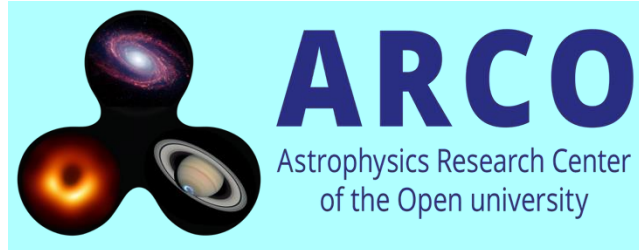
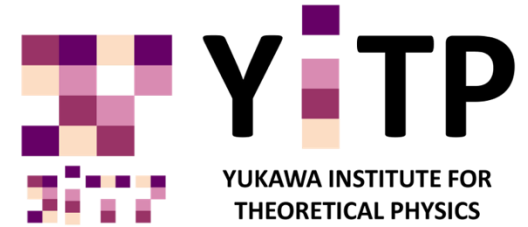


# Explosive Astrophysical Transients

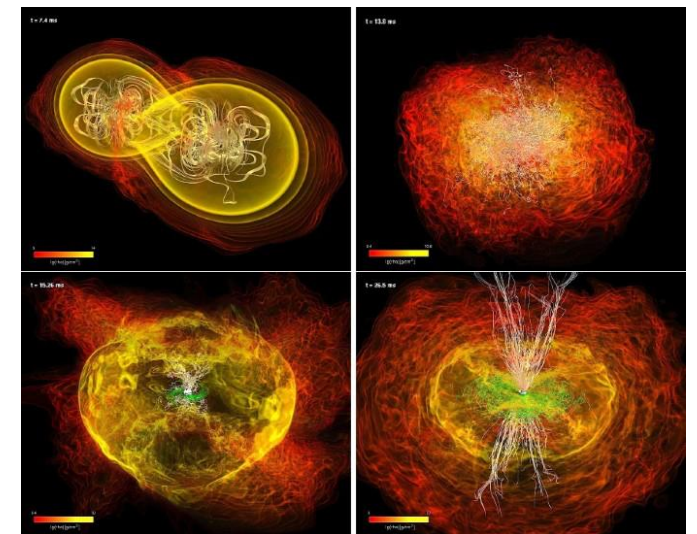
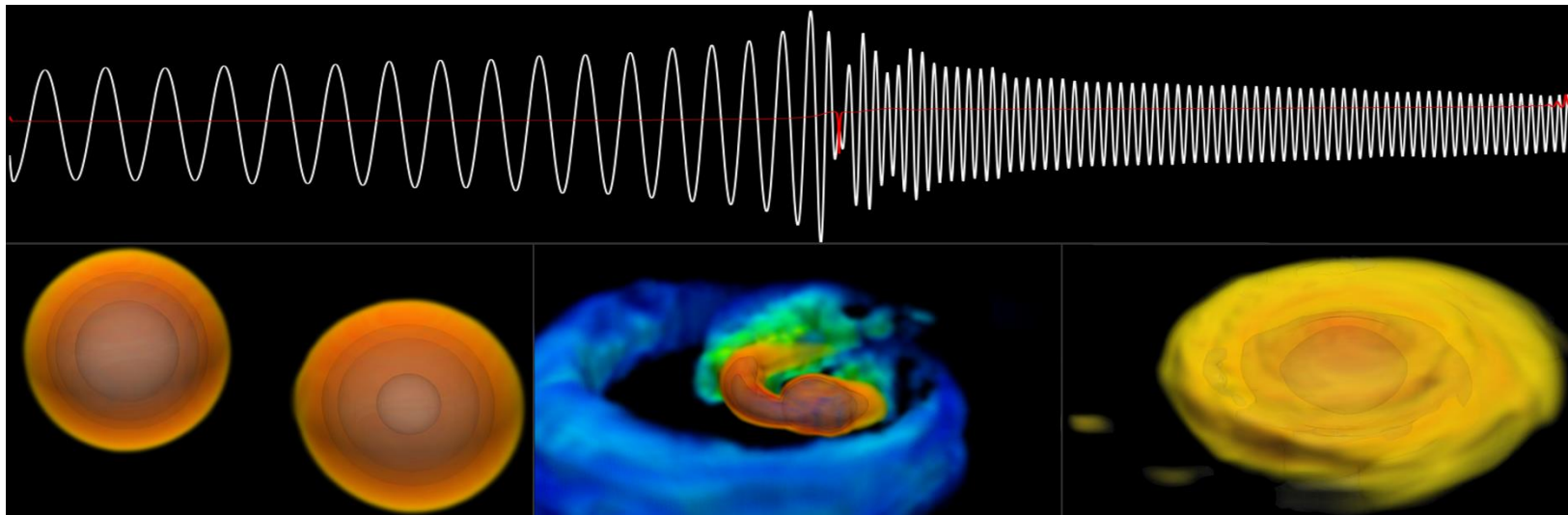
## in the Multi-Messenger Era: Some Highlights



**Jonathan  
Granot**



**Open University of Israel** & **George Washington University** & **YITP**



**YITP long-term workshop: Multi-Messenger Astrophysics in the Dynamic Universe**

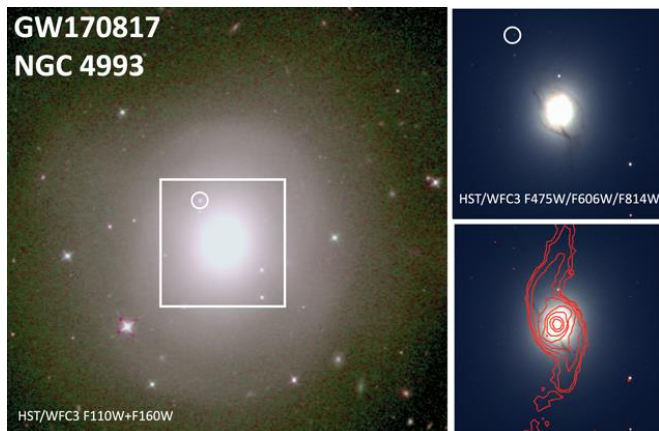
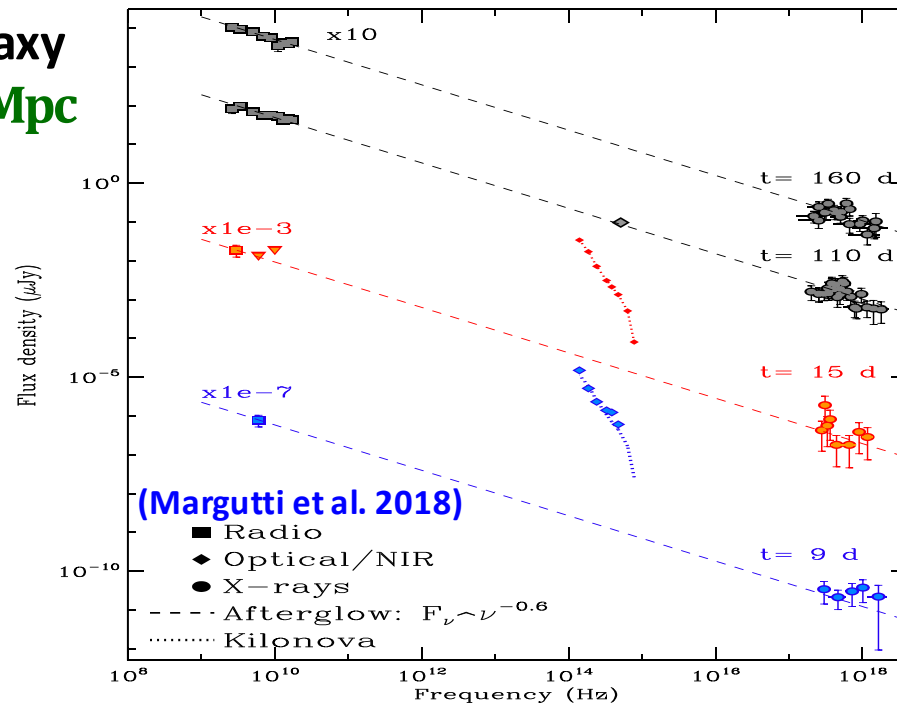
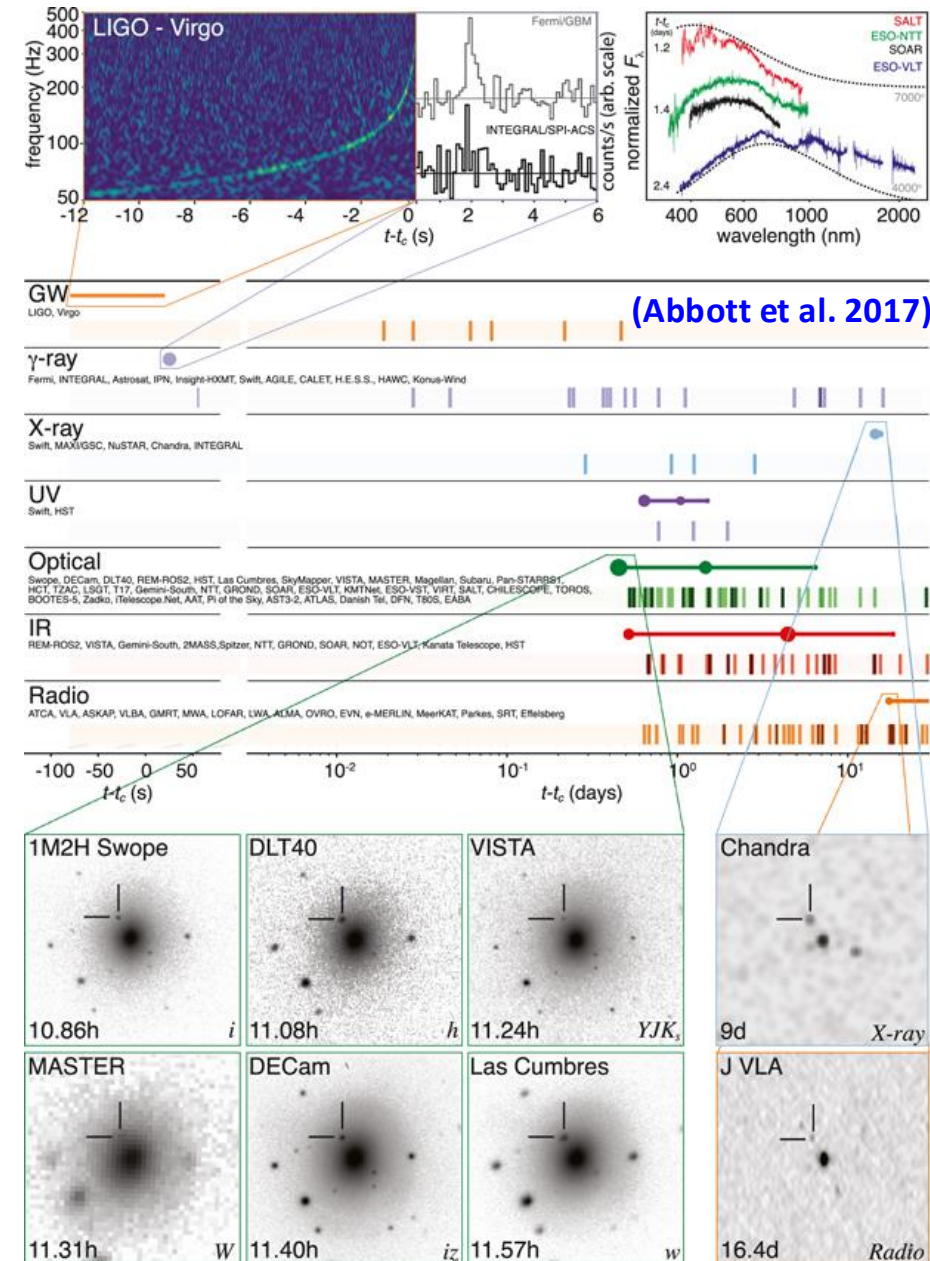
**Yukawa Institute for Theoretical Physics, Kyoto University, Kyoto, Japan, 26 January 2026**

# Outline of the Talk: what will or will not be covered

- **GRBs**: select highlights from the recent decade
  - ◆ **GRB170817A/GW170817**: 1<sup>st</sup> EM-GW counterpart (sGRB, kilonova, afterglow), r-process elements synthesis, jet angular structure & large off-axis viewing angle
  - ◆ **Polarization**: **GW170817** UL  $\Rightarrow$  constraints on B-field structure in the afterglow shock; **GRB180720B**: reverse to forward shock transition; afterglow pol. from structured jets
  - ◆ **Prompt GRB**: dissipation (IS/rec), emission (syn/Compt/SSC/had) (Rahaman)
  - ◆ **TeV emission**: from nearby GRBs – afterglow, reverse shock, prompt? (???)
  - ◆ **GRB 221009A** (B.O.A.T): bright in TeV, shallow jet, 6-12 MeV line (Salafia)
- **Einstein Probe** X-ray transients: mostly GRBs, start earlier, last longer (Hamidani)
- **ULGRB 250702B**: ~day long, unclear origin (some type of collapsar or TDE?)
- **Magnetars / FRBs**:
  - ◆ FRBs from a Galactic magnetar, SGR 1935+2154 (28.4.2020)
  - ◆ Persistent Radio Sources (**PRSs**) associated with repeating Fast Radio Bursts (**FRBs**)
  - ◆ **Extragalactic Magnetar Giant Flares**- current sample and prospects

# GW170817 / GRB170817A: NS-NS merger

- First electromagnetic counterpart to a GW event
  - The **short GRB** 170817A (very under-luminous, 1.74 s  $\gamma$ -GW delay)
  - Optical (IR to UV) **kilonova** emission (1<sup>st</sup> clear-cut) for a few weeks
  - X-ray (> 9 d; still barely detected) to radio (>16 d) **afterglow**
- First NS-NS merger detected in gravitational waves (GW)
- First direct sGRB - NS-NS merger association (Eichler+ 1989)
- The  $\gamma$ -GW 1.74 s delay constrains GW speed:  $\left| \frac{v_{GW}}{c} - 1 \right| \lesssim 4 \cdot 10^{-16}$
- $D_{GW} = 43_{-6.9}^{+2.9}$  Mpc; host galaxy is elliptical:  $D = 41.0 \pm 3.1$  Mpc ( $z = 0.009783$ ) 2 kpc from host center in projection



# GW170817 / GRB170817A: Kilonova

## Observations require two components:

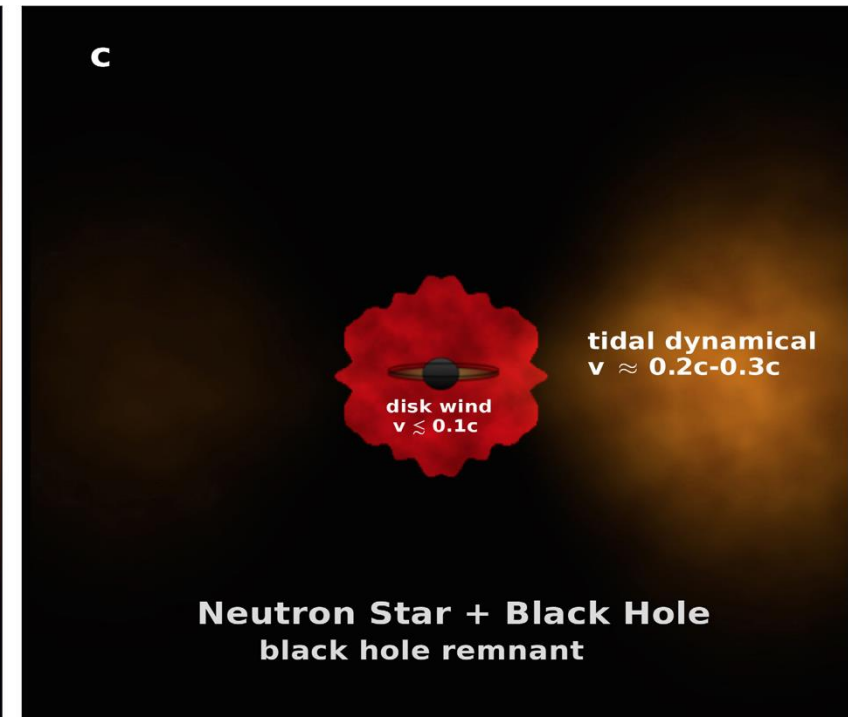
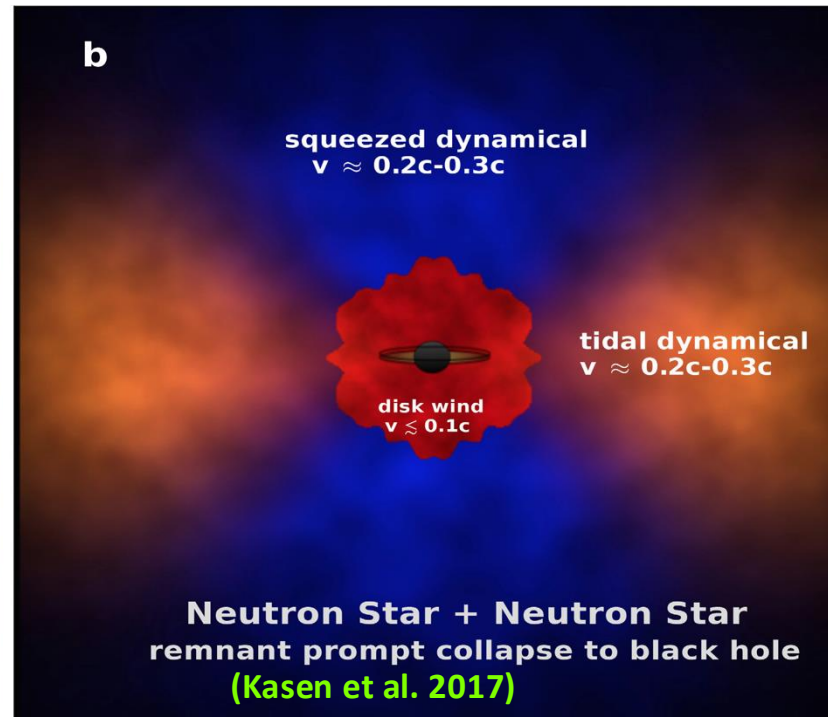
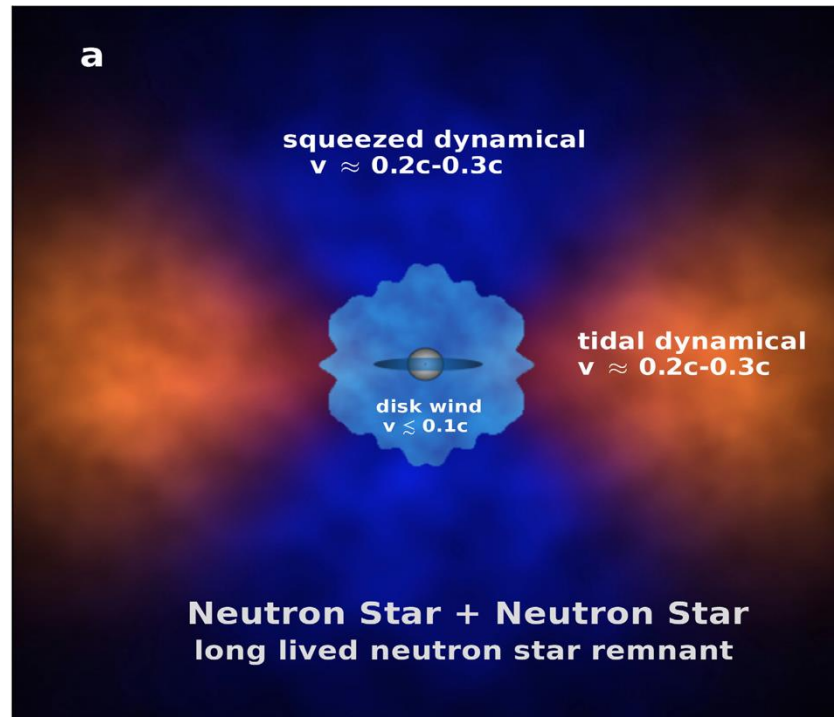
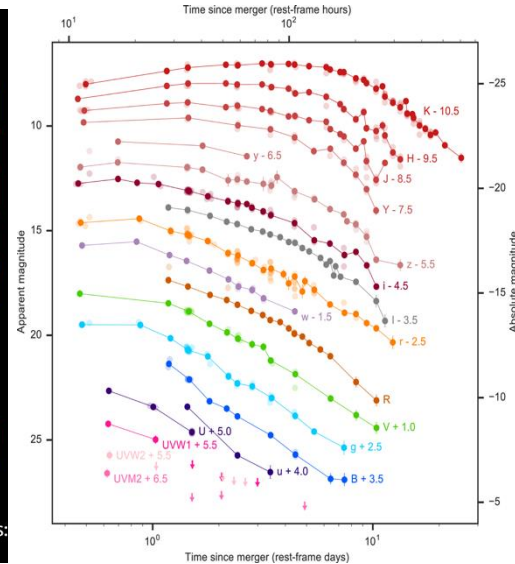
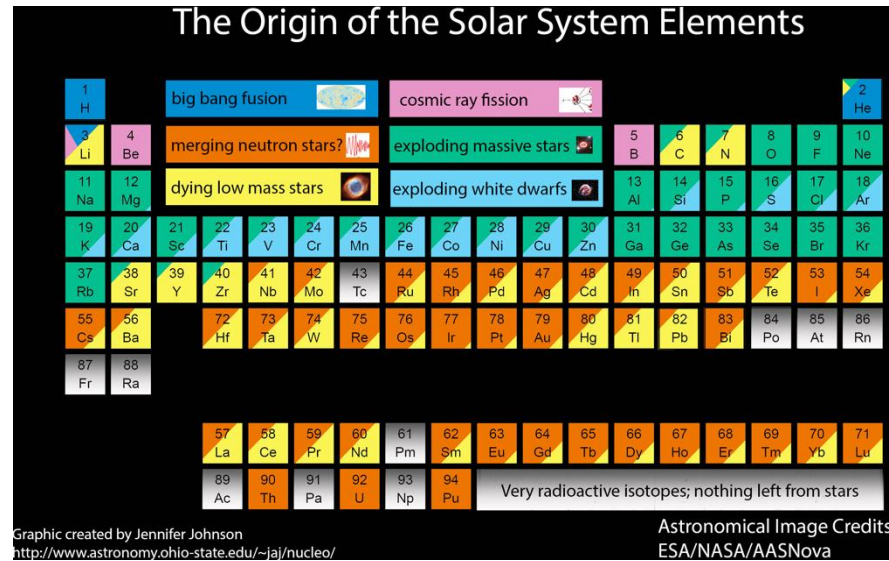
❖ First **blue/fast**, **lanthanide-poor**

$$M_{ej} \approx (1\% - 2\%)M_{\odot}, v_{ej} \approx (0.2 - 0.3)c$$

❖ Second **red/slow**, **lanthanide-rich**

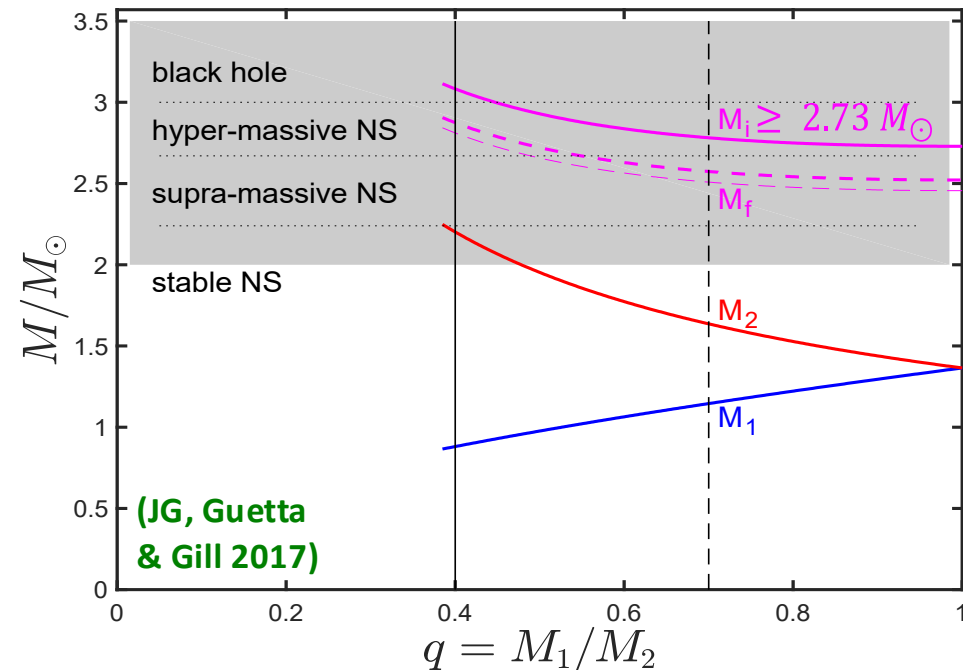
$$M_{ej} \approx (3\% - 5\%)M_{\odot}, v_{ej} \approx (0.05 - 0.2)c$$

## Synthesized large amounts of heavy elements (may dominate the cosmic r-process nucleosynthesis, heavy metals e.g. gold, platinum)

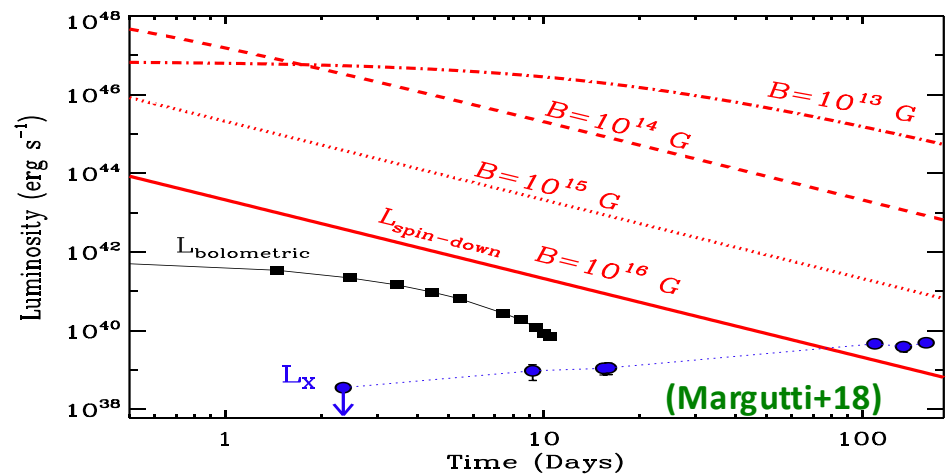


# GW170817 / GRB170817A: Remnant Type

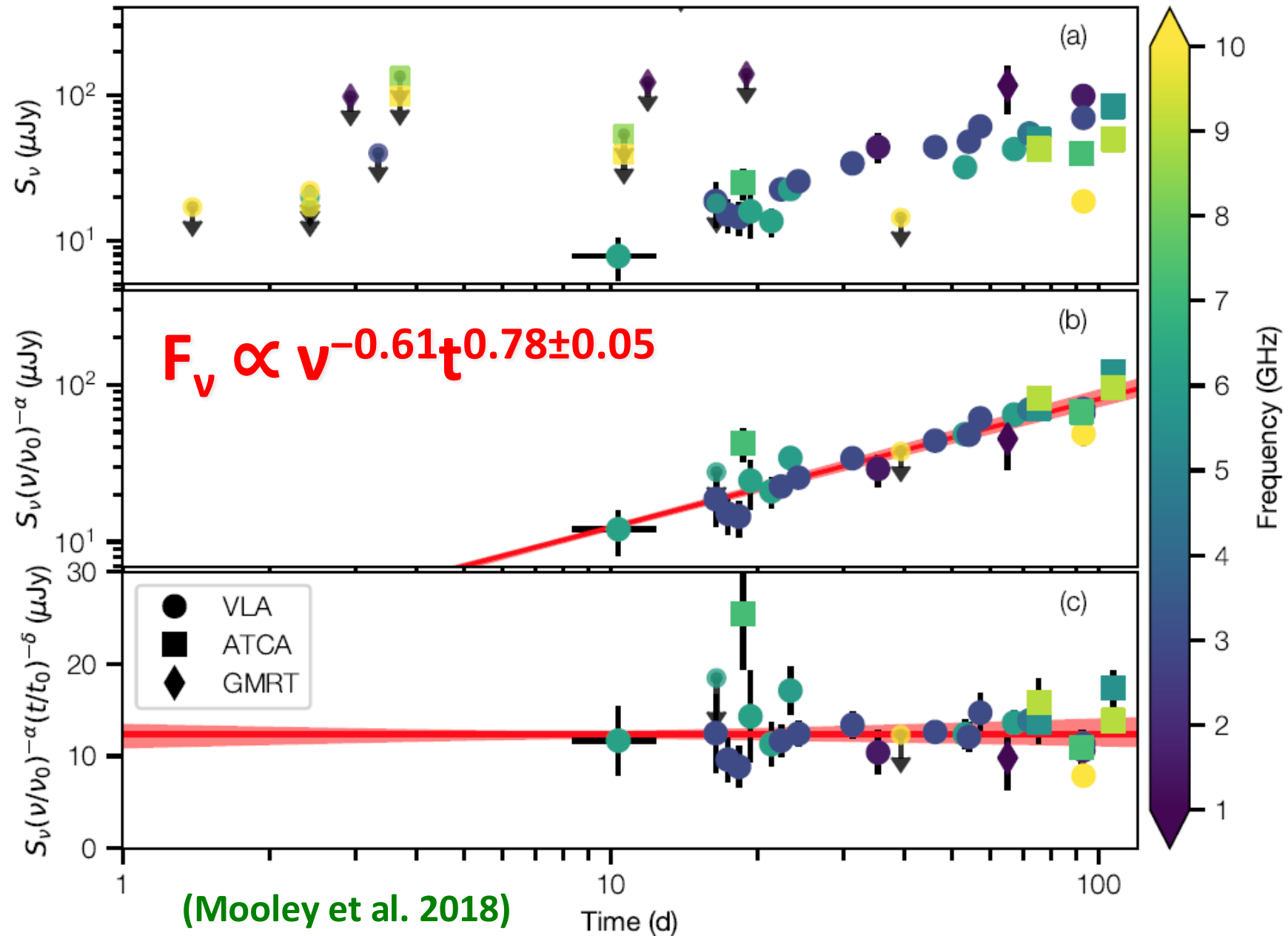
- $M_{1,2}$  = pre-merger NS  $M_{\text{gravitational}}$
- post-merger total mass:  $M_i = M_1 + M_2$
- Final mass  $M_f \approx 0.93M_i$  due to:
  - ❖ GW & neutrino energy losses
  - ❖ Mass ejection during the merger
- A stable NS or SMNS  $\Rightarrow P_0 \approx 1 \text{ ms} \Rightarrow E_{\text{rot}} \gtrsim 10^{52.5} \text{ erg}$ ,  
 $\tau_{\text{sd}} \approx 20B_{13}^{-2} \text{ days} \Rightarrow$  would contradict afterglow observations (also what produces the GRB/afterglow?)
- The argument can be reversed to constrain NS EoS &  $M_{\text{max}} \lesssim 2.17M_{\odot}$  (Margalit & Metzger 2017; Rezzolla et al. 2018)



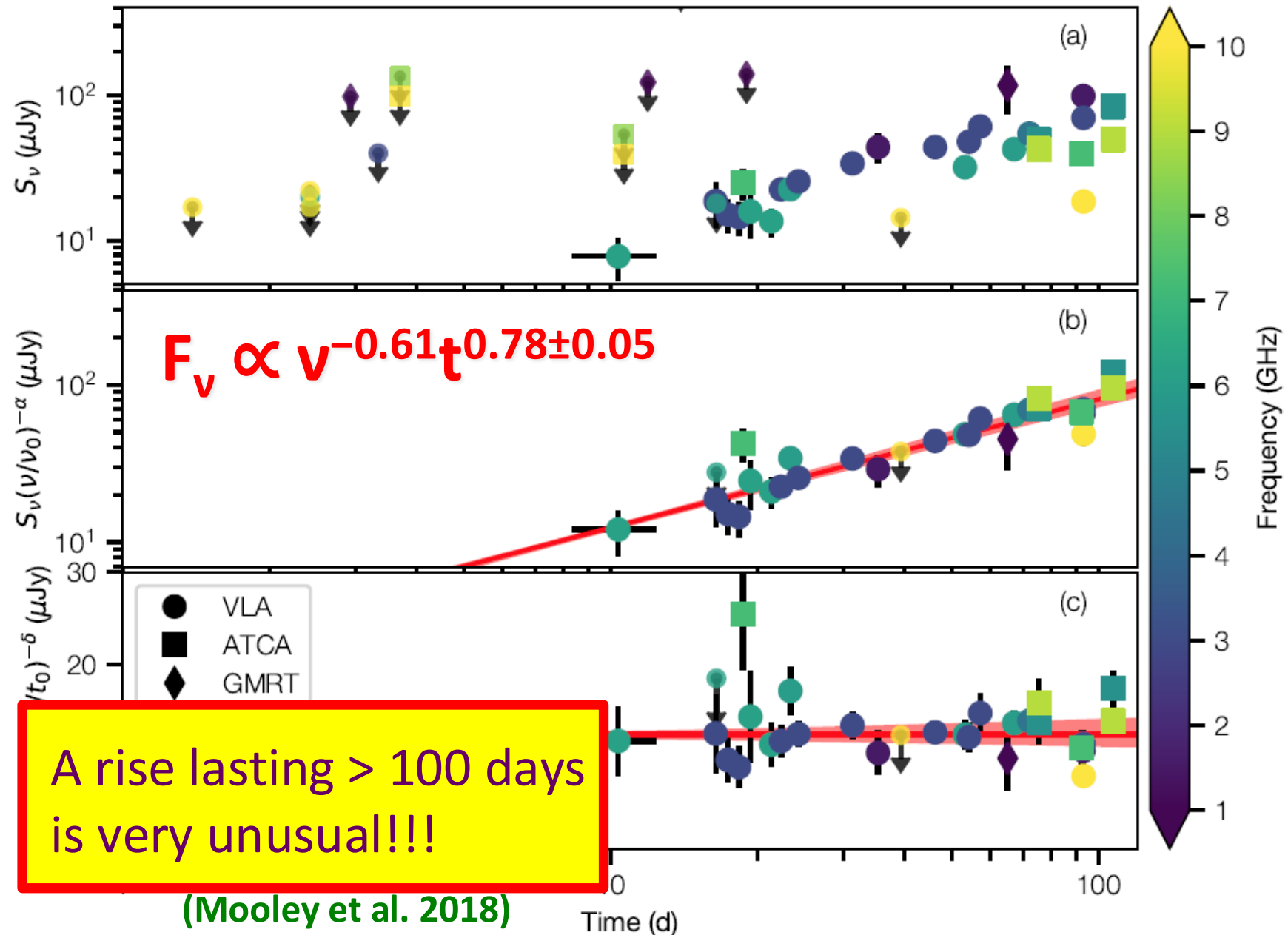
Chirp mass:  $\mathcal{M} = \left( \frac{M_1^3 M_2^3}{M_1 + M_2} \right)^{1/5} = 1.188^{+0.004}_{-0.002} M_{\odot}$  (Abbott+ 2017)



# GRB170817A: Afterglow Observations



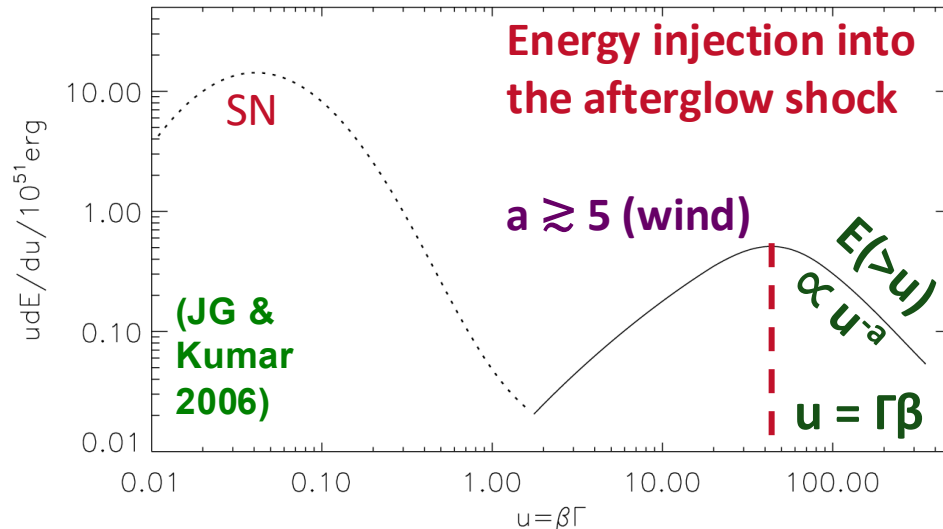
# GRB170817A: Afterglow Observations



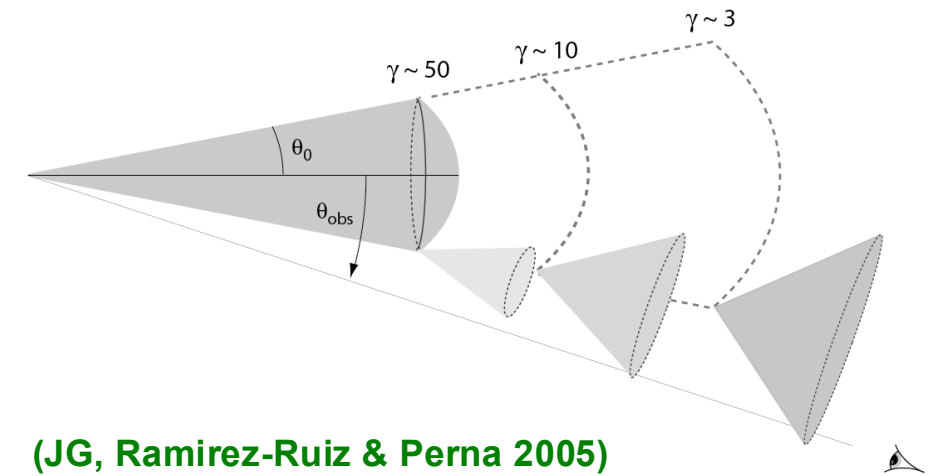
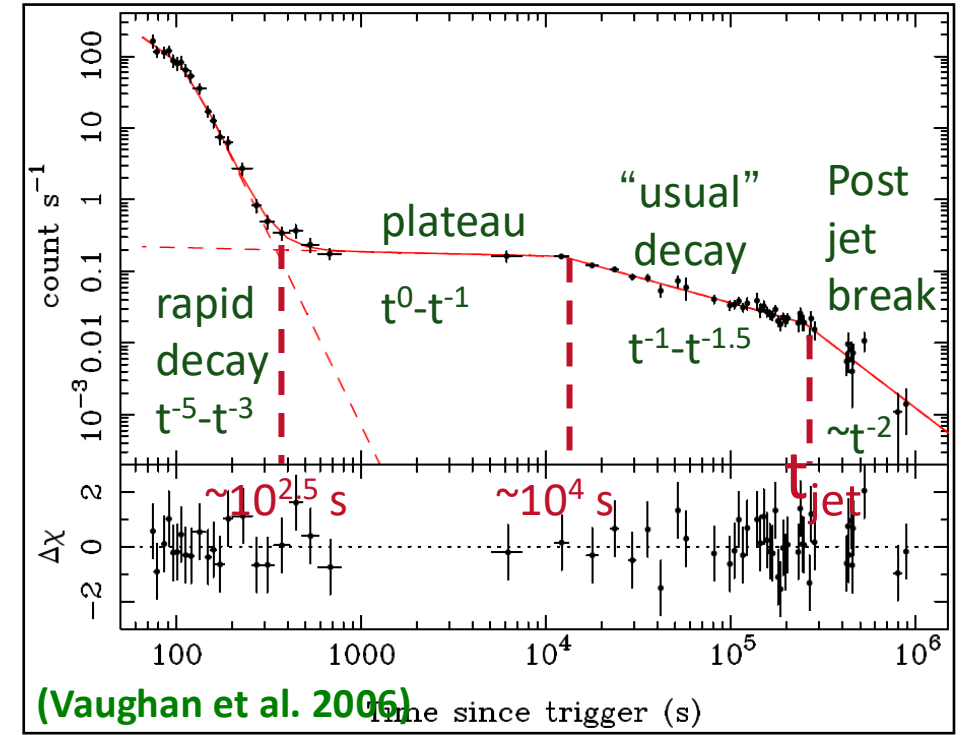
# Analogy to rising $F_\nu$ : X-ray Plateaus

## ■ Possible solutions:

- ◆ Evolution of shock microphysical parameters (JG, Konigl & Piran 2006)
- ◆ Energy injection into external shock:
  1. long-lived relativistic wind
  2. slower ejecta catching up  
(Sari & Meszaros 00; Nousek+ 06; JG & Kumar 06)



## ◆ Viewing angle effects

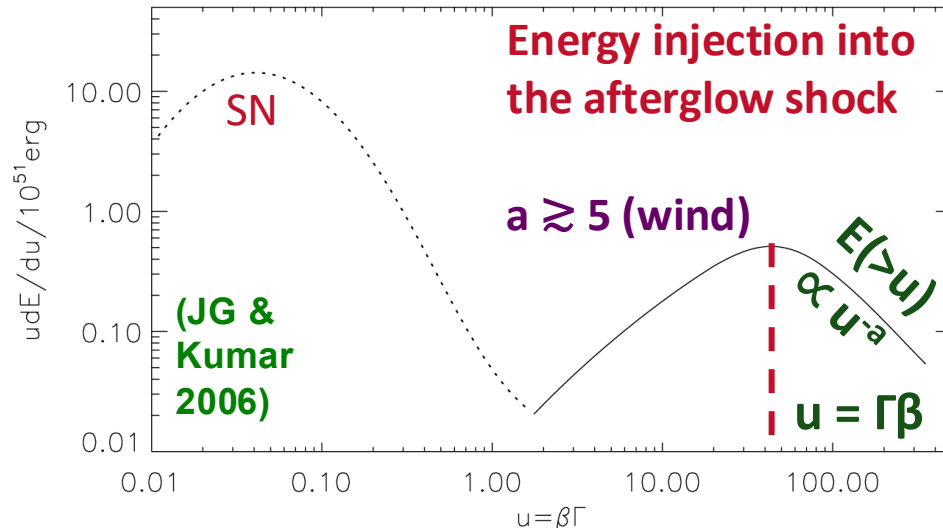


(JG, Ramirez-Ruiz & Perna 2005)

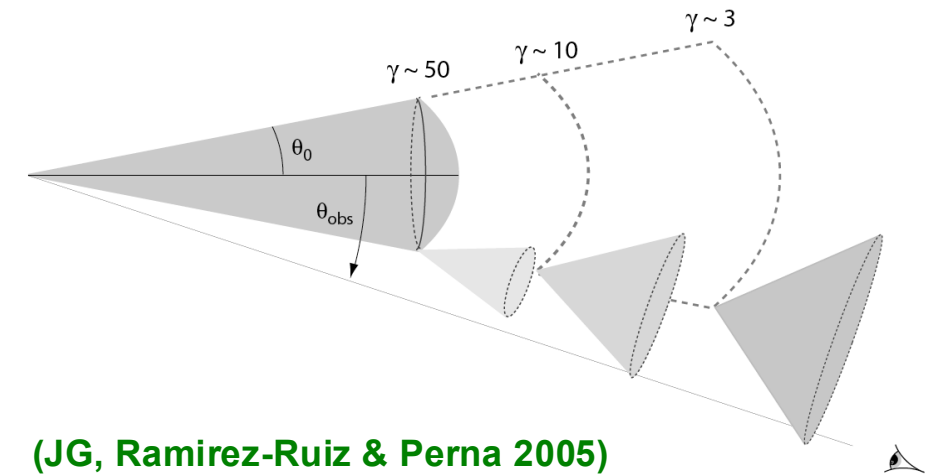
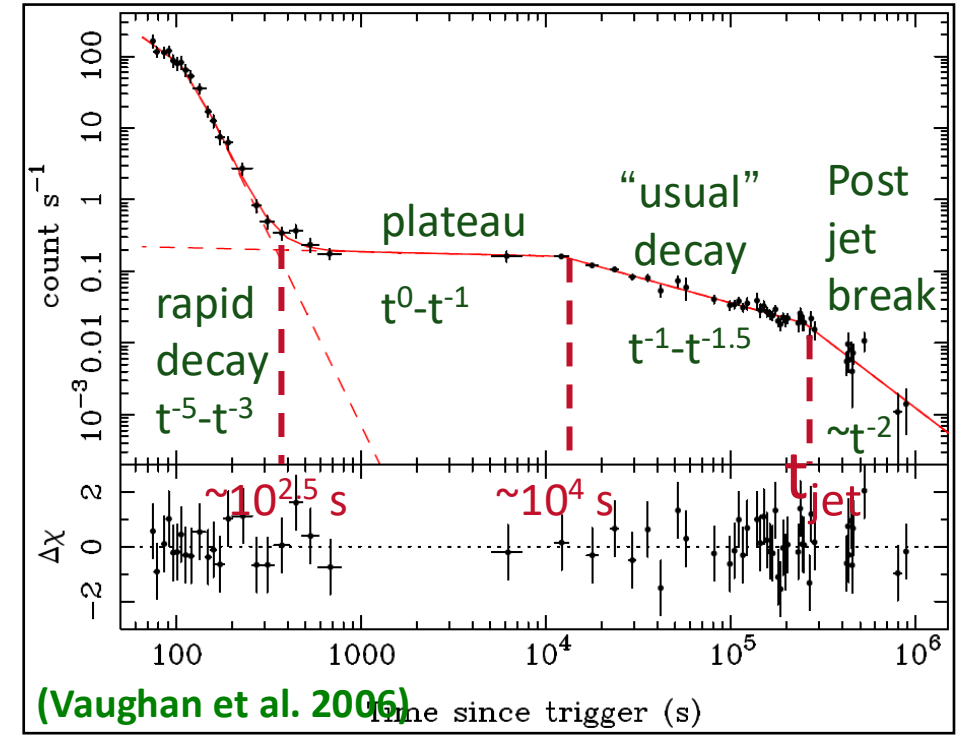
# Analogy to rising $F_\nu$ : X-ray Plateaus

## ■ Possible solutions:

- ◆ Evolution of shock microphysical parameters (JG, Konigl & Piran 2006)
- ◆ Energy injection into external shock:
  1. long-lived relativistic wind
  2. **slower ejecta catching up** radial  
(Sari & Meszaros 00; Nousek+ 06; JG & Kumar 06)

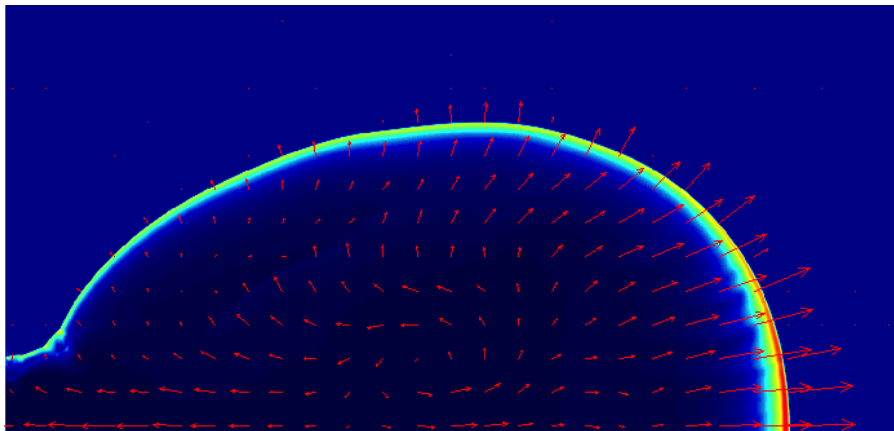


- ◆ **Viewing angle effects** angular



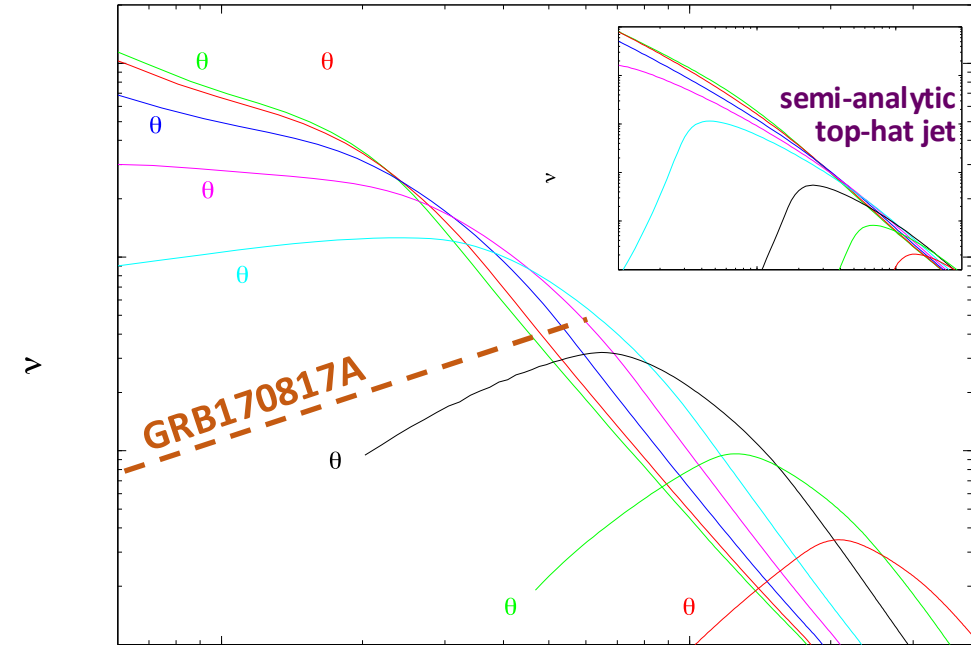
# Analogy to rising $F_\nu$ : Off-Axis Viewing

- The emission is initially strongly beamed away from our L.o.S
- $F_\nu$  rises as beaming cone widens
- When beaming cone reaches LoS  $F_\nu$  peaks & approaches on-axis  $F_\nu$
- The rise is much more gradual for hydrodynamic simulations due to slower matter at the jet's sides with non-radial velocities

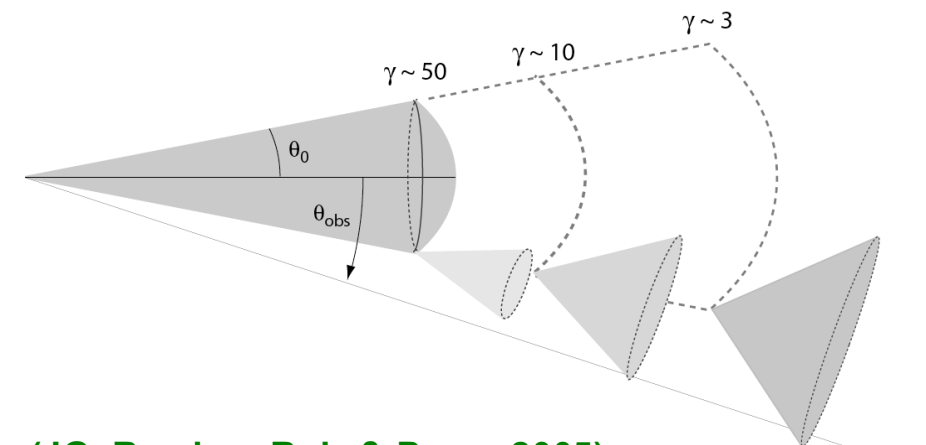


(JG et al. 2001)

0.311E-12  0.163E-05



(JG et al. 2002)

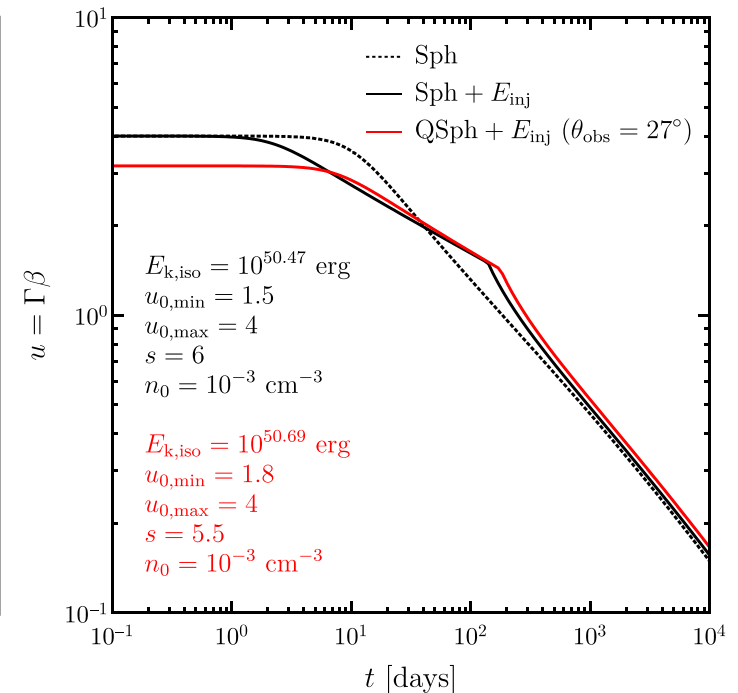
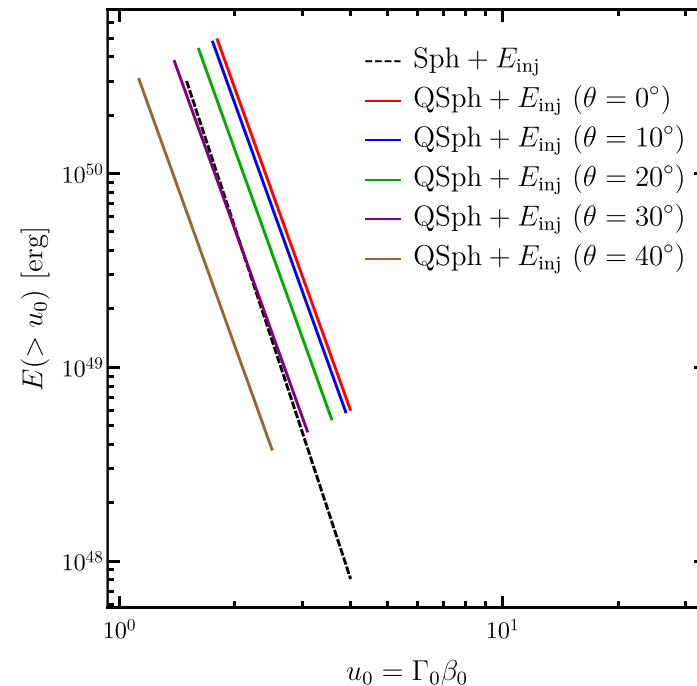


(JG, Ramirez-Ruiz & Perna 2005)

# Outflow Structure: Breaking the Degeneracy (Gill & JG 18)

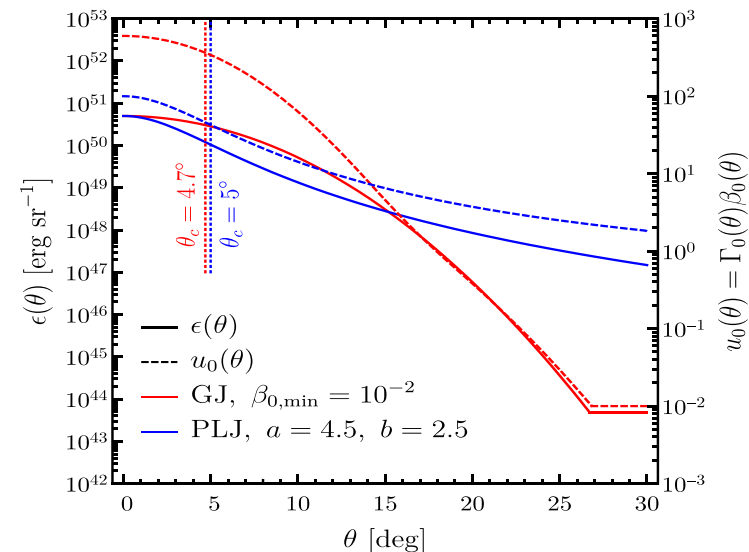
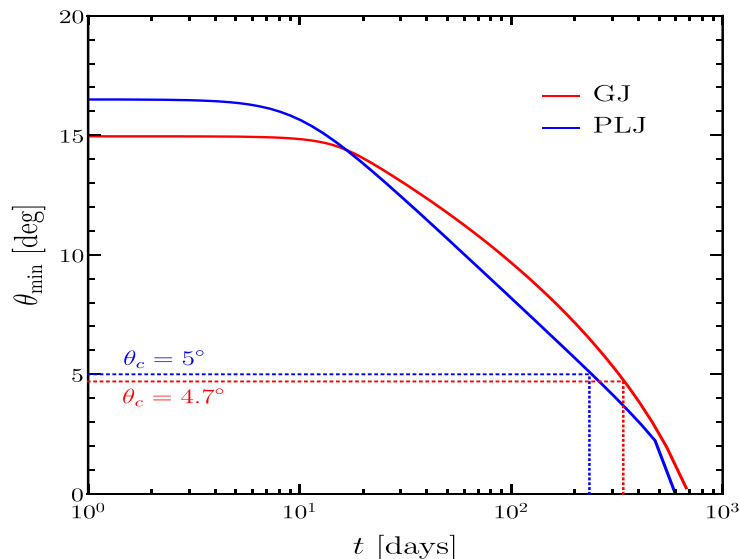
- The lightcurves leave a lot of degeneracy between models
- The degeneracy may be lifted by calculation the afterglow **images** & **polarization** (e.g. Nakar & Piran 2018; Nakar et al. 2018)
- We considered 4 different models including both main types
  - ◆ Sph+ $E_{inj}$ : Spherical with energy injection  $E(>u=\Gamma\beta) \propto u^{-6}$ ,  $1.5 < u < 4$
  - ◆ QSph+ $E_{inj}$ : Quasi-Spherical + energy injection  $E(>u) \propto u^{-s}$ ,  $u_{min,0} = 1.8$   $u_{max,0} = 4$ ,  $s = 5.5$ ,  $\zeta = 0.1$

$$\frac{\epsilon(\theta)}{\epsilon_0} = \frac{u_{0,min}(\theta)}{u_{min,0}} = \frac{u_{0,max}(\theta)}{u_{max,0}} = \frac{\zeta + \cos^2 \theta}{\zeta + 1}$$



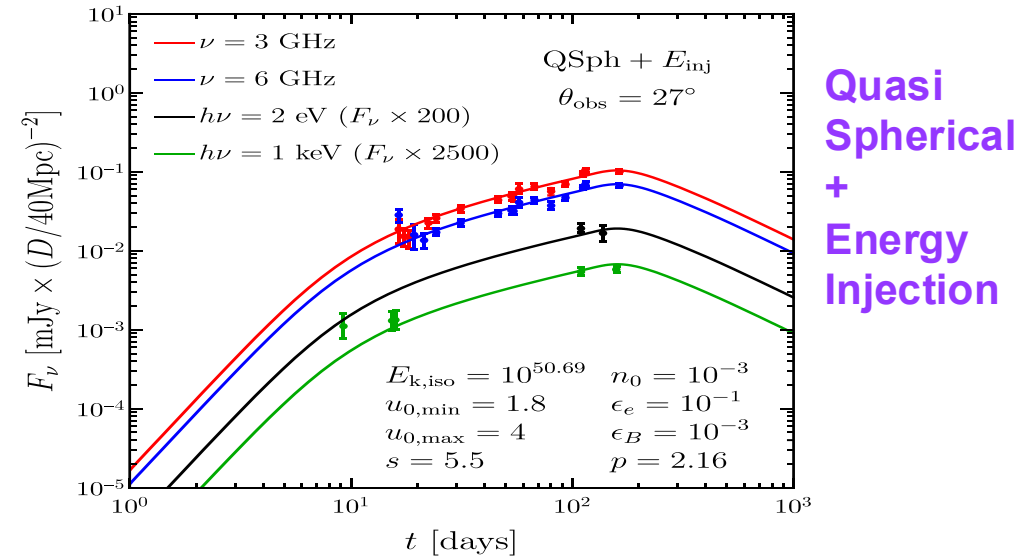
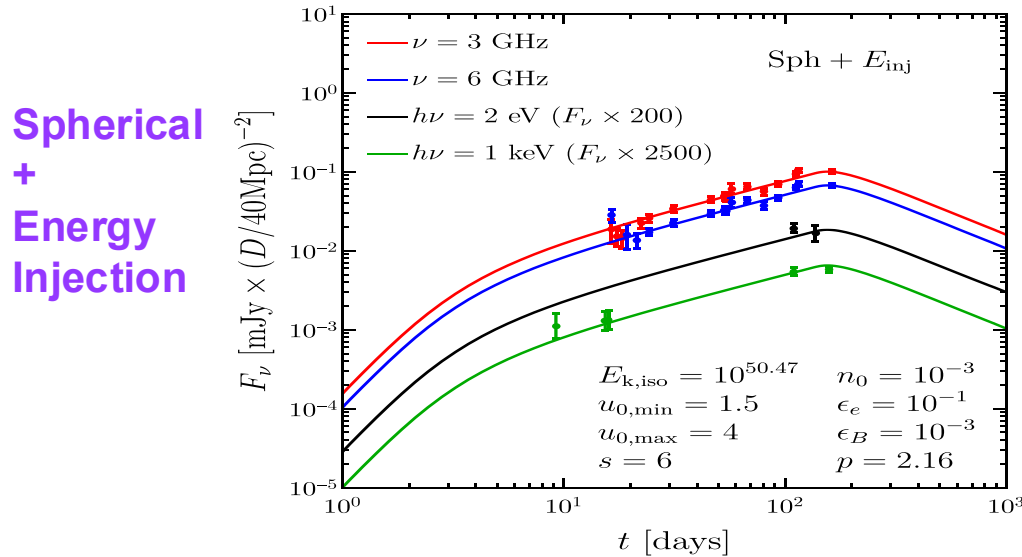
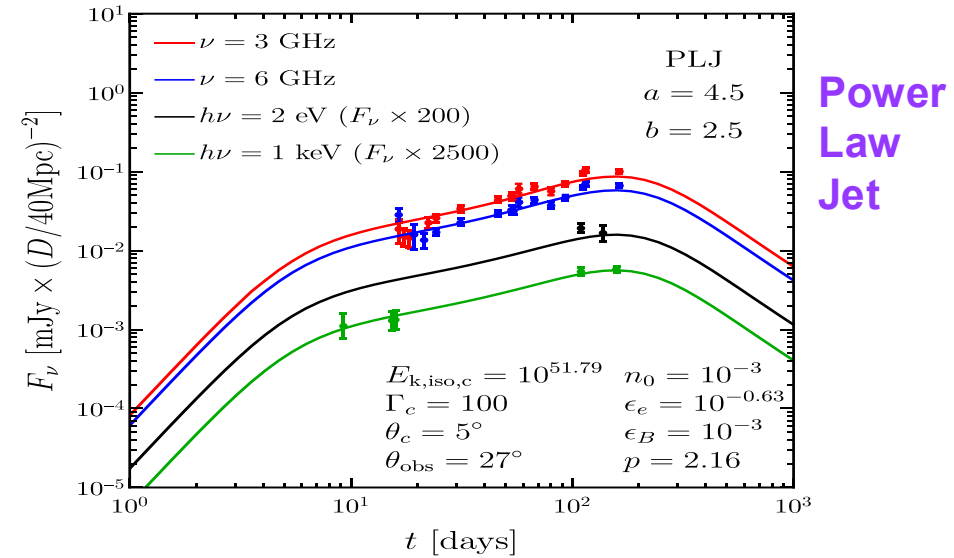
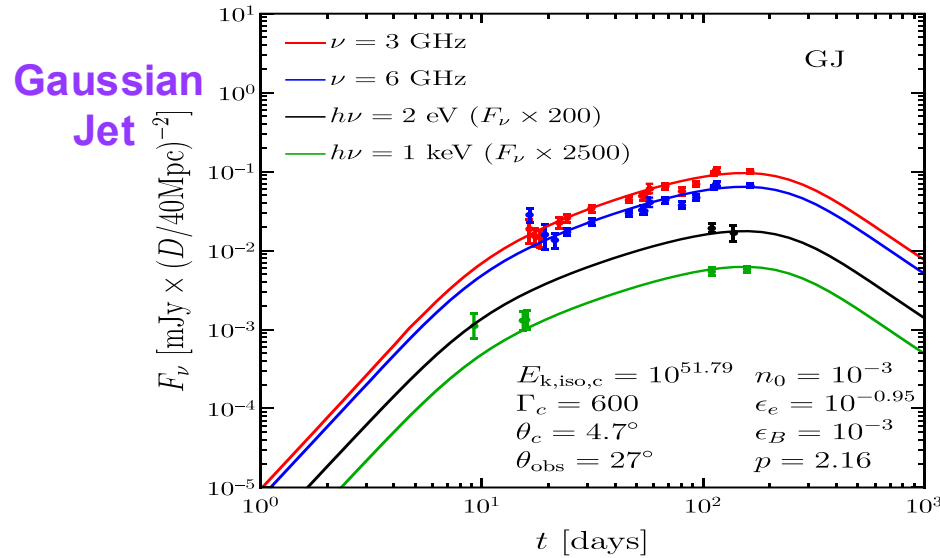
# Outflow Structure: Breaking the Degeneracy (Gill & JG 18)

- The lightcurves leave a lot of degeneracy between models
- The degeneracy may be lifted by calculation the afterglow **images** & **polarization** (e.g. Nakar & Piran 2018; Nakar et al. 2018)
- We considered 4 different models including both main types
  - ◆ GJ: Gaussian Jet (in  $\epsilon = dE/d\Omega$ ,  $\Gamma_0 - 1$ )  $\Gamma_c = 600$ ,  $\theta_c = 4.7^\circ$
  - ◆ PLJ: Power-Law Jet;  $\epsilon = \epsilon_c \Theta^{-a}$ ,  $\Gamma_0 - 1 = (\Gamma_c - 1) \Theta^{-b}$ ,  $\Theta = [1 + (\theta/\theta_c)^2]^{1/2}$ ,  $\Gamma_c = 100$ ,  $\theta_c = 5^\circ$ ,  $a = 4.5$ ,  $b = 2.5$
- As there is a lot of freedom we fixed:  $p = 2.16$ ,  $\epsilon_B = n_0 = 10^{-3}$ ,  $\theta_{\text{obs}} = 27^\circ$



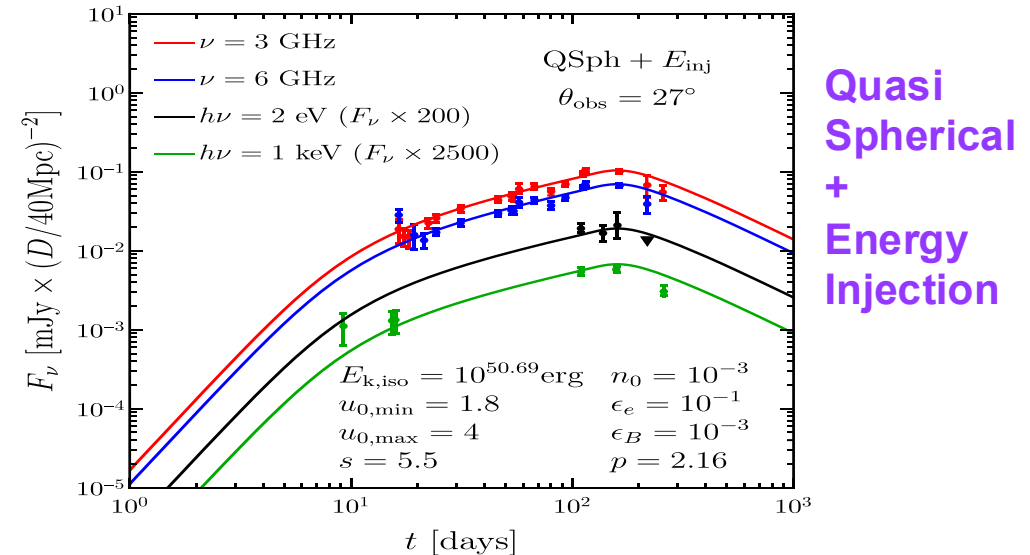
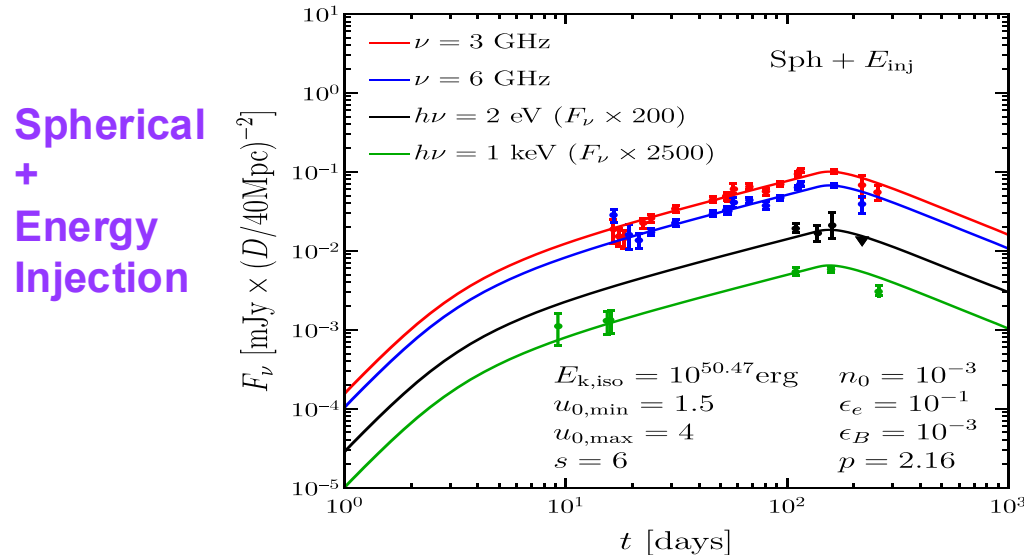
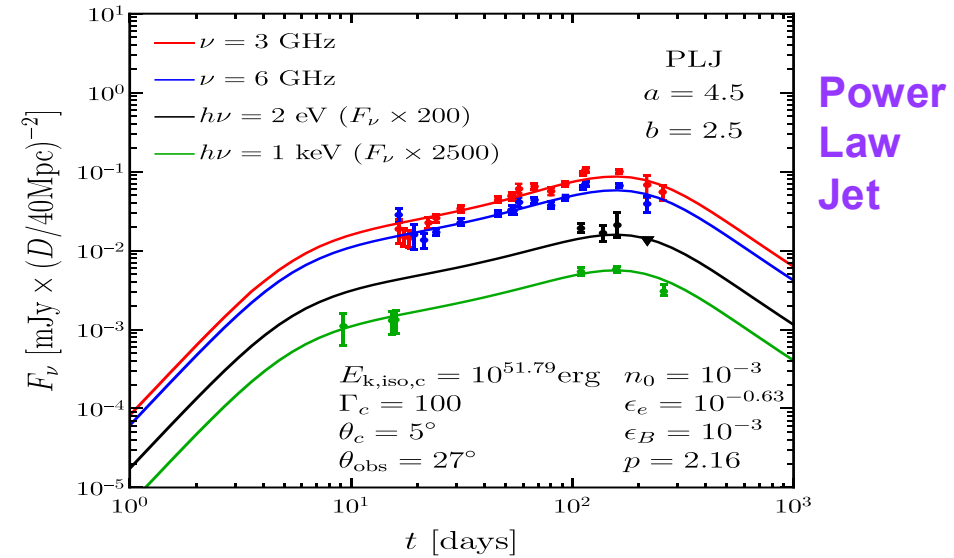
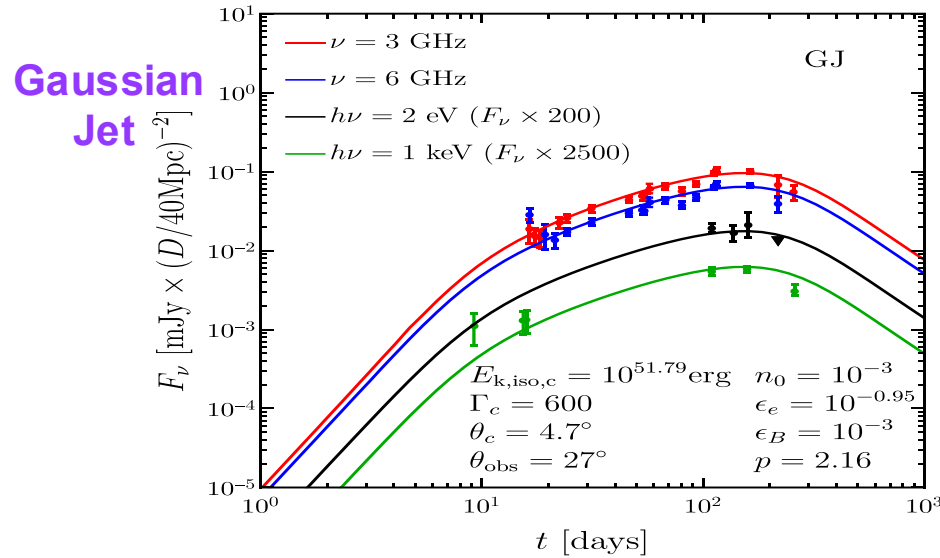
# Outflow Structure: Breaking the Degeneracy (Gill & JG 18)

## ■ Tentative fit to GRB170817A afterglow data (radio to X-ray)



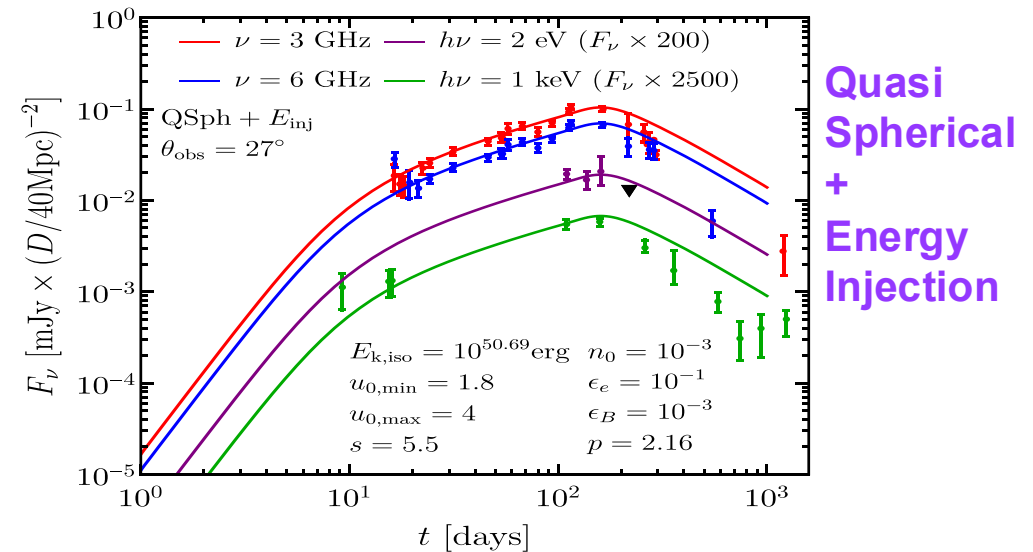
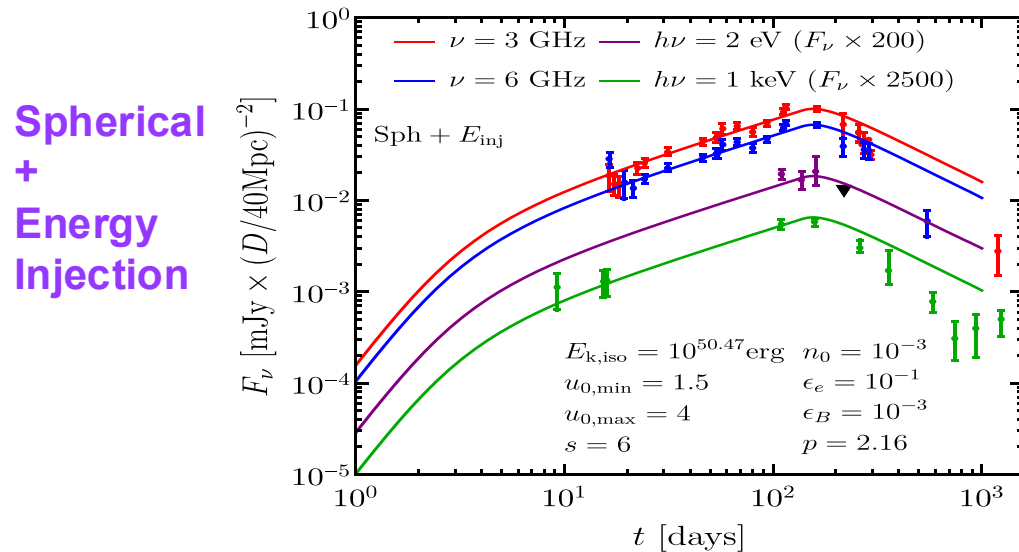
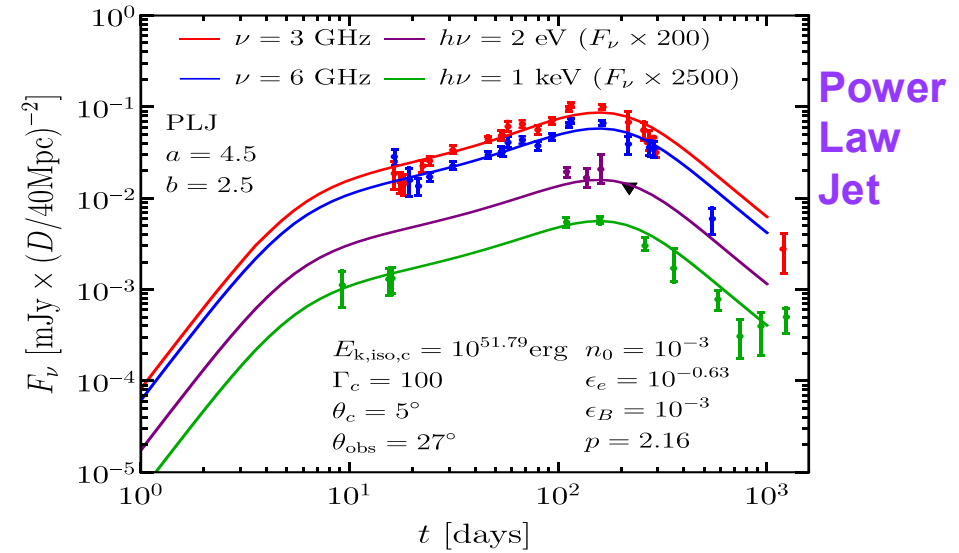
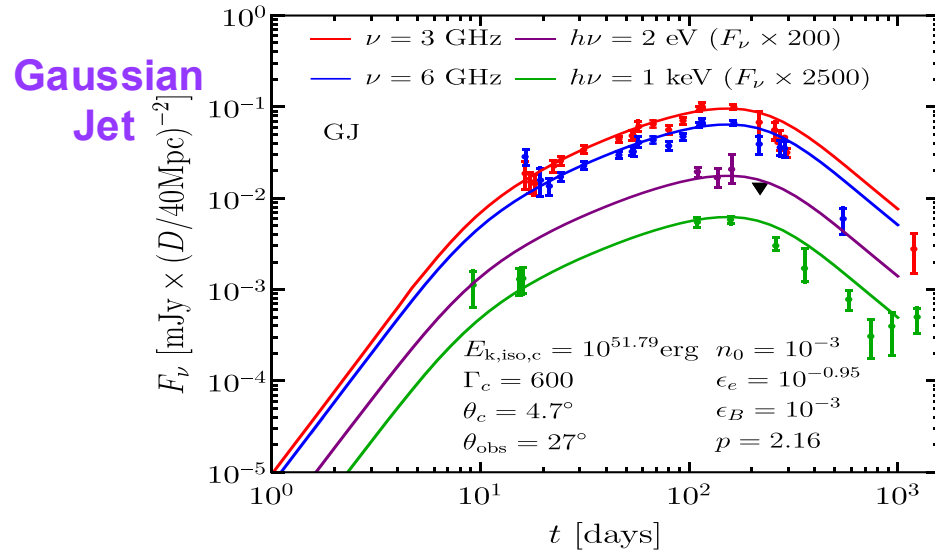
# Outflow Structure: Breaking the Degeneracy (Gill & JG 18)

- New data that came out established a peak at  $t_{\text{peak}} \sim 150$  days



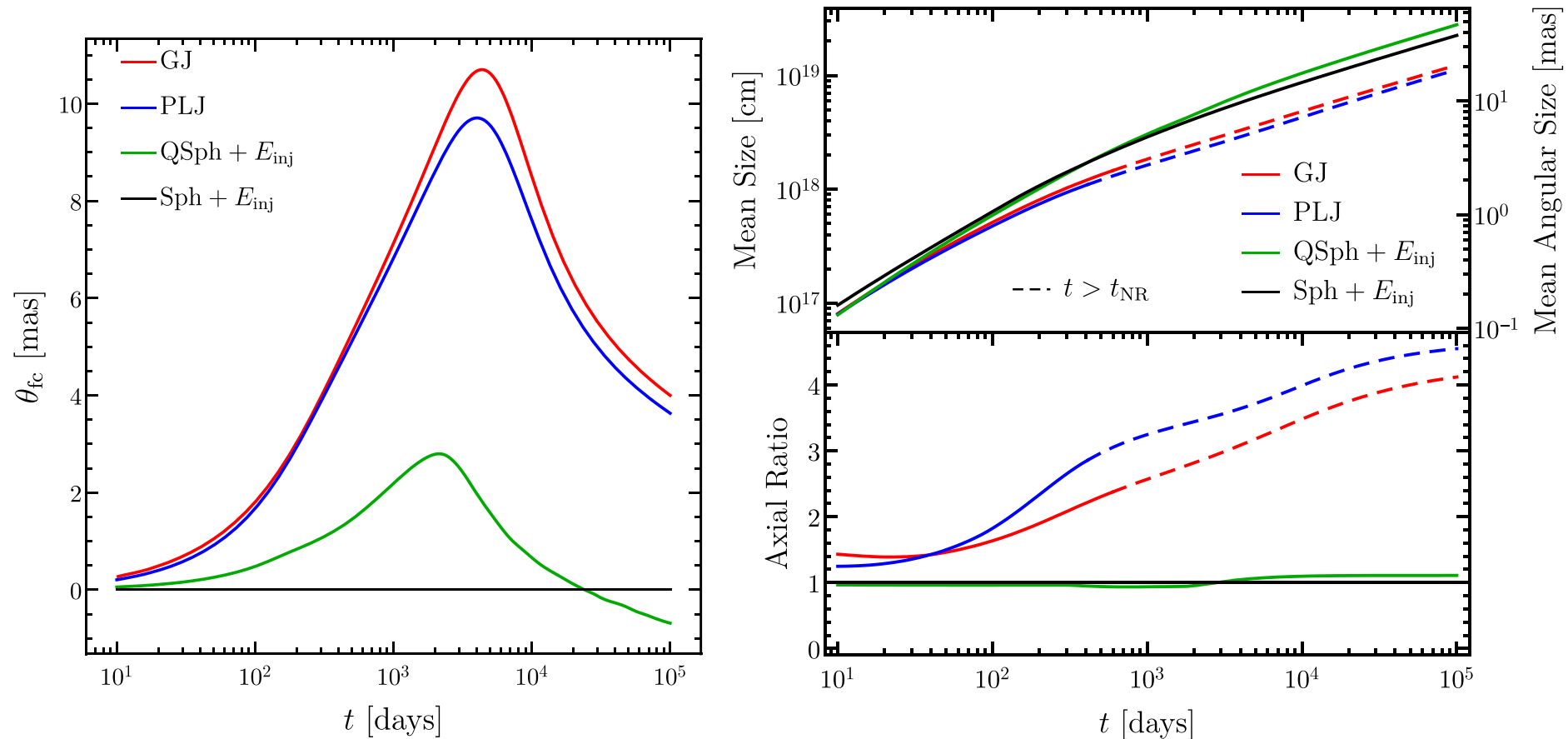
# Outflow Structure: Breaking the Degeneracy (Gill & JG 18)

- The jet models decay faster (closer to post-peak data:  $F_\nu \propto t^{-2.2}$ )



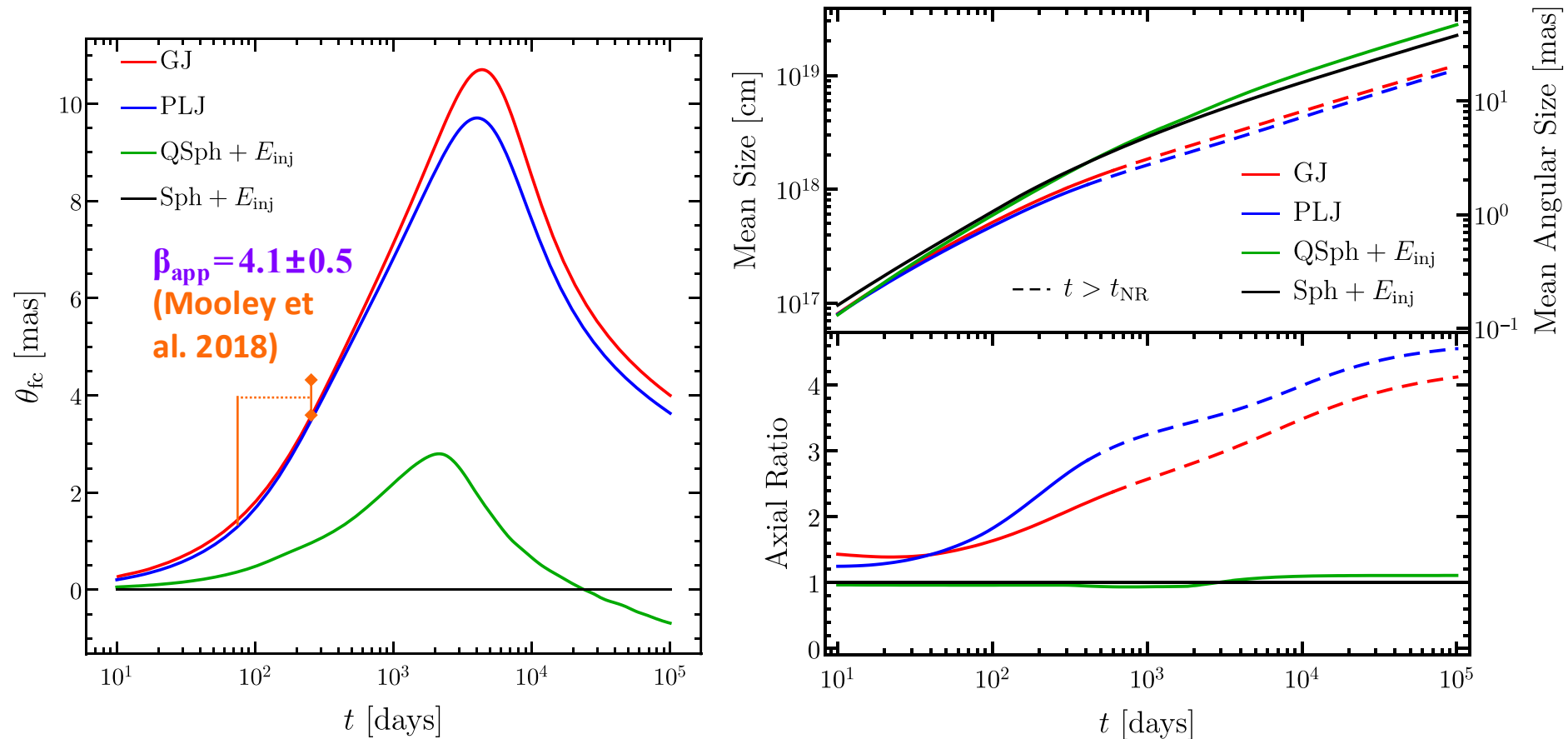
# Afterglow Images: Flux Centroid, Size, Shape

- The flux centroid motion: a potentially powerful diagnostic
- It may be hard to tell apart models based on the image size alone, but a much higher axis-ratio is expected for jet models



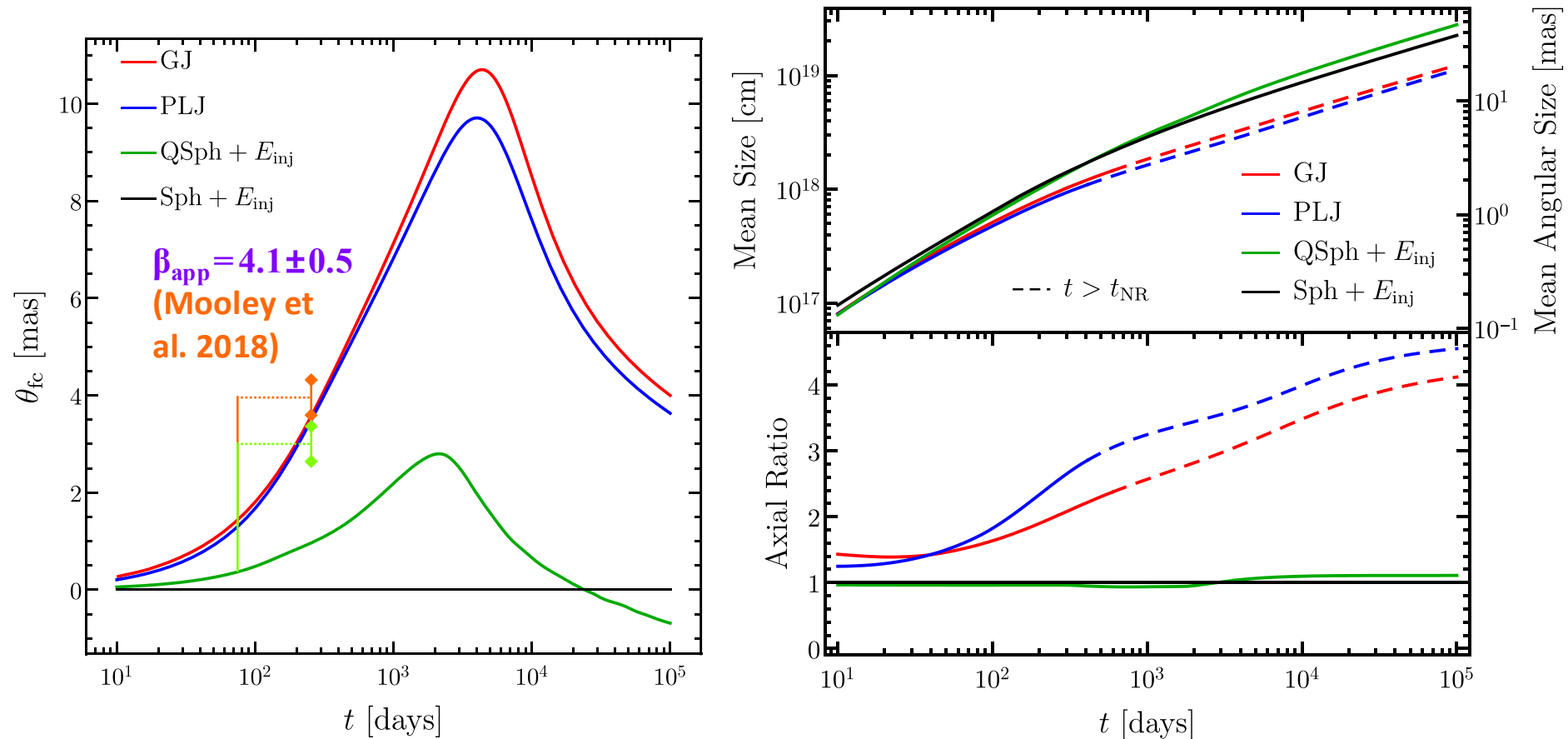
# Afterglow Images: Flux Centroid, Size, Shape

- The flux centroid motion: a potentially powerful diagnostic
- It may be hard to tell apart models based on the image size alone, but a much higher axis-ratio is expected for jet models



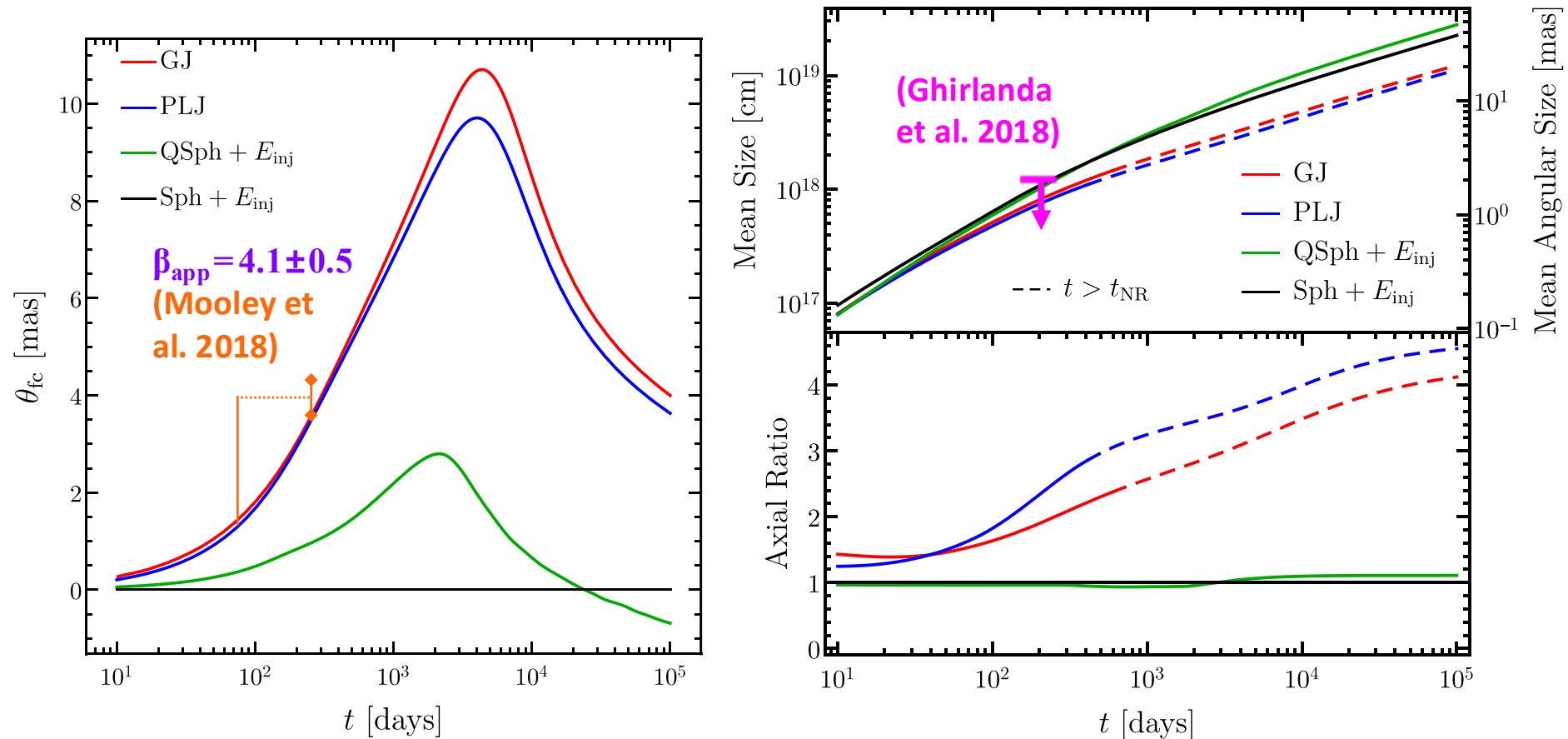
# Afterglow Images: Flux Centroid, Size, Shape

- The flux centroid motion: a potentially powerful diagnostic
- It may be hard to tell apart models based on the image size alone, but a much higher axis-ratio is expected for jet models



# Afterglow Images: Flux Centroid, Size, Shape

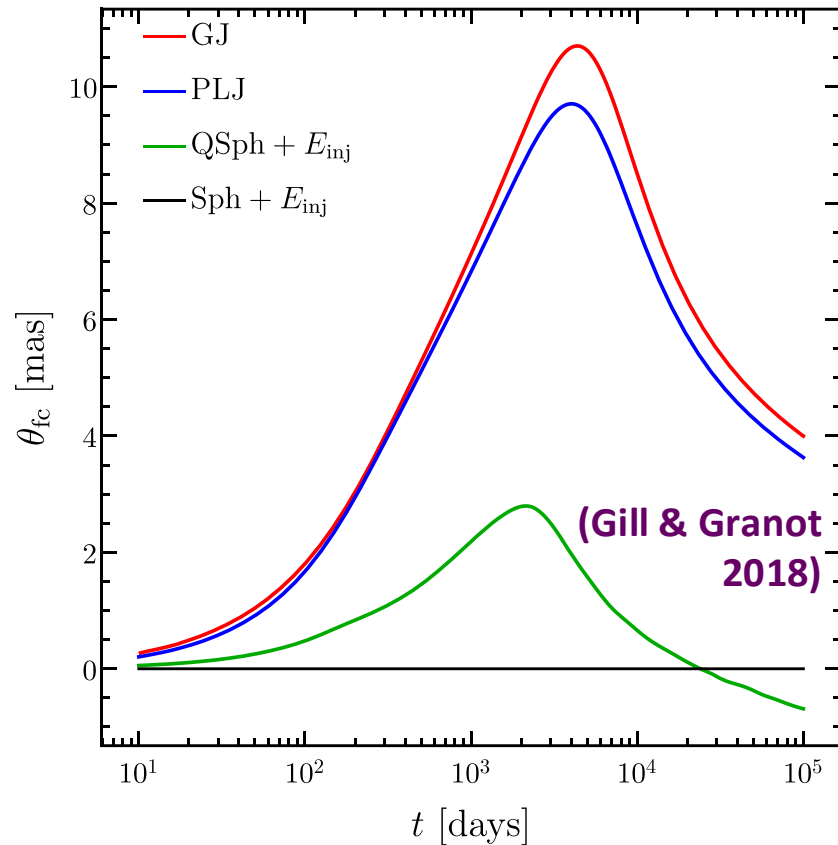
- The flux centroid motion: a potentially powerful diagnostic
- It may be hard to tell apart models based on the image size alone, but a much higher axis-ratio is expected for jet models



# Afterglow Images: Flux Centroid, Size, Shape

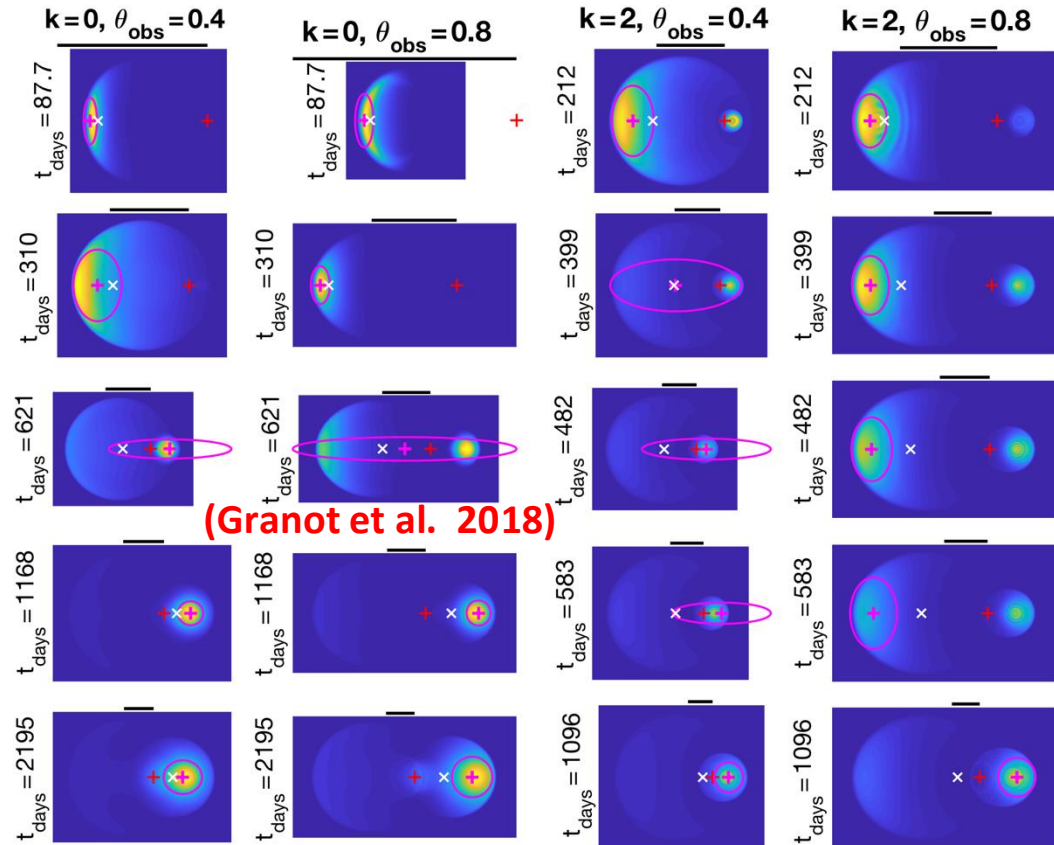
- The flux centroid motion: a potentially powerful diagnostic
- It may be hard to tell apart models based on the image size alone, but a much higher axis-ratio is expected for jet models

Radio flux centroid motion: semi-analytic



(Gill & JG 2018)

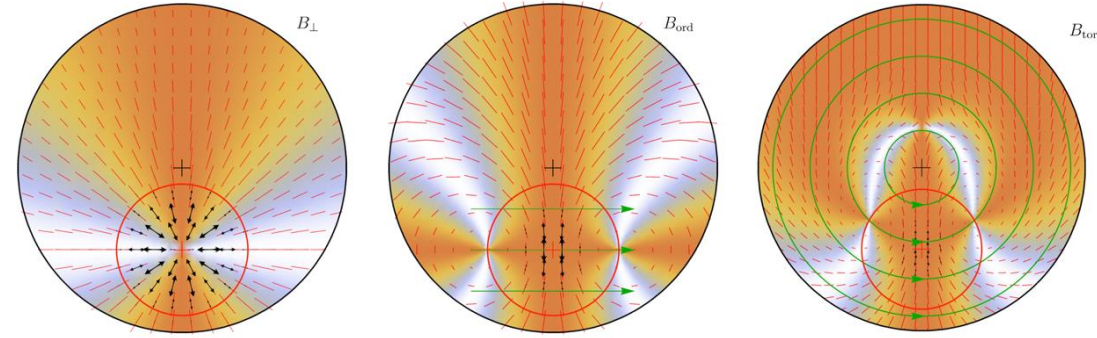
Agree with radio afterglow images from simulations



(JG, De Colle & Ramirez-Ruiz 2018)

# GRB Polarization probes the B-field & Jet structures:

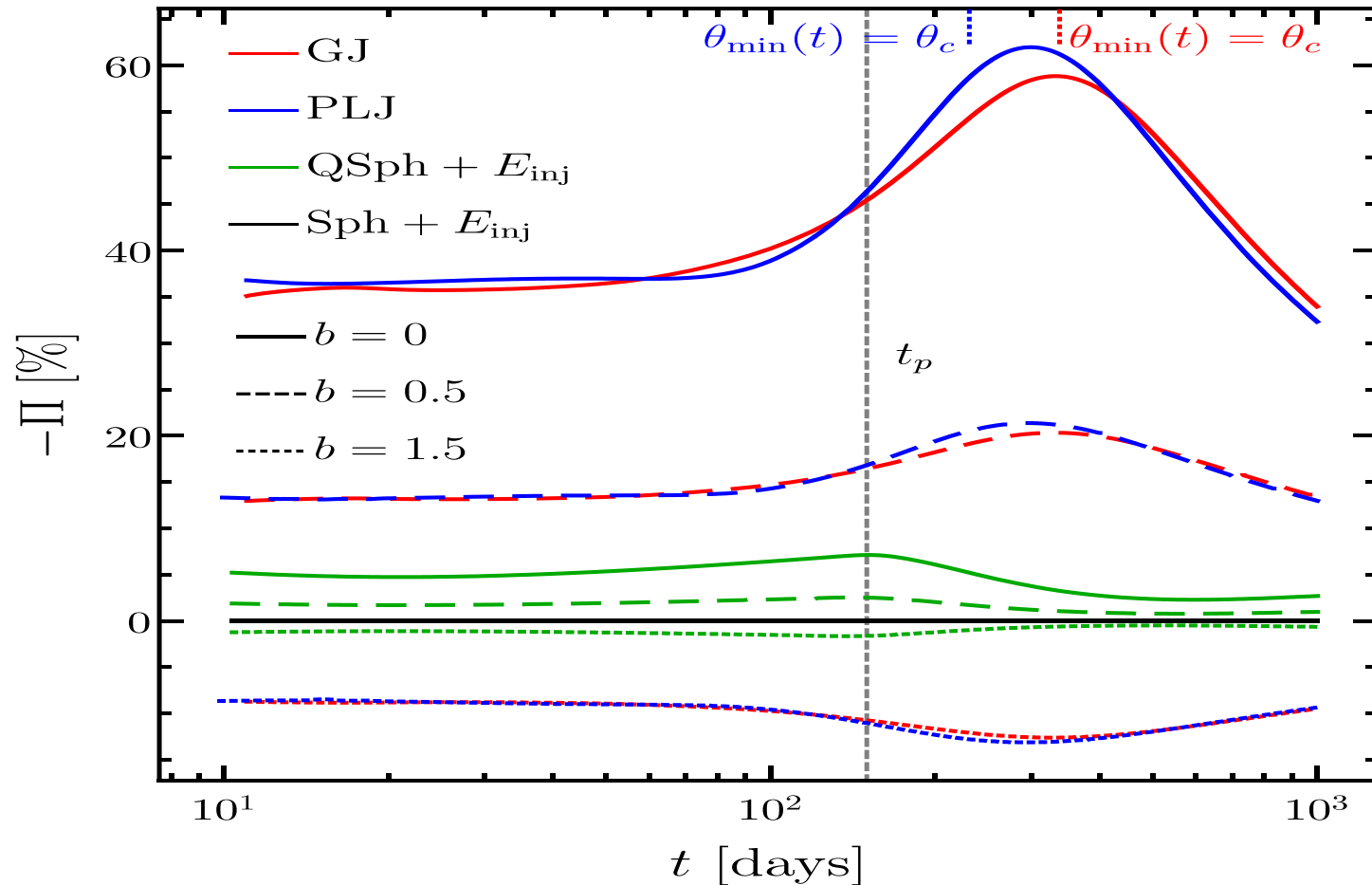
- **Prompt GRB:** hard X-ray – soft  $\gamma$ -ray  
⇒ hard to measure ⇒ no clear detections  
(stay tuned: POLAR-2, LEAP, COSI, eXTP)



- **Reverse Shock:** also probes original ejecta, but in optical to radio ⇒ detections
  - ❖ Probes B-field structure & turbulence in the ejecta near the deceleration epoch
  - ❖ Radio UL  $\Pi_{8.5\text{GHz}}(1 \text{ day}) < 7\%$  ⇒ rules out ordered B-field (coherent over  $\theta_B \gtrsim 1/\Gamma$ ) or toroidal B-field +  $dE/d\Omega \propto \theta^{-2}$  structured jet; allows  $\theta_B \lesssim 10^{-2}$  patches (JG & Taylor 2005)
  - ❖ RINGO2 GRB120308A:  $\Pi_{opt}(240 - 323 \text{ s}) = 28 \pm 4\%$  ⇒ ordered B-field (Mundell et al. 2013)
  - ❖ ALMA GRB190114C:  $\Pi_{97.5\text{GHz}}(2.2 \rightarrow 5.2 \text{ hr}) = 0.9 \rightarrow 0.6\%$  with  $\Delta\theta_p(2.2 \rightarrow 5.2 \text{ hr}) = 54^\circ$  (first GRB radio polarization) ⇒ favors patches with  $\theta_B \sim 10^{-3}$  (Laskar et al. 2019)
- **Afterglow:** optical & radio – probes jet angular structure & B-field structure in collisionless relativistic shocks

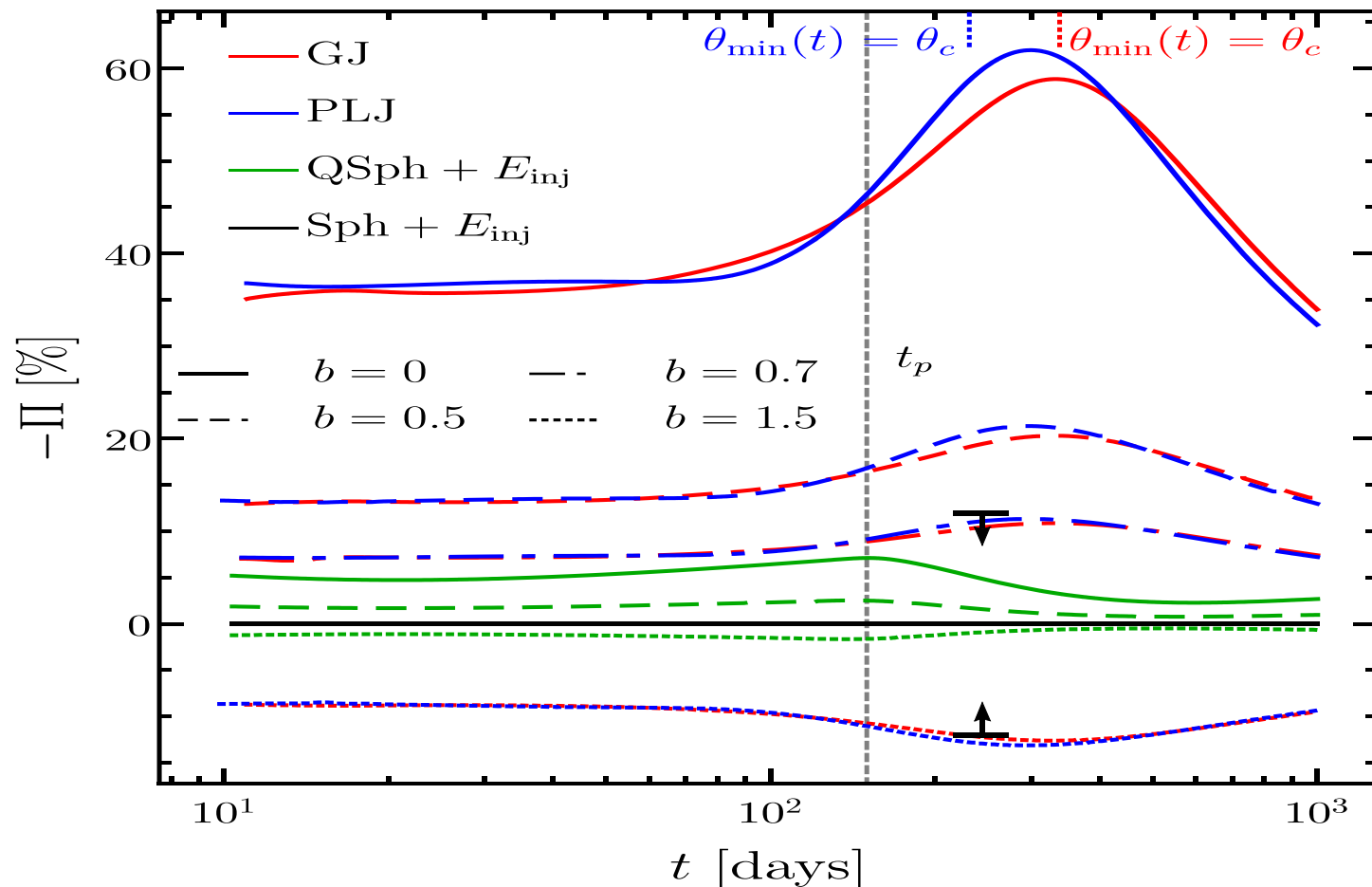
# GRB 170817A: polarization UL $\Rightarrow$ post-shock B-field

- Jet angular structure &  $\theta_{\text{obs}}$  well constrained  $\Rightarrow$  breaks degeneracies
- Assuming a shock-produced B-field with  $b \equiv 2\langle B_{\parallel}^2 \rangle / \langle B_{\perp}^2 \rangle$  (JG & König 03; Gill & JG 18)



# GRB 170817A: polarization UL $\Rightarrow$ post-shock B-field

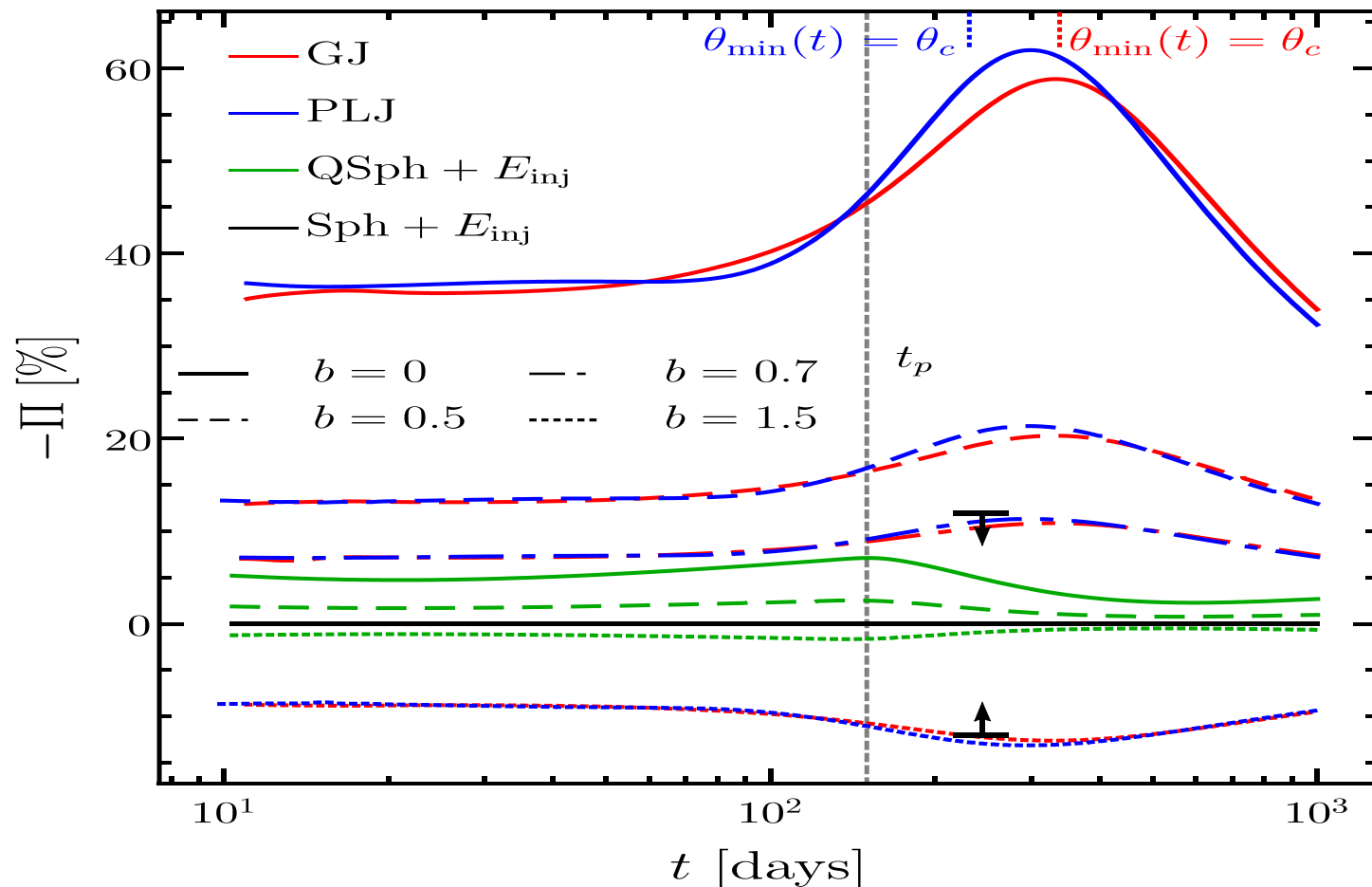
- Jet angular structure &  $\theta_{\text{obs}}$  well constrained  $\Rightarrow$  breaks degeneracies
- Assuming a shock-produced B-field with  $b \equiv 2\langle B_{\parallel}^2 \rangle / \langle B_{\perp}^2 \rangle$  (JG & König 03; Gill & JG 18)



Later: upper limit  
 $P_{\text{lin}} < 12\%$  @  
 $\nu = 2.8 \text{ GHz}$ ,  
 $t = 244 \text{ days}$   
(Corsi+ 2018)

# GRB 170817A: polarization UL $\Rightarrow$ post-shock B-field

- Jet angular structure &  $\theta_{\text{obs}}$  well constrained  $\Rightarrow$  breaks degeneracies
- Assuming a shock-produced B-field with  $b \equiv 2\langle B_{\parallel}^2 \rangle / \langle B_{\perp}^2 \rangle$  (JG & König 03; Gill & JG 18)



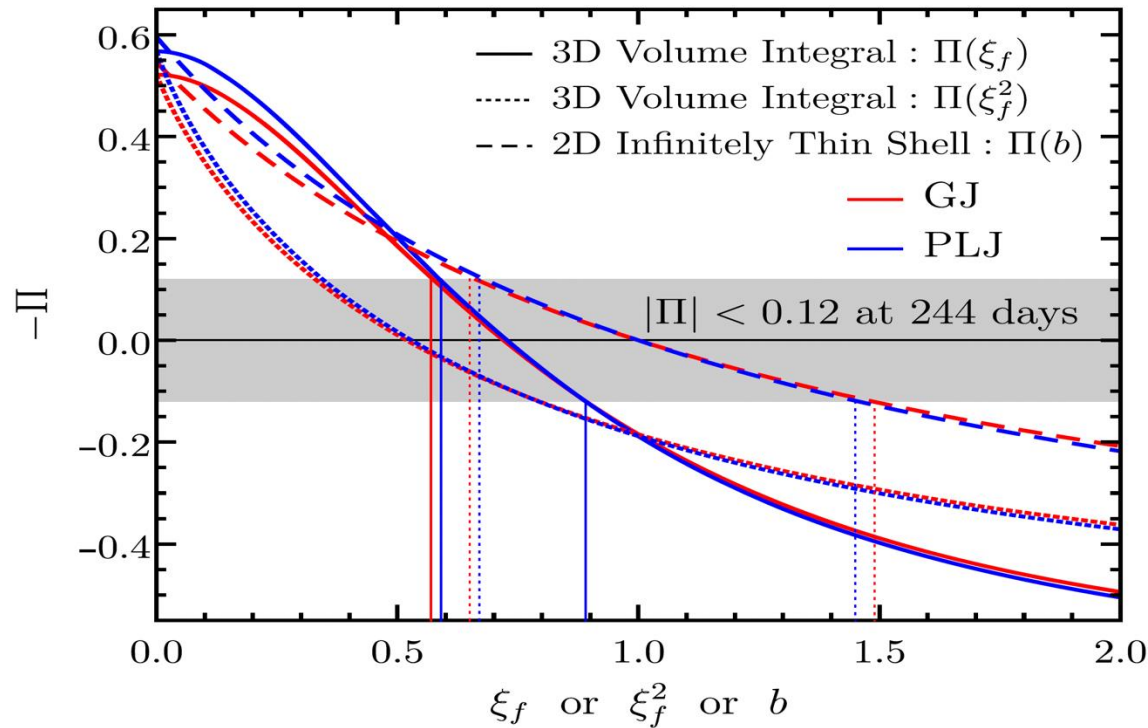
$0.7 \lesssim b \lesssim 1.5$   
for jet models

Later: upper limit  
 $P_{\text{lin}} < 12\%$  @  
 $\nu = 2.8 \text{ GHz}$ ,  
 $t = 244 \text{ days}$   
 (Corsi+ 2018)

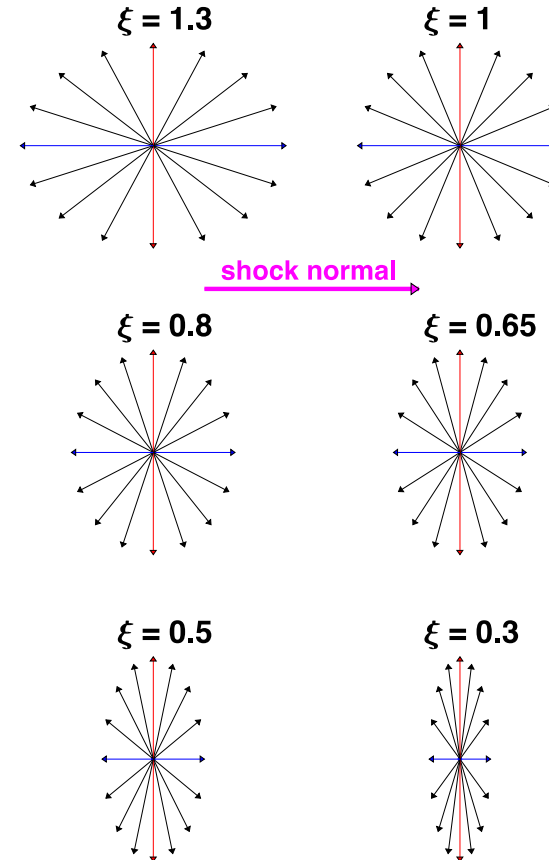
# GRB 170817A: polarization UL $\Rightarrow$ post-shock B-field

More realistic assumptions  $\Rightarrow$  B-field in collisionless shocks: (Gill & JG 2020)

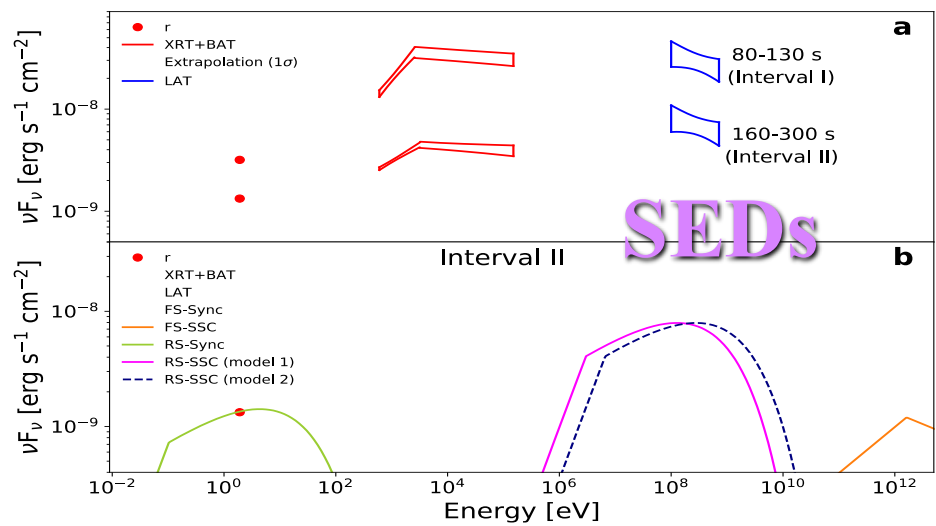
- 2D emitting shell  $\rightarrow$  3D emitting volume (local BM76 radial profile)
- B-field evolution by faster radial expansion:  $L'_r / L'_{\theta,\phi} \propto \chi^{(7-2k)/(8-2k)}$
- B-field isotropic in 3D with  $B'_r \rightarrow \xi B'_r$  (Sari 1999);  $\xi = \xi_f \chi^{(7-2k)/(8-2k)}$



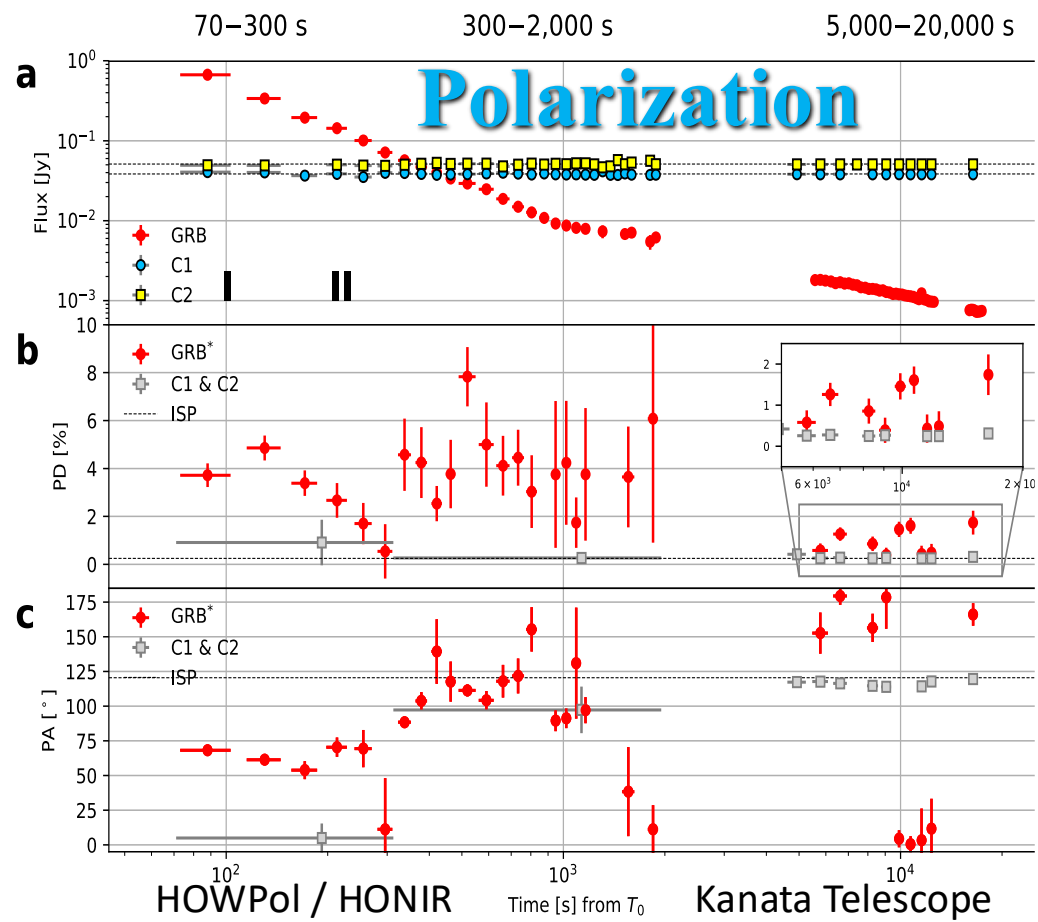
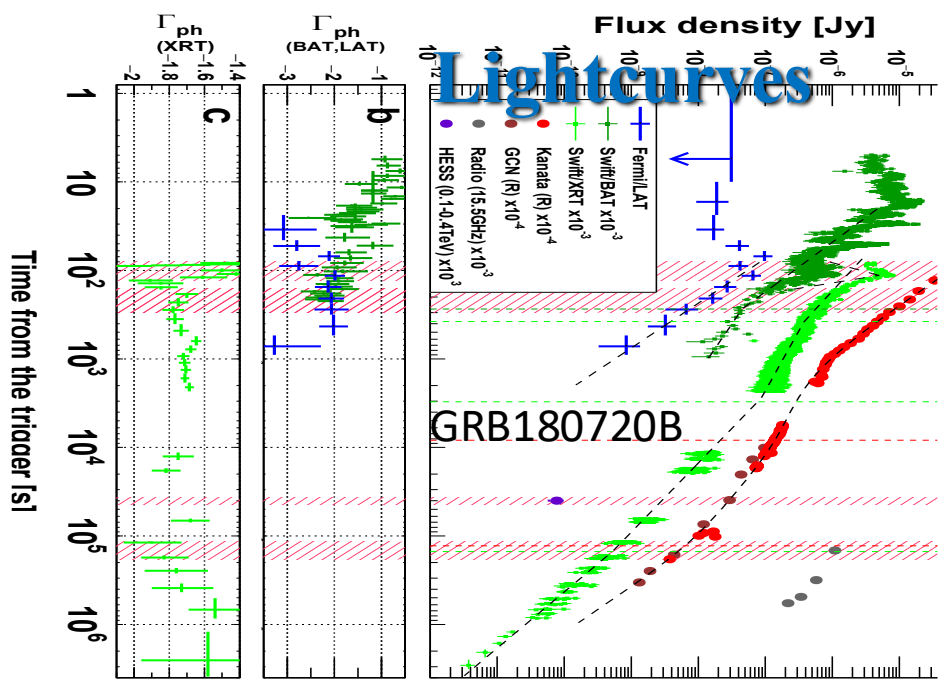
$$0.57 \lesssim \xi_f \lesssim 0.89$$



# Reverse + Forward Shock Polarization: (Arimoto et al. 2023)



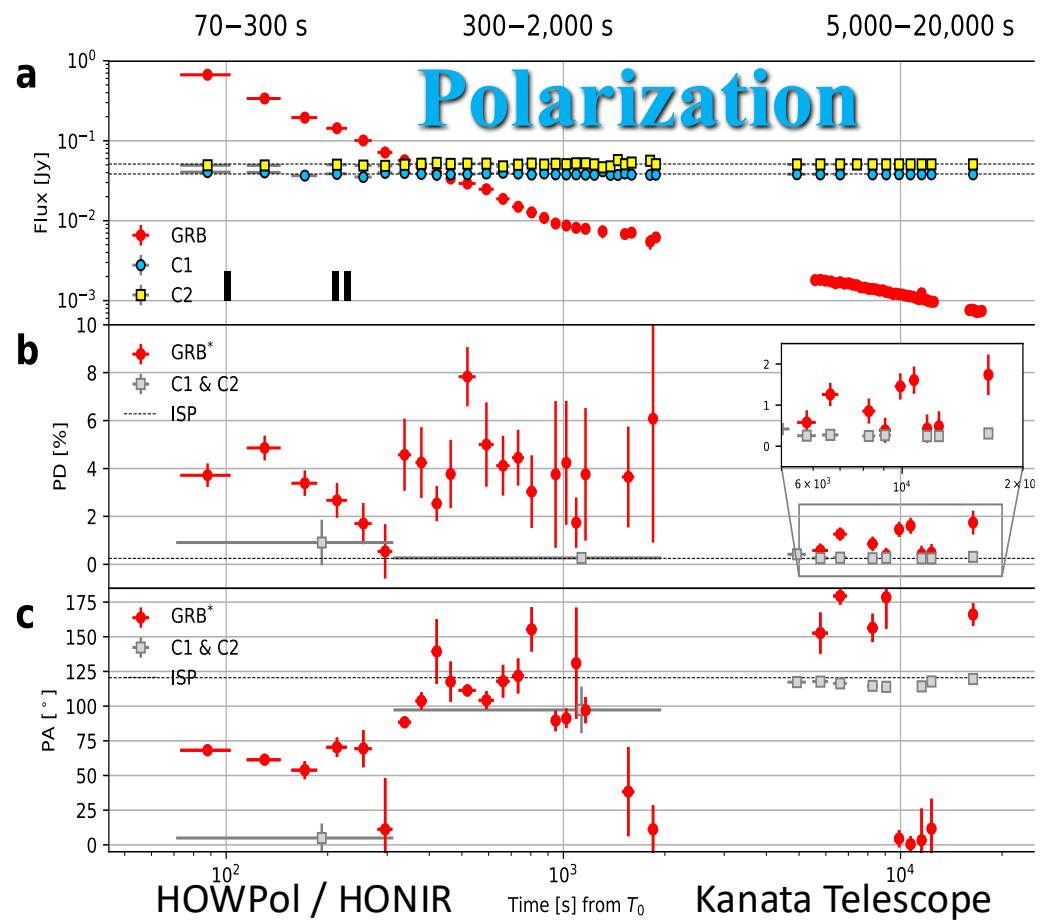
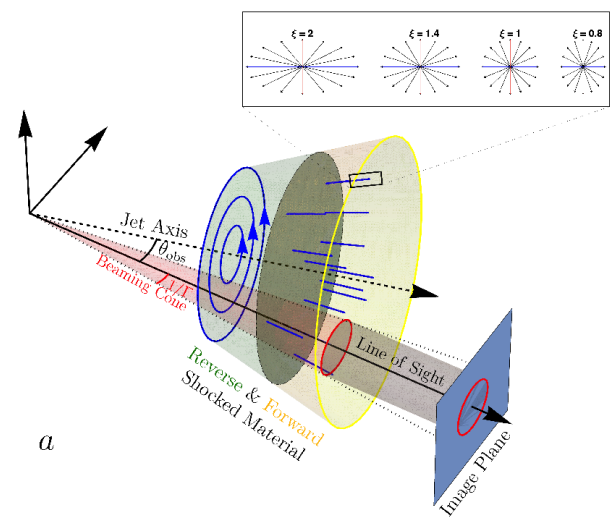
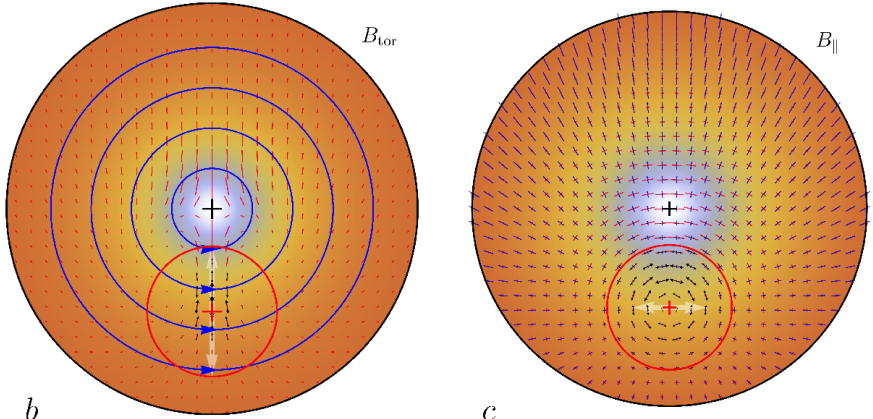
- **< 300 s: RS; P: 5  $\rightarrow$  1%,  $\theta_p \approx 70^\circ$**
- **0.3-2 ks: P  $\sim$  2-8%,  $\theta_p$  varies**
- **5-20 ks: FS; P  $\sim$  0.5-2%,  $\theta_p \approx 160^\circ$**
- **RS  $\rightarrow$  FS dominance @  $\sim 10^3$  s**



# Reverse + Forward Shock Polarization: (Arimoto et al. 2023)

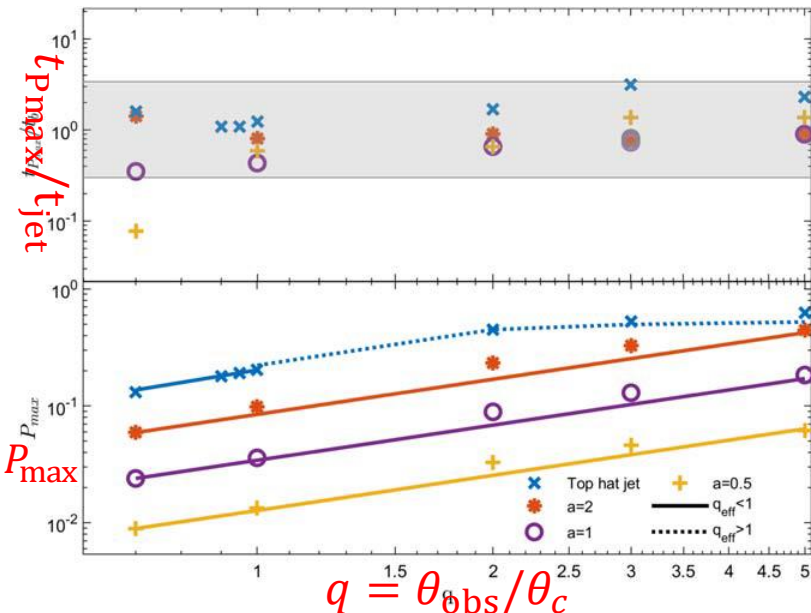
- < 300 s: ejecta;  $B_{\text{tor}}$  + turbulence
- 0.3-2 ks: turbulence-induced P
- 5-20 ks: CSM; radial stretching

- < 300 s: RS; P: 5  $\rightarrow$  1%,  $\theta_p \approx 70^\circ$
- 0.3-2 ks: P  $\sim$  2-8%,  $\theta_p$  varies
- 5-20 ks: FS; P  $\sim$  0.5-2%,  $\theta_p \approx 160^\circ$
- RS  $\rightarrow$  FS dominance @  $\sim 10^3$  s

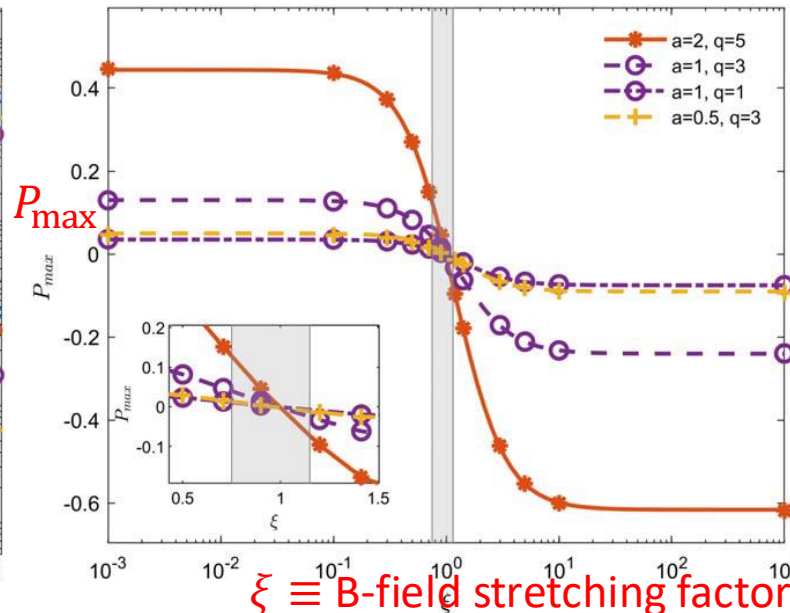


# Afterglow Polarization from Shallow Jets (Birenbaum et al. 2024)

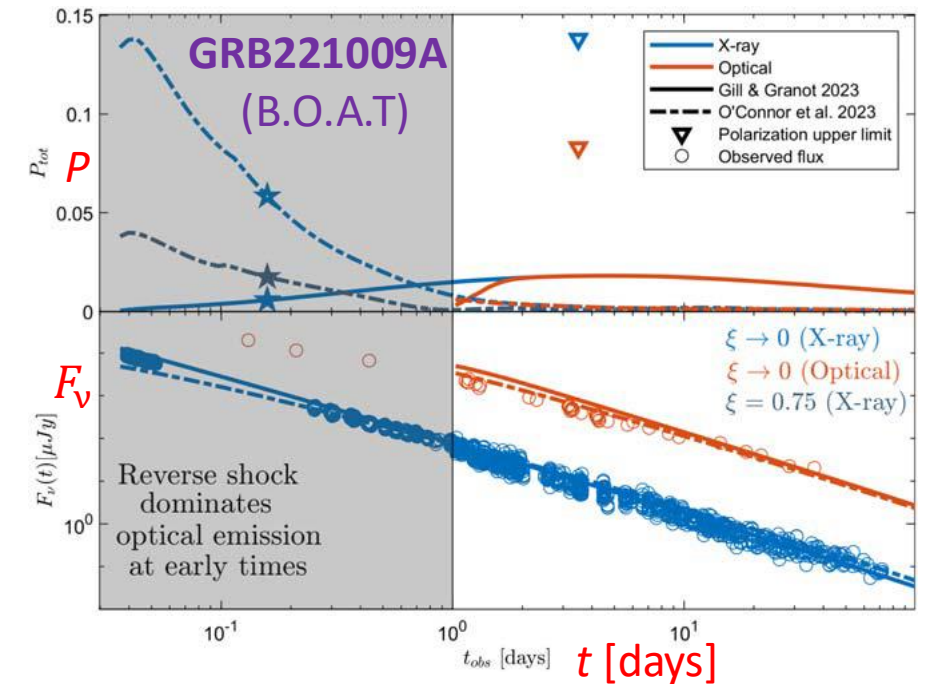
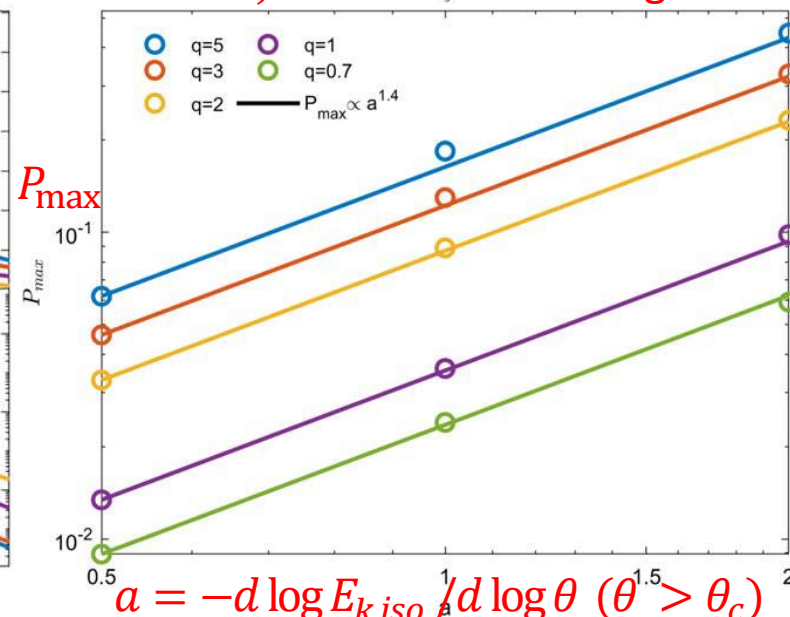
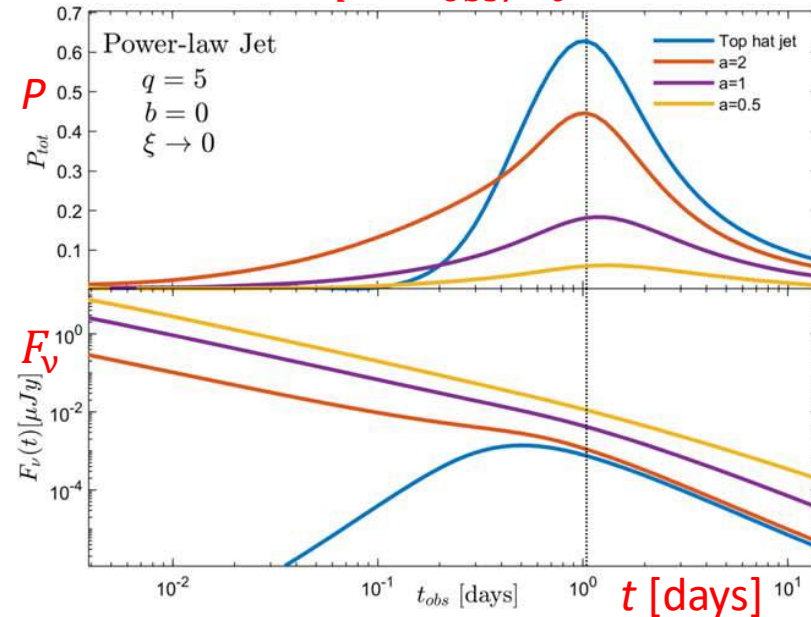
$P$  peaks near the jet break time



$$P_{\max} \approx qa^{1.4} [0.055 \tanh(0.34 - 2.3 \log_{10} \xi) - 0.02]$$

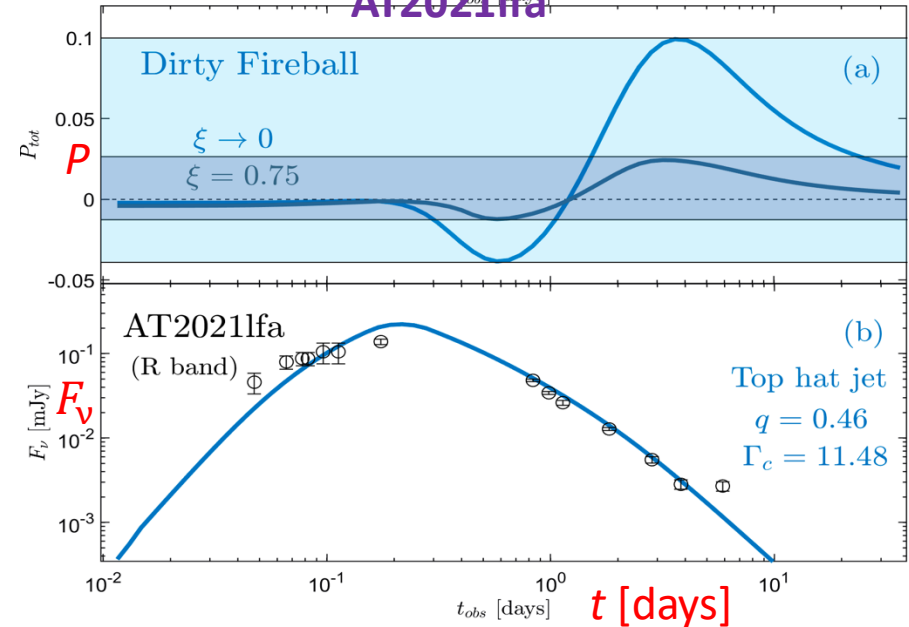
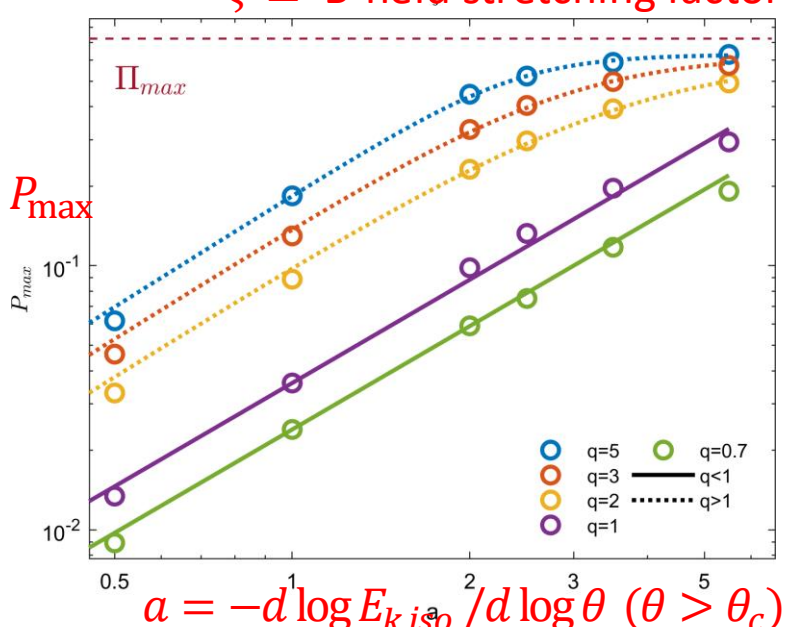
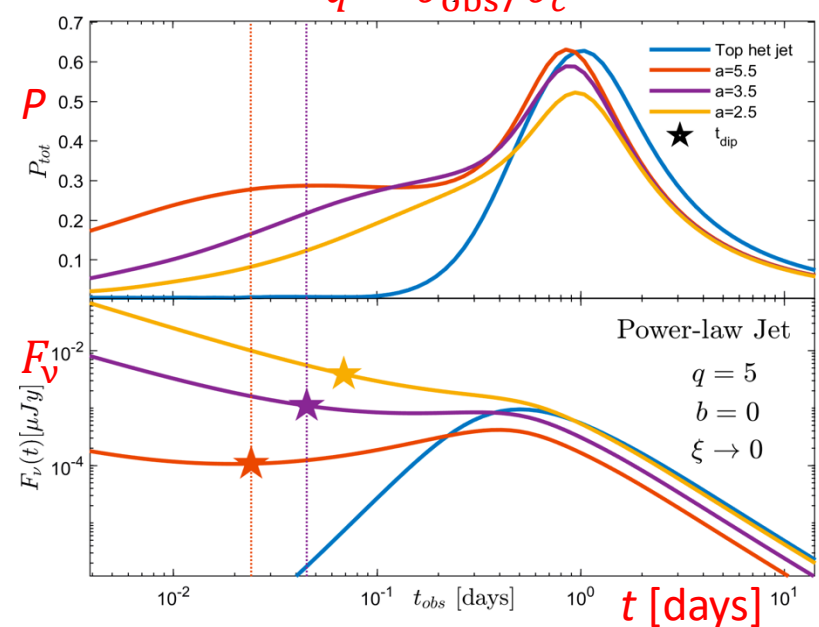
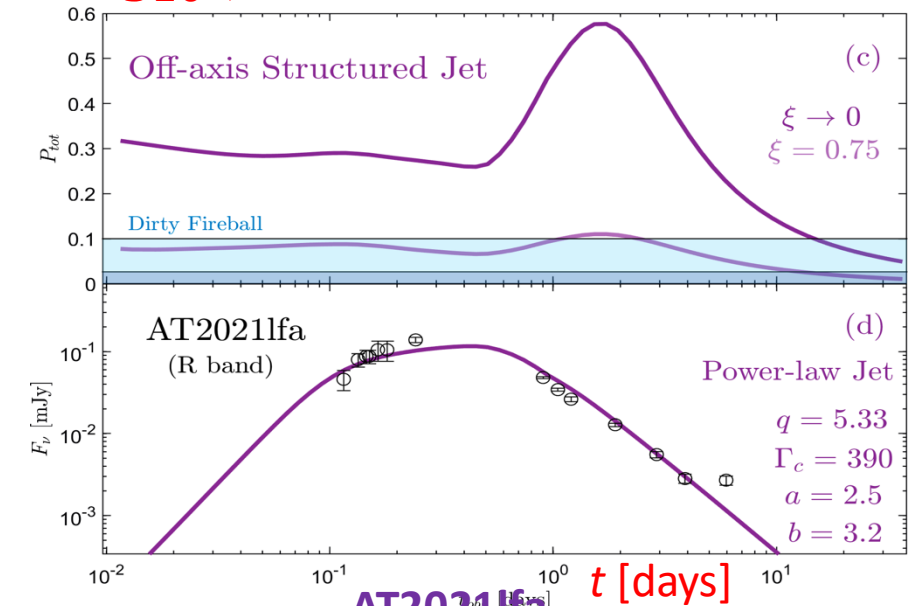
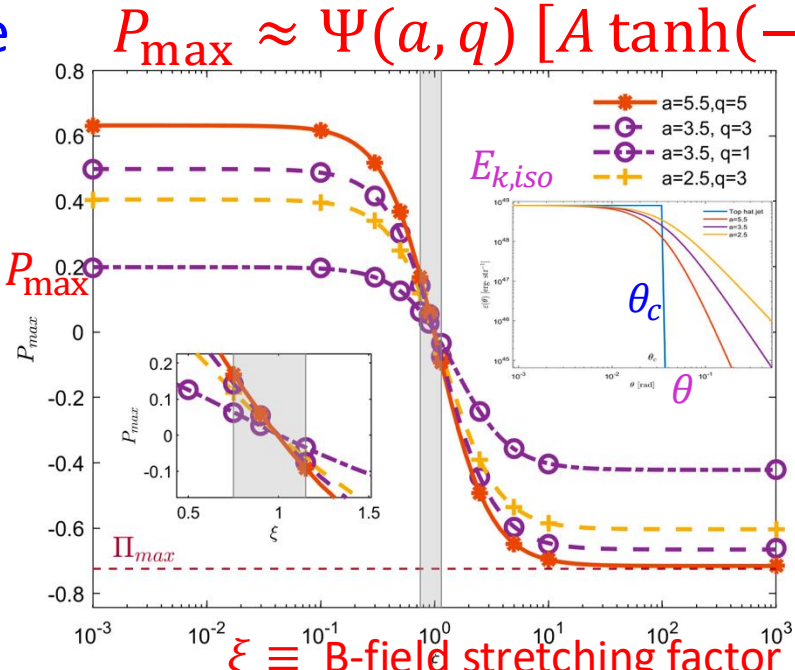
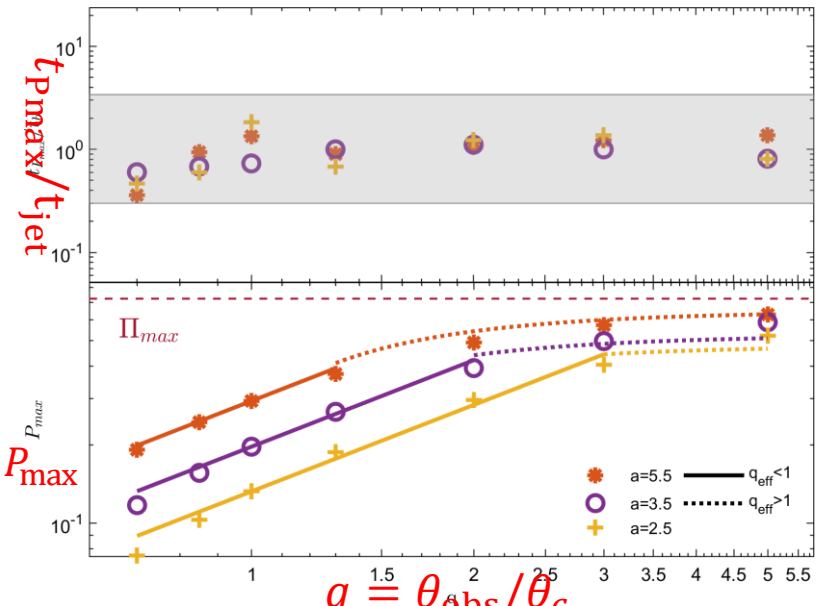


- Particularly energetic GRBs seem to have **shallow Jets**
- Earlier polarimetry of the B.O.A.T could have helped constrain its jet structure & post-shock B-field structure



# Afterglow Polarization from Steep Jets ( $a \geq 2$ ; Birenbaum et al. 2026)

$P$  peaks near the jet break time



# ULGRB250702B: Prompt Emission

$T_{GRB} \approx 25$  ks (longest ever)

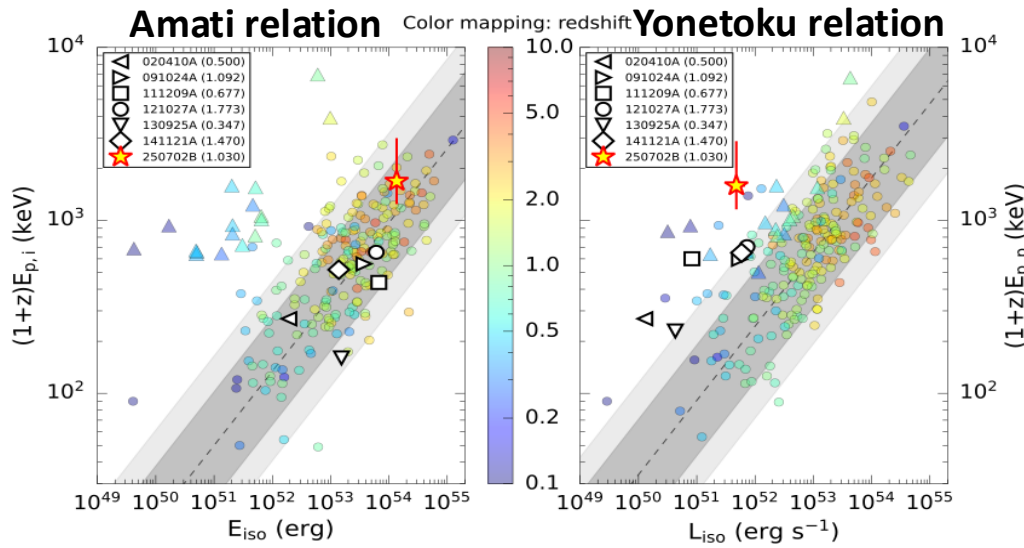
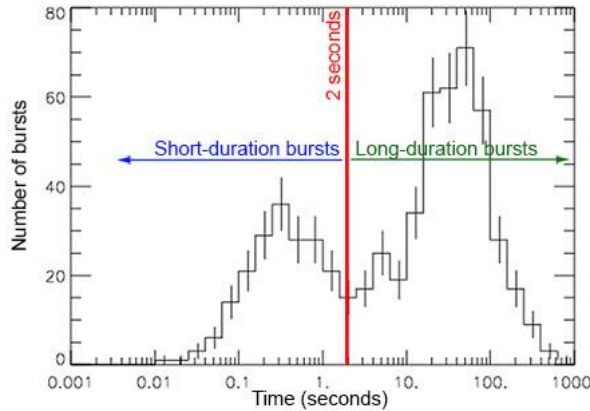
$E_{\gamma,iso} \geq 1.4 \times 10^{54}$  erg;

$L_{\gamma,iso} \approx 5 \times 10^{51}$  erg/s

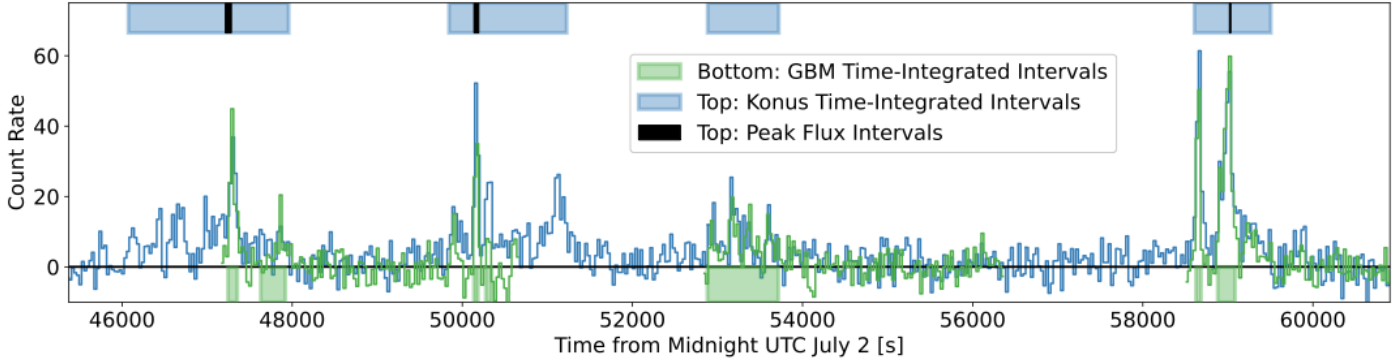
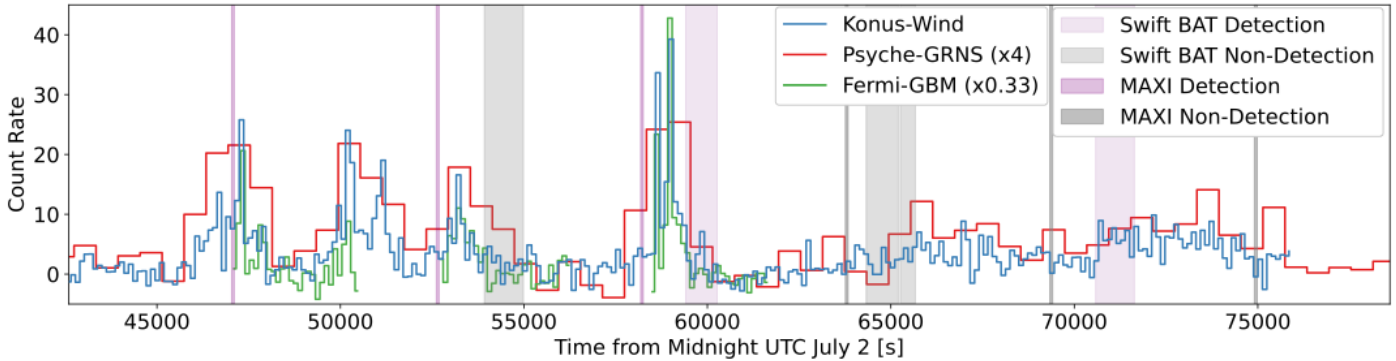
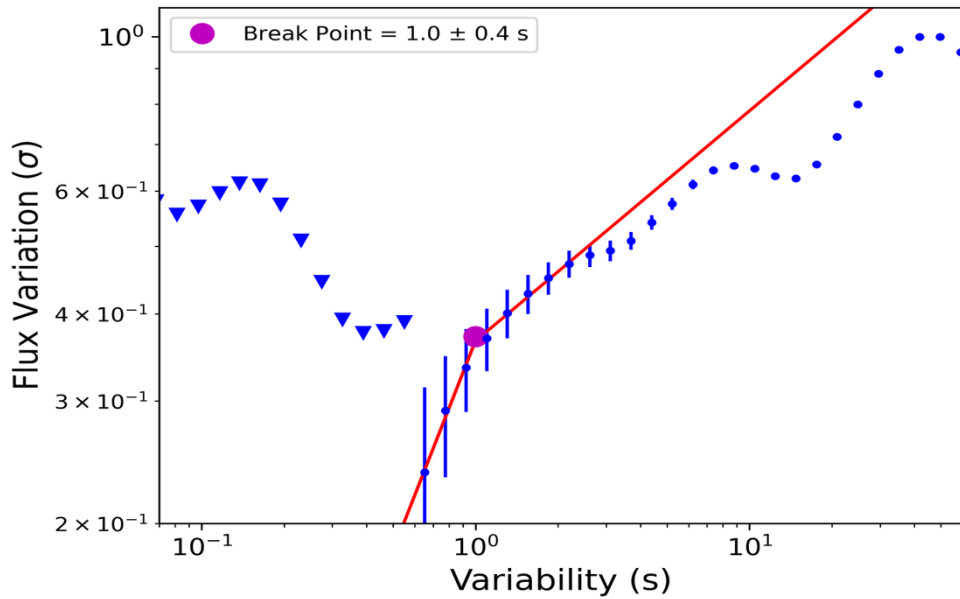
$E_{p,z} \sim 1.5 - 6$  MeV

$t_{MV} \approx 1$  s,  $E_{max} \approx 5$  MeV  $\Rightarrow \Gamma > 56$

$E_{cut} \approx 4$  MeV  $\Rightarrow \Gamma \approx 81$



(Neights et al. 2025)



# Ultra-Long GRBs:

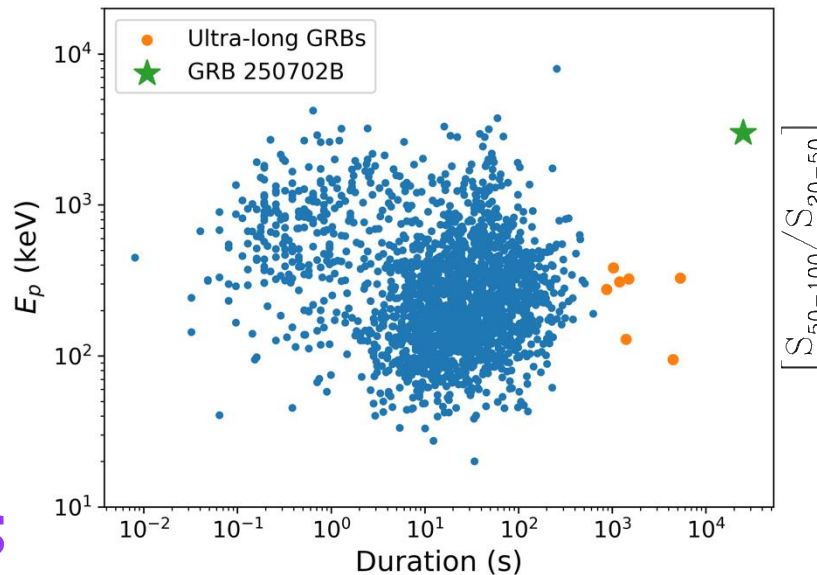
$$T_{\text{GRB}} \approx 25 \text{ ks}$$

$$E_{\gamma, \text{iso}} \geq 1.4 \times 10^{54} \text{ erg}$$

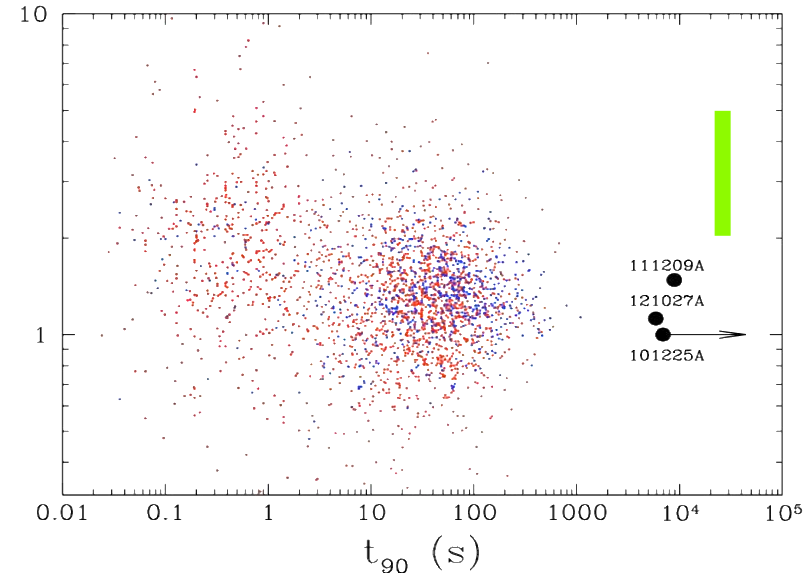
$$L_{\gamma, \text{iso}} \approx 5 \times 10^{51} \text{ erg/s}$$

$$\bar{L}_{\gamma, \text{iso}} \geq 1.1 \times 10^{50} \text{ erg/s}$$

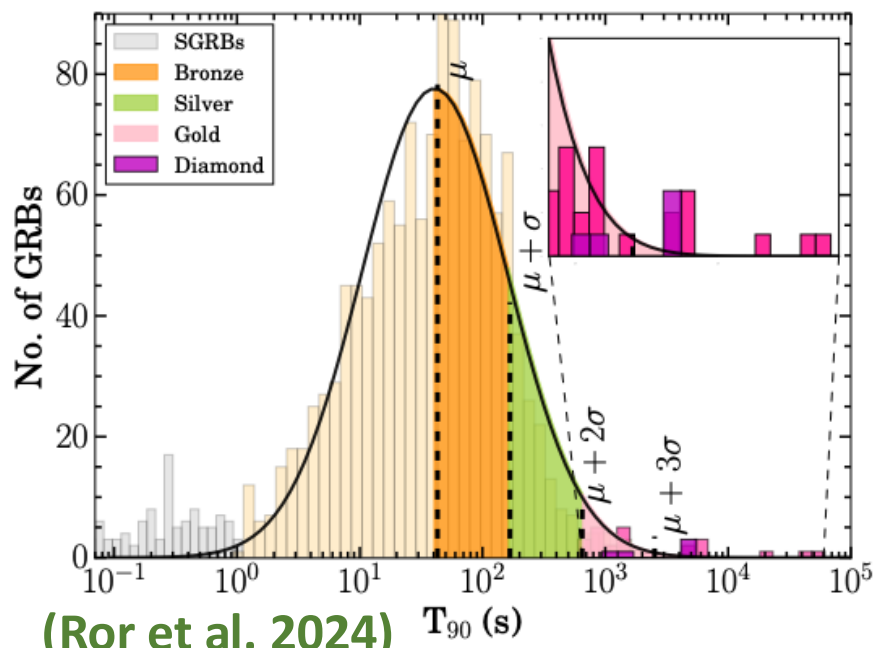
$$E_{p,z} \sim 1.5 - 6 \text{ MeV}$$



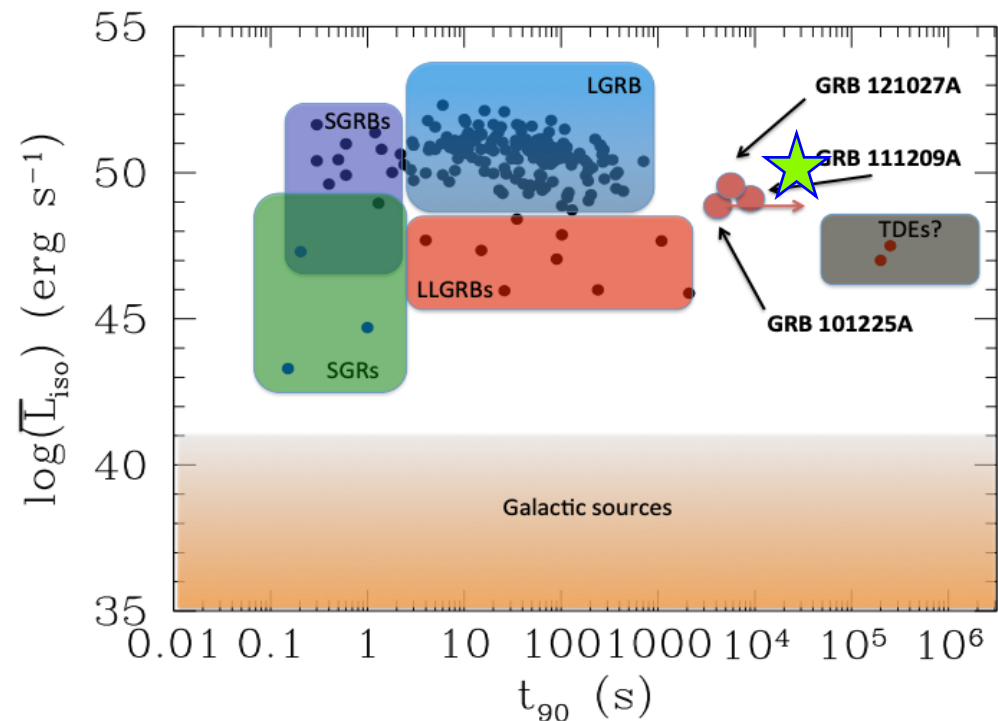
(Neights et al. 2025)



(Levan et al. 2014)



(Ror et al. 2024)



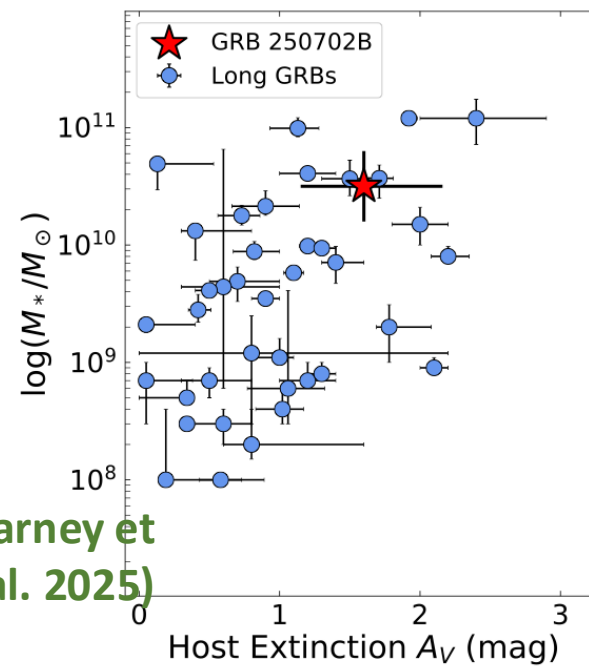
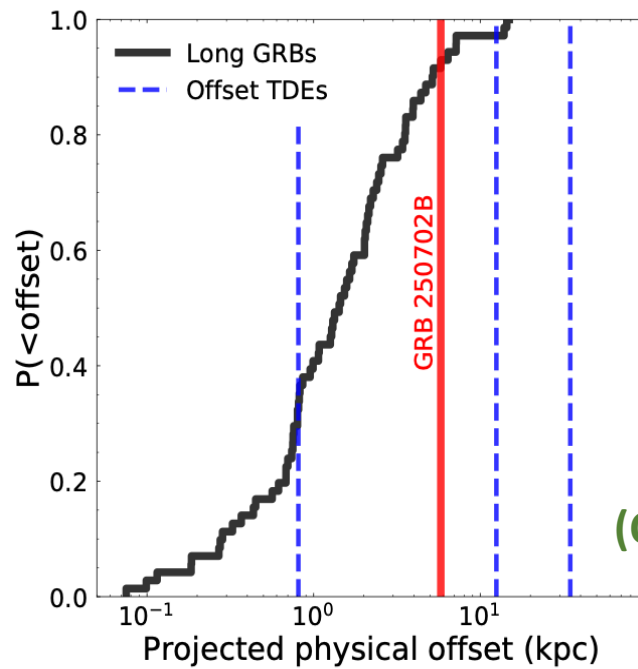
# ULGRB250702B

Redshift &

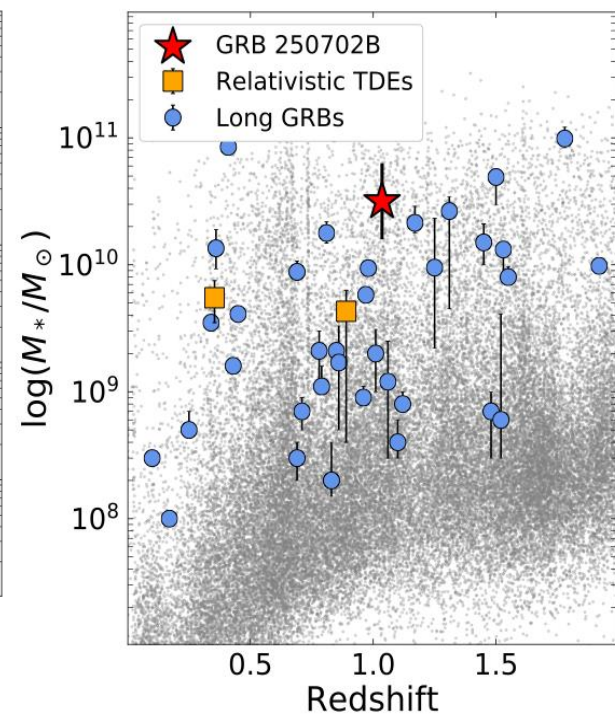
Host galaxy:

JWST:  $z = 1.036$

Massive spiral galaxy (with dust lane?) or merger

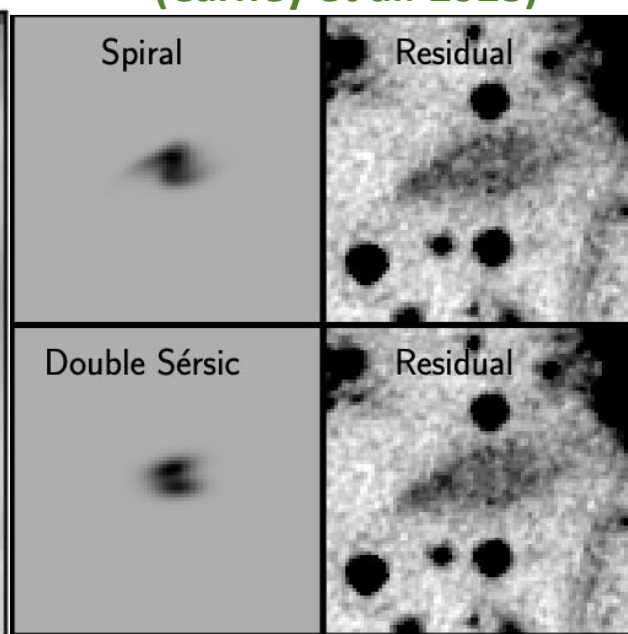
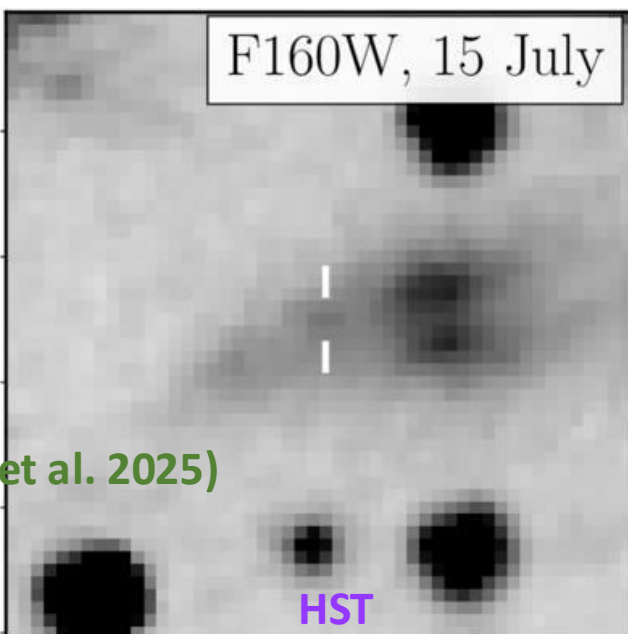
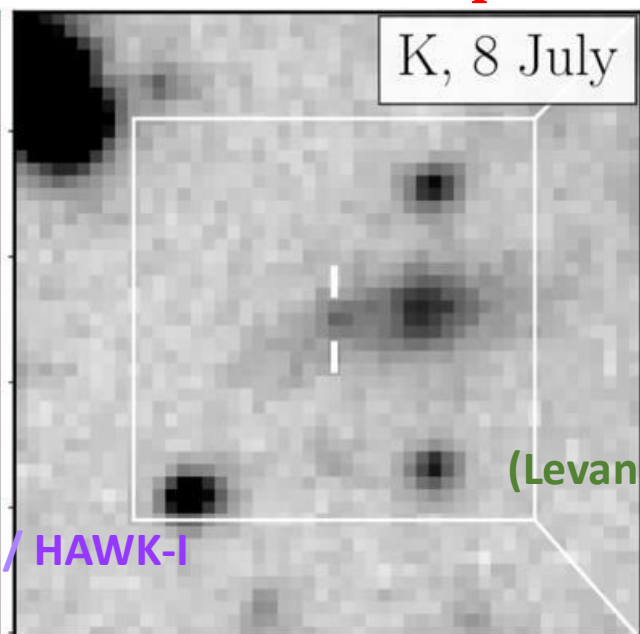
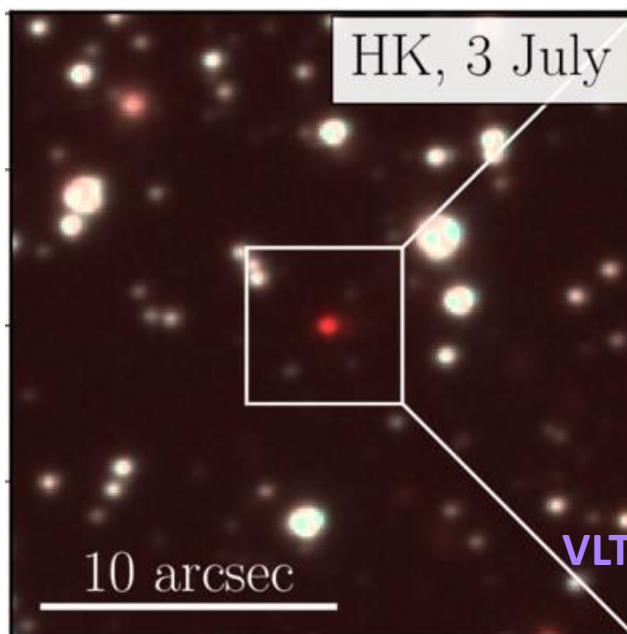


(Carney et al. 2025)



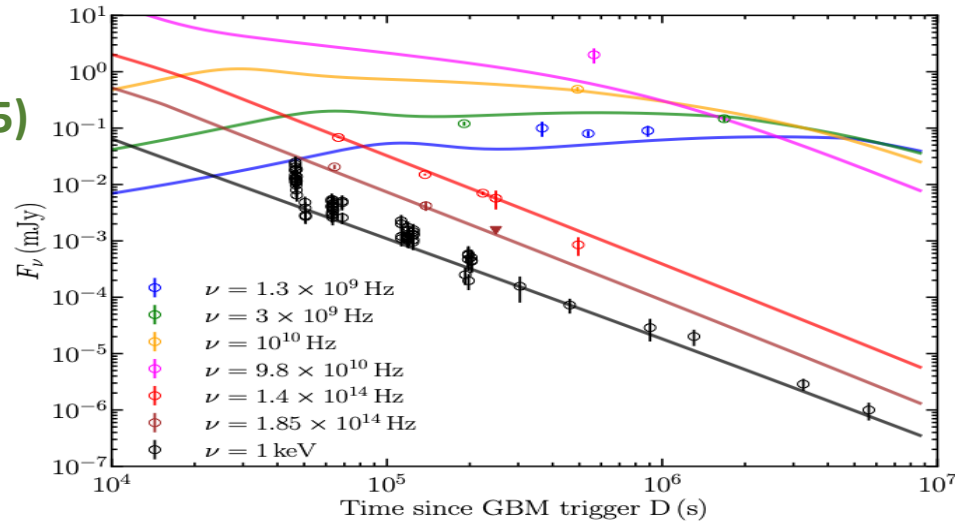
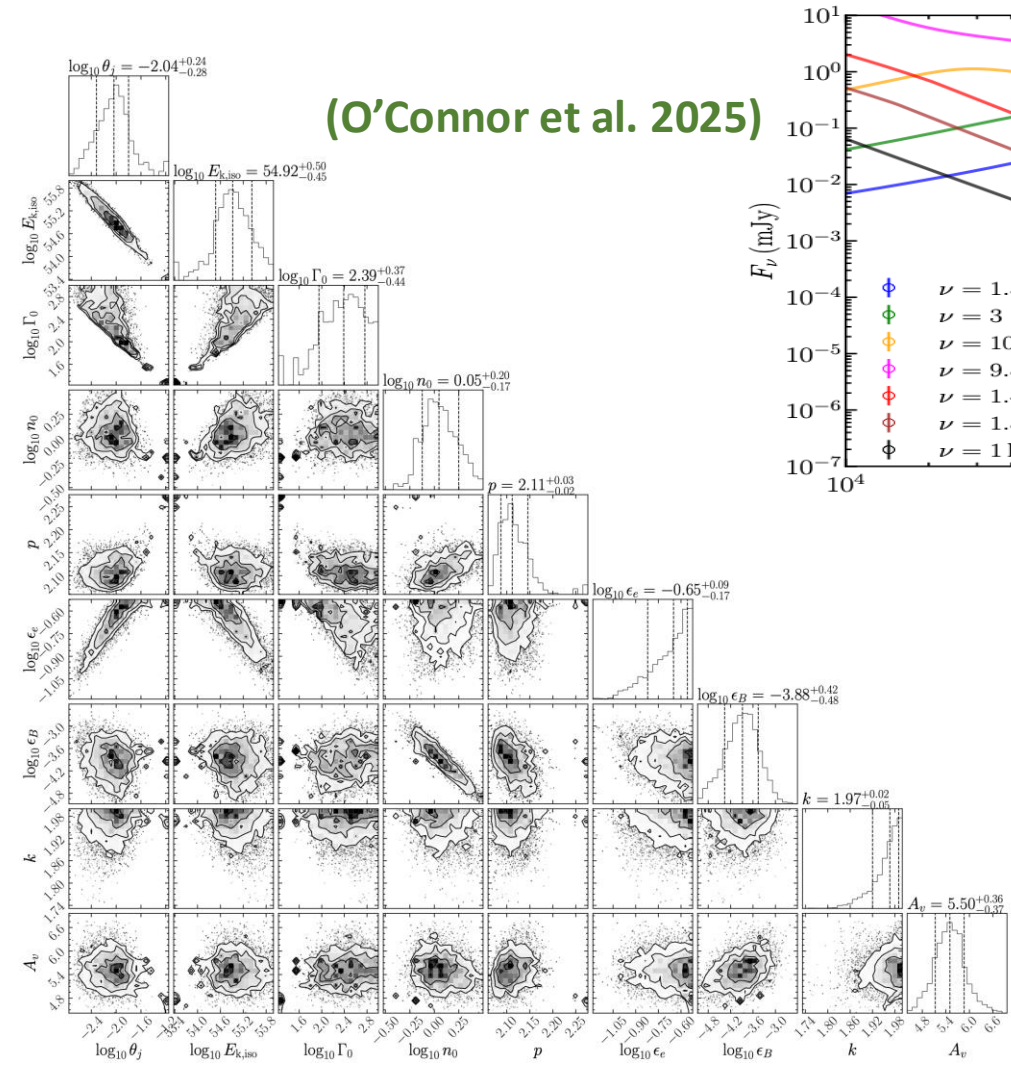
(Carney et al. 2025)

offset = 5.7 kpc

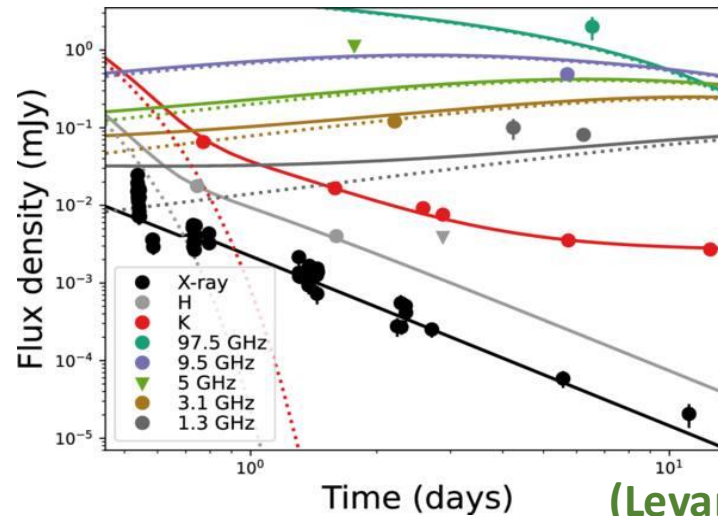


# ULGRB250702B Afterglow: X-ray, IR, radio

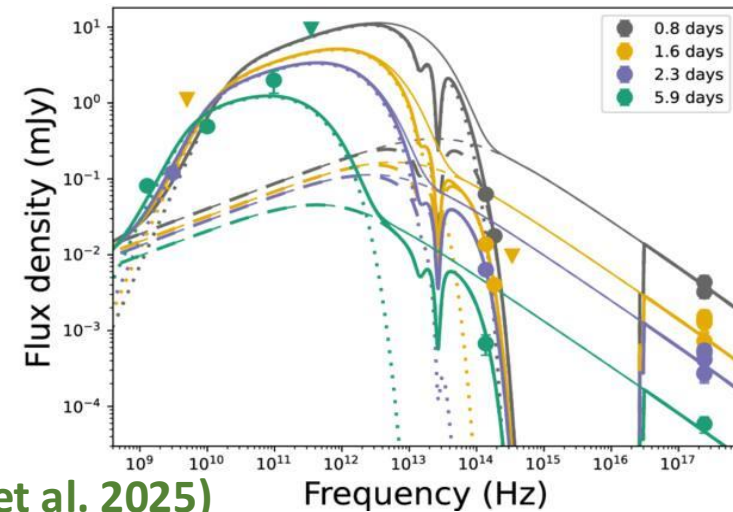
- **Extinction:**  $A_V = 0.847$  mag (MW) + 2 – 9 mag (host);  $N_H \approx (3 - 5) \times 10^{22} \text{ cm}^{-2}$



- **Stratified external medium**
- $E_{k,iso} \sim \text{few} \times E_{\gamma,iso}$
- **Narrow jet:**  $\theta_{jet} \sim 10^{-2}$  rad
- **Still many degeneracies; more data expected**



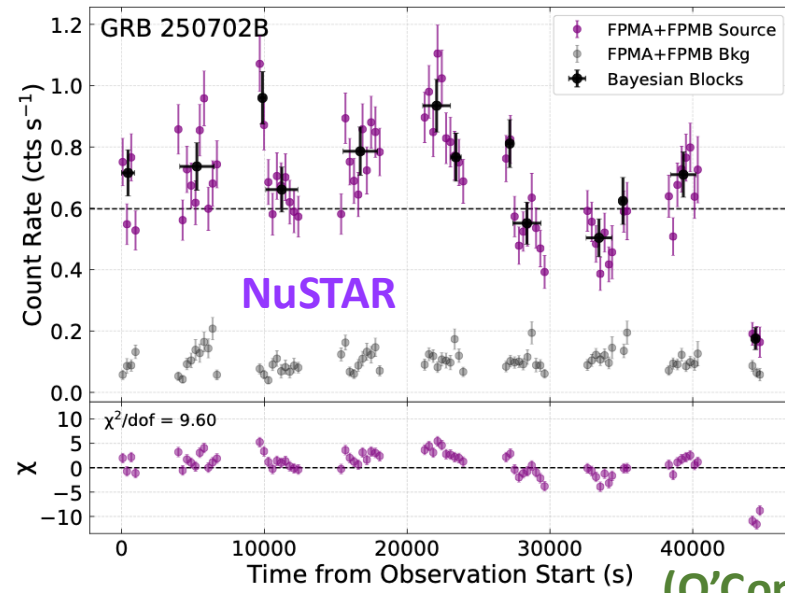
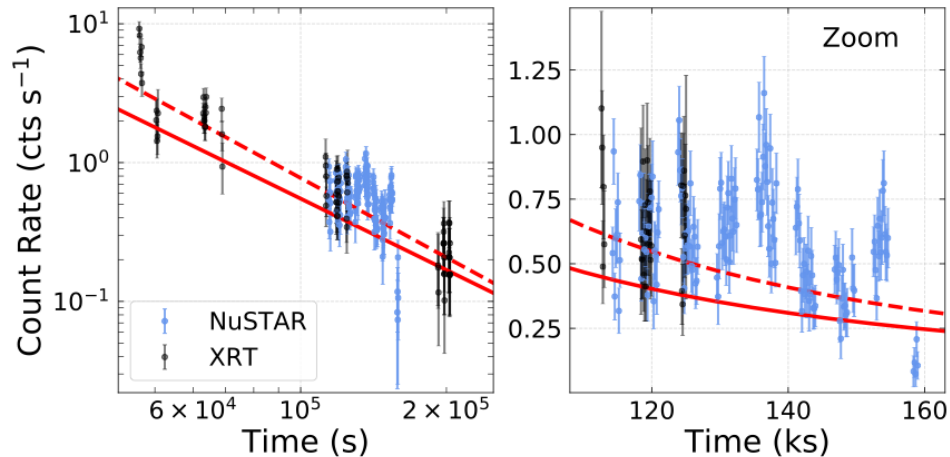
(Levan et al. 2025)



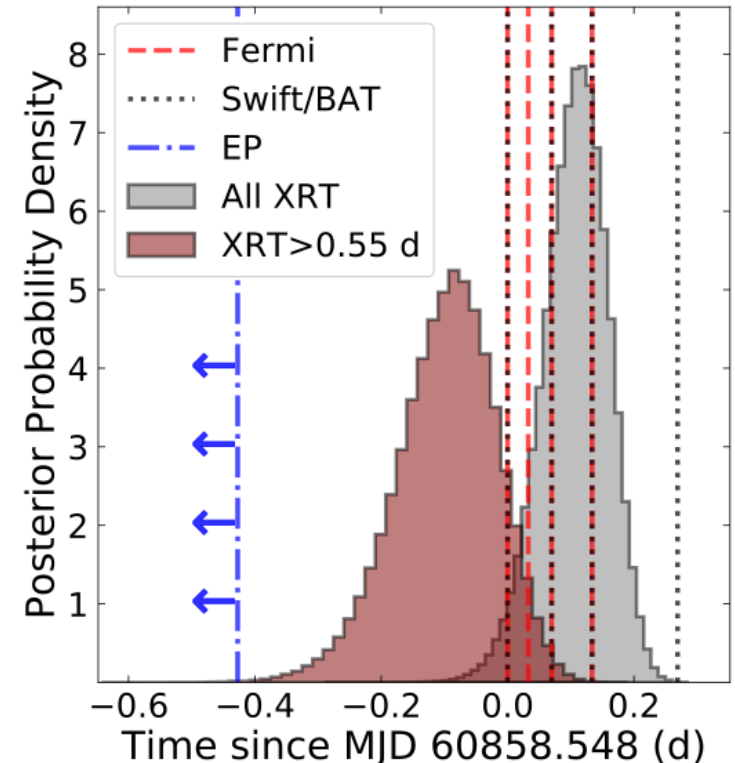
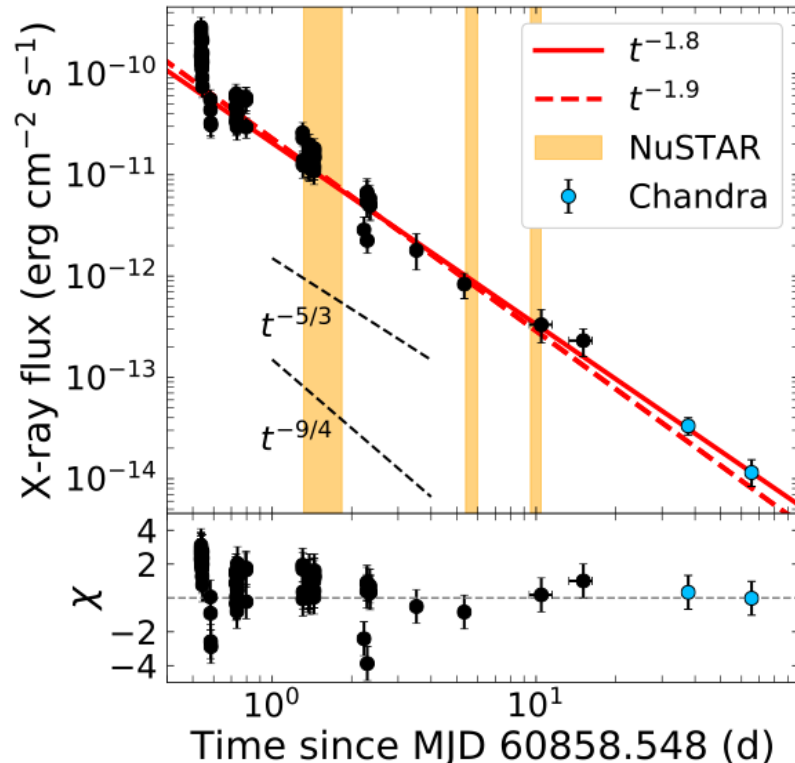
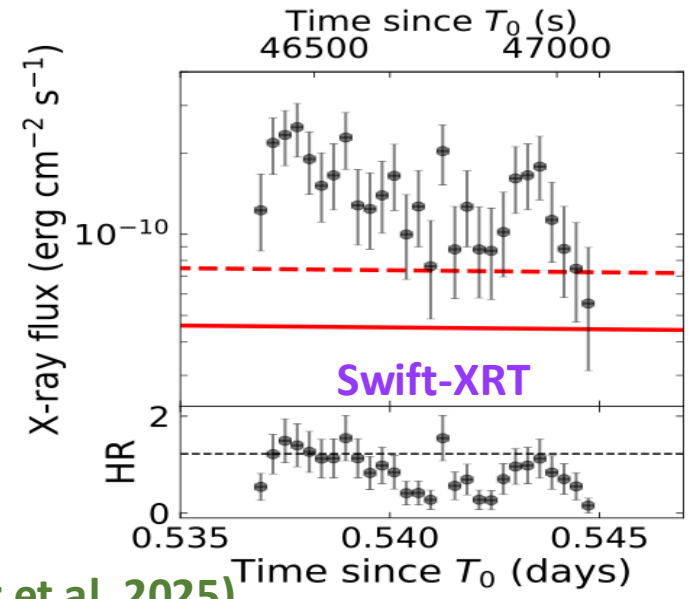
# ULGRB250702B

## X-ray Afterglow:

- Very rapid variability in first few days:  $\Delta t/t \sim 10^{-2.5}$   
 $\Rightarrow$  rules out afterglow origin
- Likely late time residual source activity (accretion powered jet)
- Decay slope broadly consistent with TDE expectations

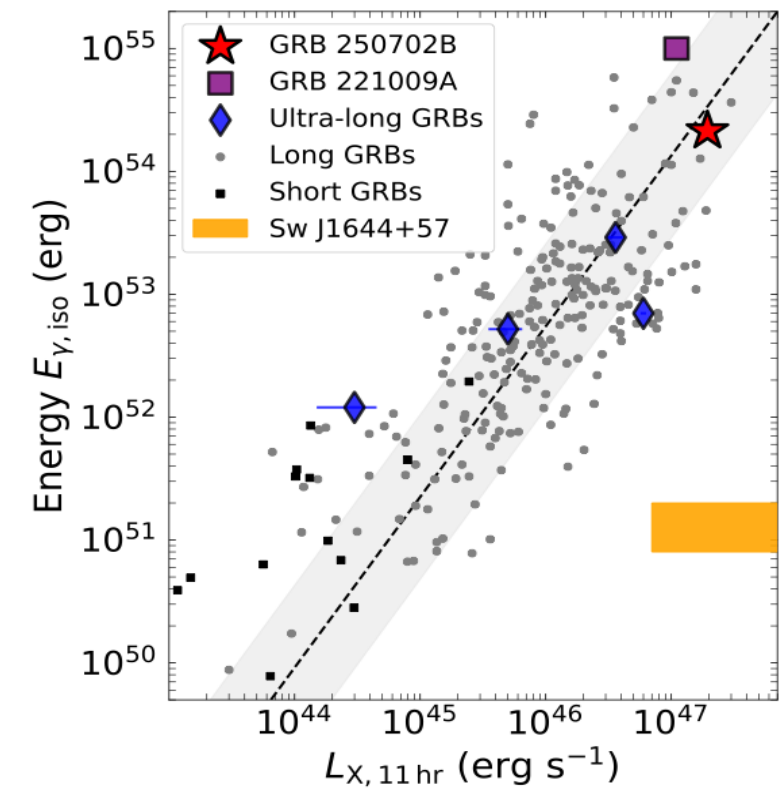
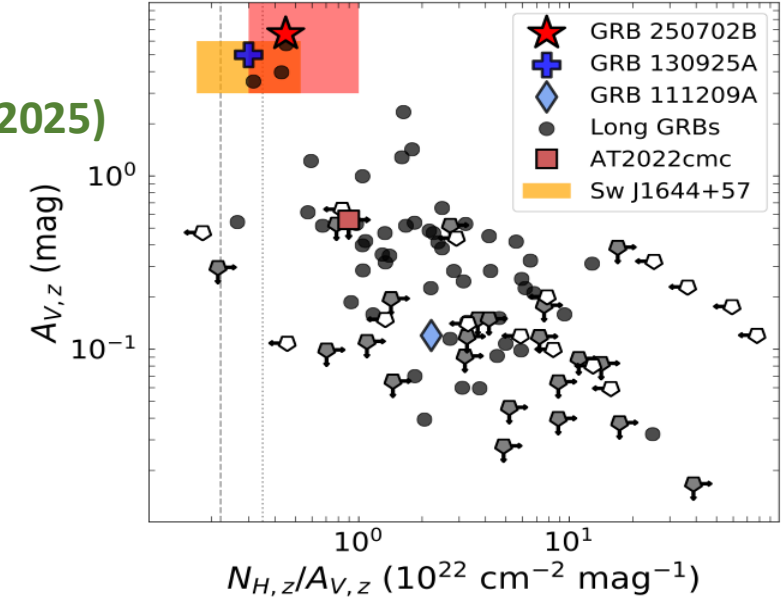
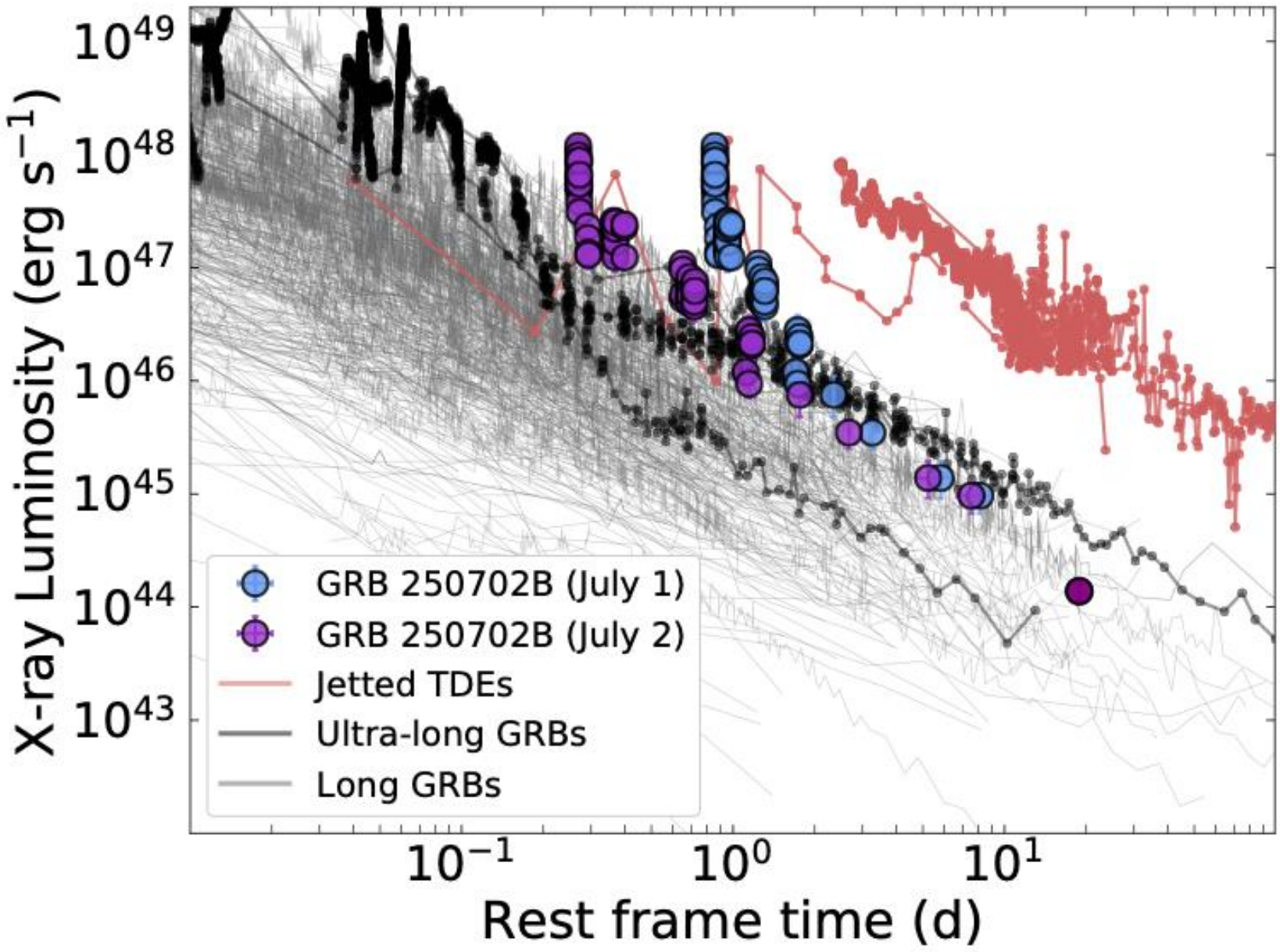


(O'Connor et al. 2025)



# ULGRB250702B: GRB or TDE?

(O'Connor et al. 2025)



# ULGRB250702B: Einstein Probe: X-ray starts 1 day earlier

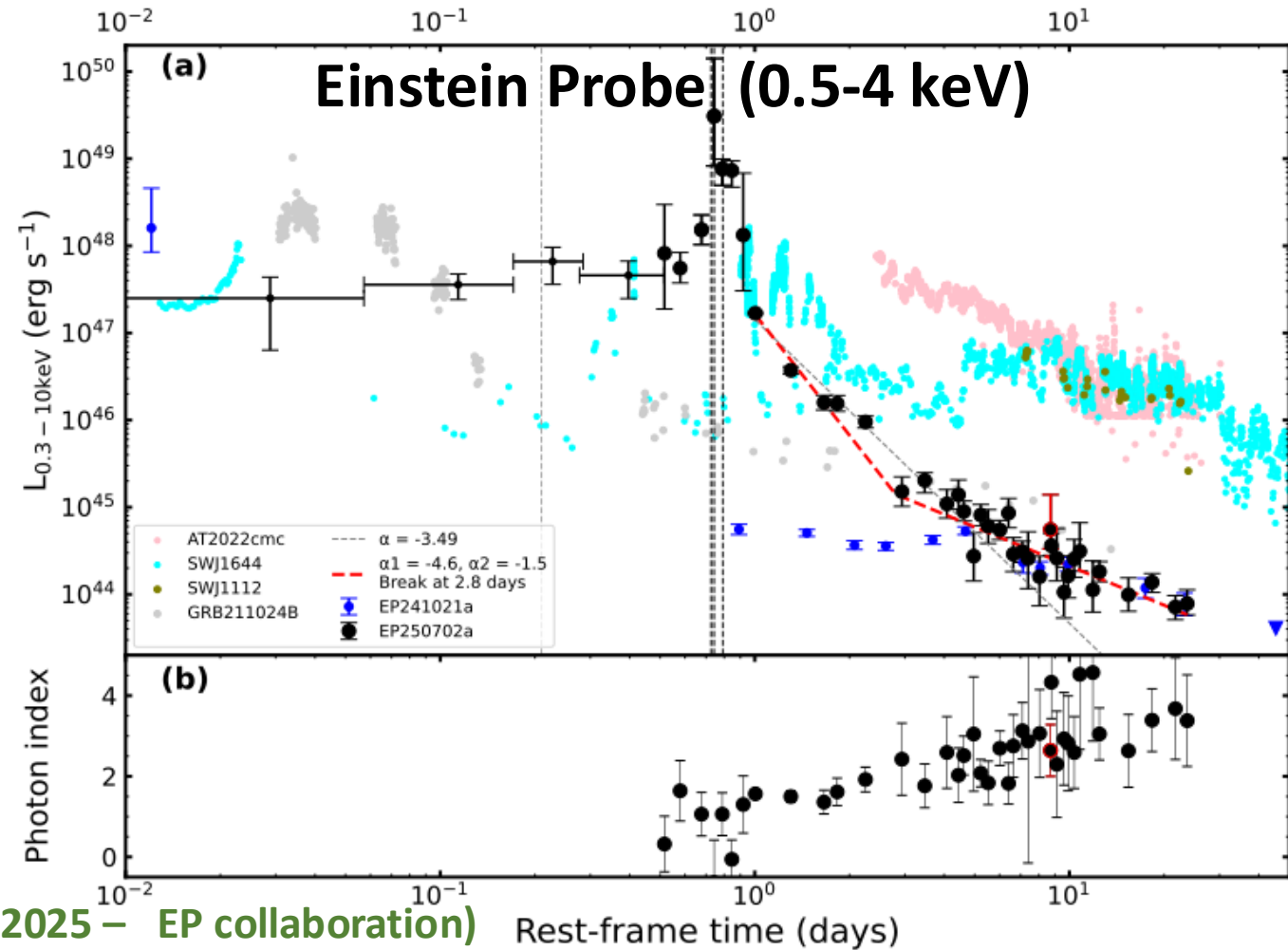
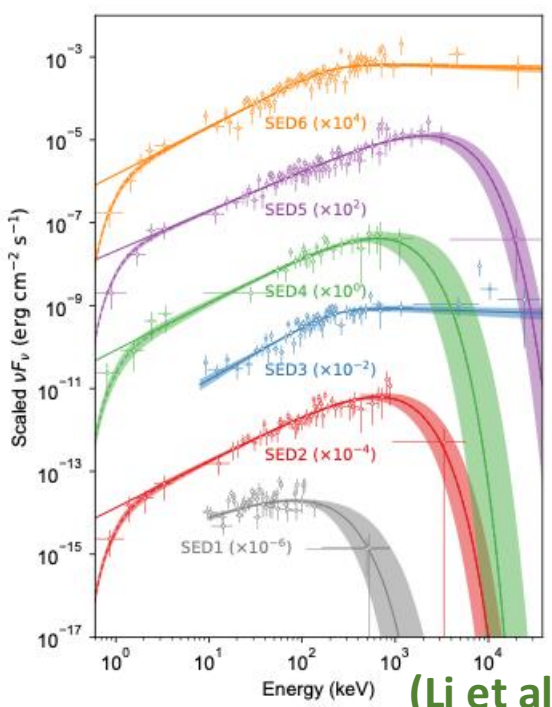
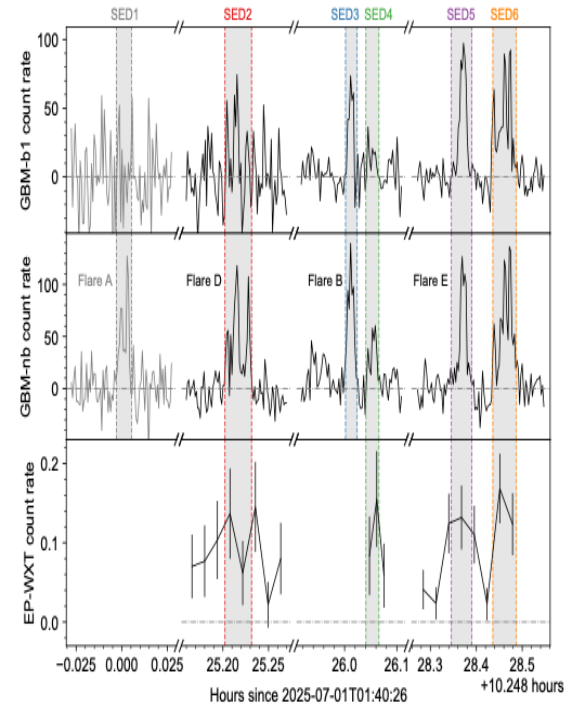
$E_{X,iso}$  (pre-peak)  $\sim 10^{52.5}$  erg

$E_{X,iso}$  (peak)  $\sim 10^{53}$  erg

$E_{\gamma,iso}$  (peak)  $\geq 1.4 \times 10^{54}$  erg

$\Rightarrow$  likely beamed relativistic jet

- Insight-HXMT/HE + Fermi /GBM:  $\sim 50$  s precursor found  $\sim 25$  hr before the main peak (Zhang+26)



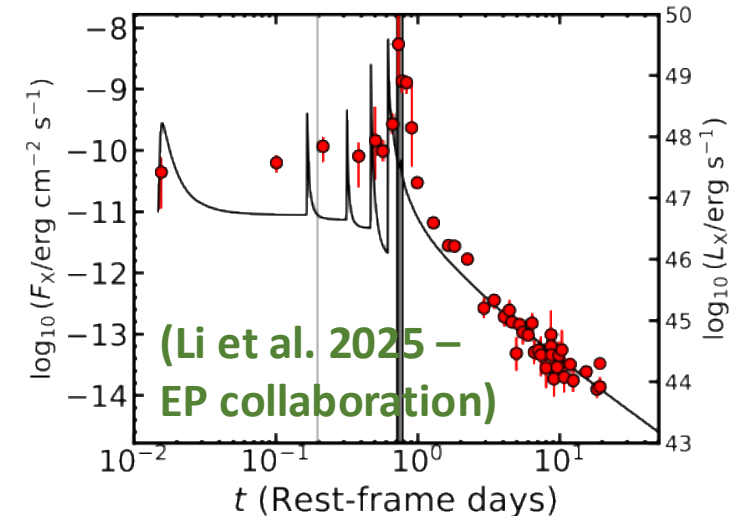
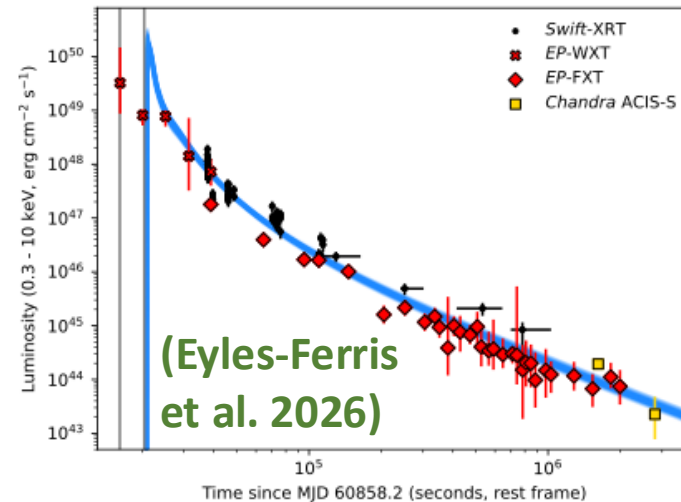
(Li et al. 2025 – EP collaboration)

# What can it be?

- Unusual type of collapsar (variant of long GRBs)? He-core + NS/BH? (JWST rules out a typical broad-line SN Ic, associated with LGRSs)
- Extreme Ultra-Long GRB? (maybe, but unclear what ULGRBs are...)
- TDE-SMBH: offset from host +  $t_{MV,z} \approx 0.5 \text{ s} > \frac{r_g}{c} \Rightarrow M_{BH} < 5 \times 10^4 M_{\odot}$
- TDE-stellar-mass-BH (micro-TDE): possible (Beniamini, Perets & JG 2025)
- TDE-IMBH: possible (MS or WD?);  $t_{MV,z} \approx 0.5 \text{ s} & \Gamma > 56$  still favor a stellar-mass BH engine

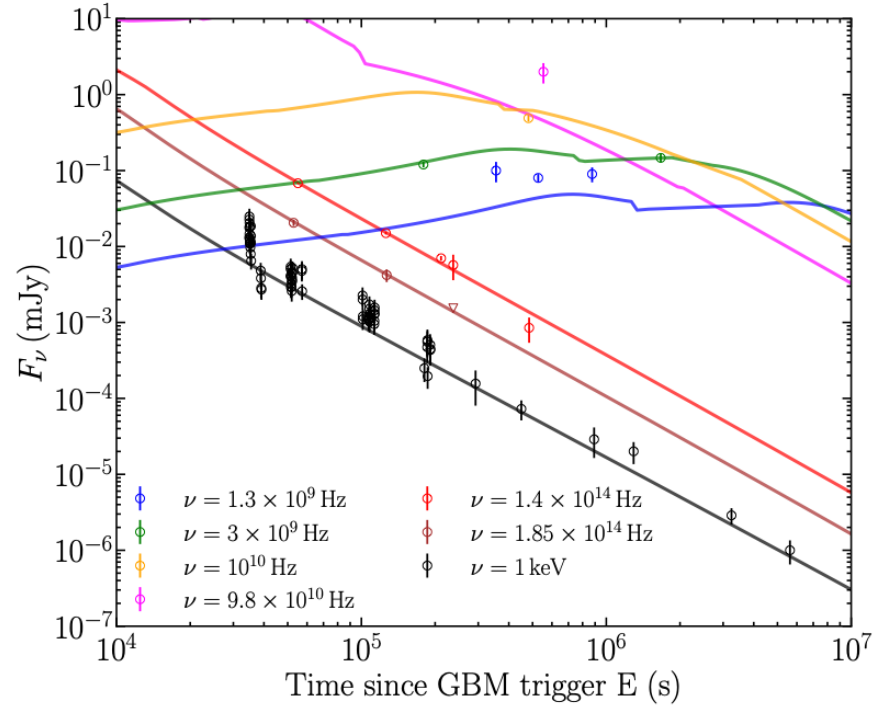
## TDE-IMBH of WD:

Timescales & lightcurve shape don't quite match



# A milli-TDE Model for GRB250702B: MS Star Disrupted by IMBH (JG, Peters, Gill, Beniamini, O'Connor 2025)

## GRB250702B Afterglow Fit:



$k = -1.60 \pm 0.17$  (consistent with  $-3/2$ )

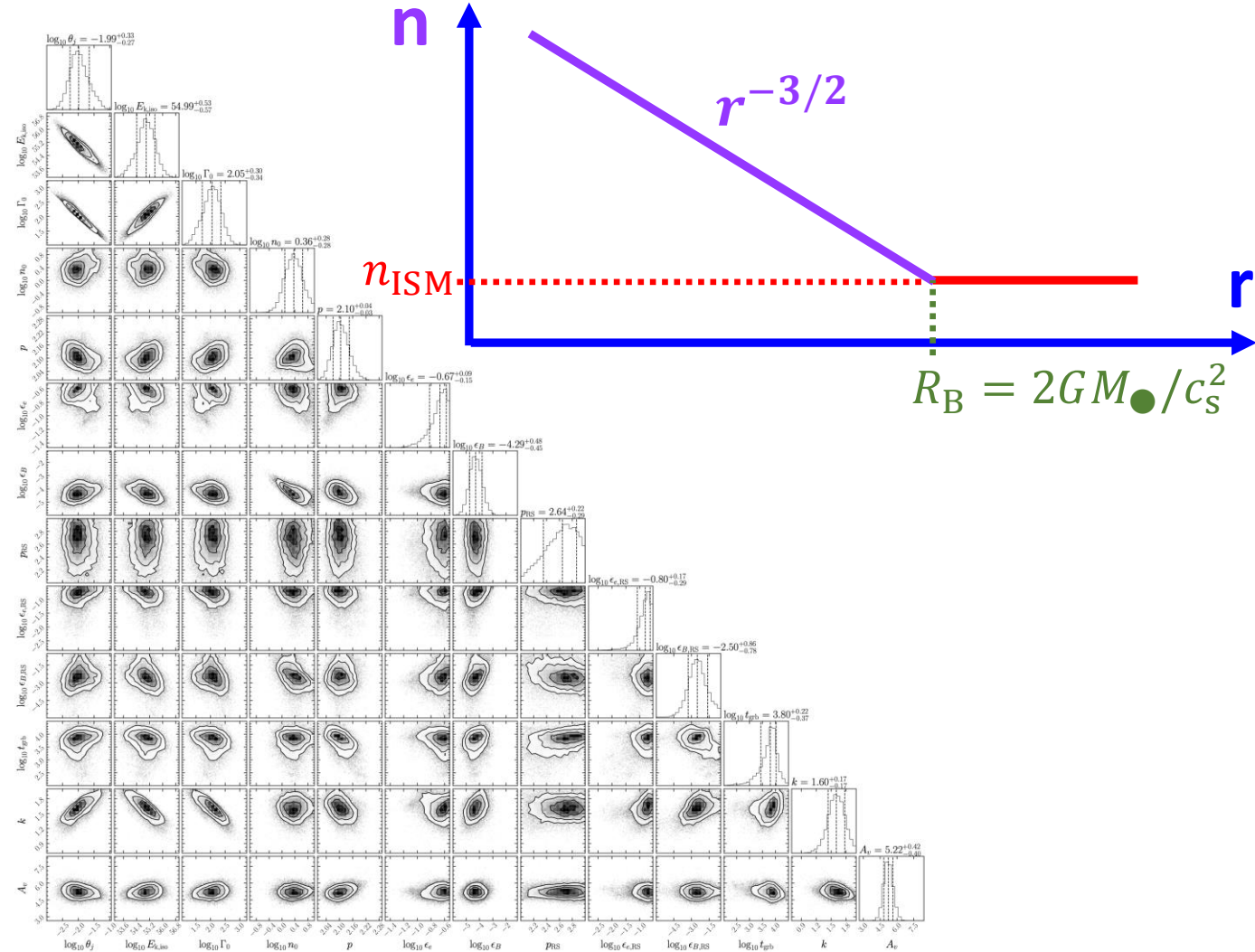
$n(r) = n_d (r/R_d)^{-k}, R_d = 10^{18} \text{ cm}$

$\log_{10} n_{d,0} = 0.36 \pm 0.28$

$(\log_{10} \theta_j = -1.99^{+0.33}_{-0.27}; \log_{10} E_{k,iso} = 54.99^{+0.53}_{-0.57})$

$50 \lesssim \log_{10} E_k \lesssim 51$

## Bondi Accretion:



# A milli-TDE Model for GRB250702B: MS Star Disrupted by IMBH (JG, Peters, Gill, Beniamini, O'Connor 2025)

Inferred Bondi Radius:

$$R_B = R_d (n_d/n_{\text{ISM}})^{2/3} \\ = 0.56^{+0.31}_{-0.19} n_0^{-2/3} \text{ pc}$$

Inferred IMBH Mass:

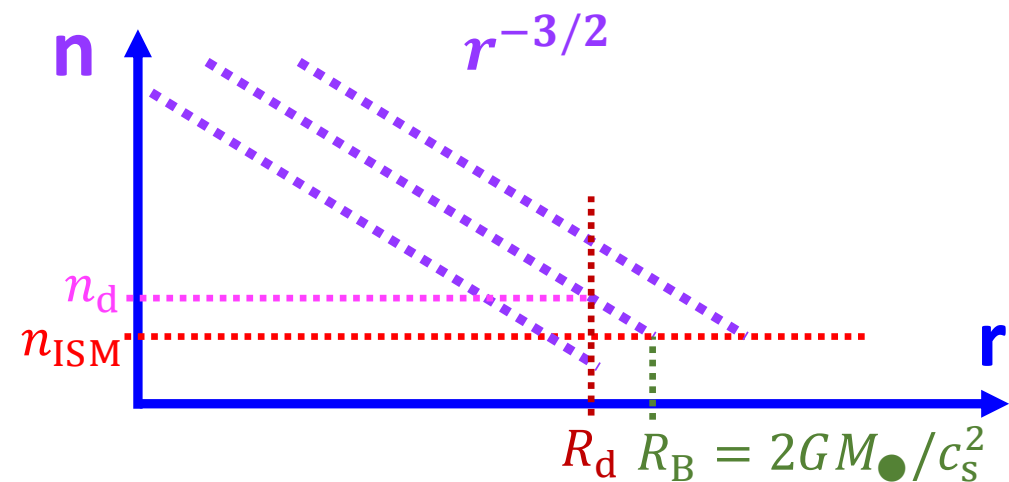
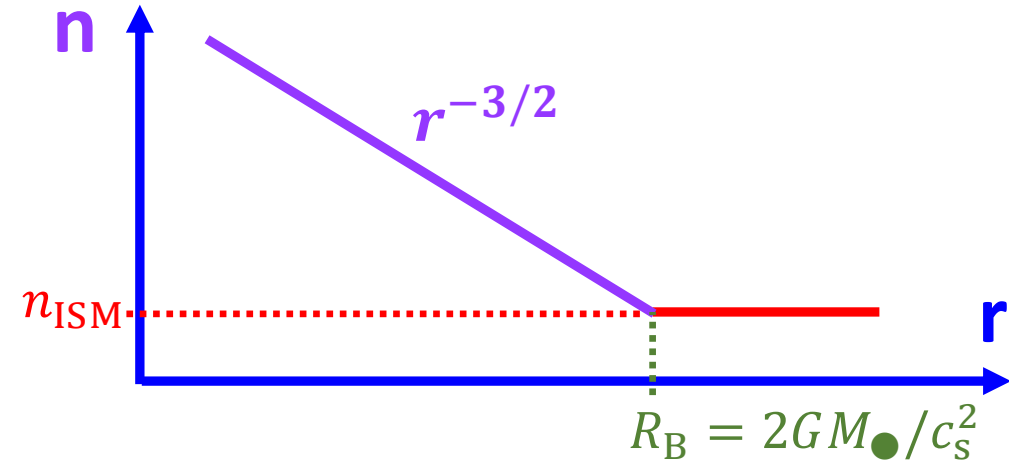
$$M_{\bullet} \\ = 6.55^{+3.51}_{-2.29} \times 10^3 n_0^{-2/3} c_{s,6}^2 M_{\odot}$$

$$k = -1.60 \pm 0.17 \text{ (consistent with } -3/2)$$

$$n(r) = n_d (r/R_d)^{-k}, R_d = 10^{18} \text{ cm}$$

$$\log_{10} n_{d,0} = 0.36 \pm 0.28$$

Bondi Accretion:



# A milli-TDE Model for GRB250702B: MS Star Disrupted by IMBH (JG, Peters, Gill, Beniamini, O'Connor 2025)

## Inferred Bondi Radius:

$$R_B = R_d (n_d/n_{\text{ISM}})^{2/3}$$

$$= 0.56^{+0.31}_{-0.19} n_0^{-2/3} \text{ pc}$$

## Inferred IMBH Mass:

$$M_{\bullet}$$

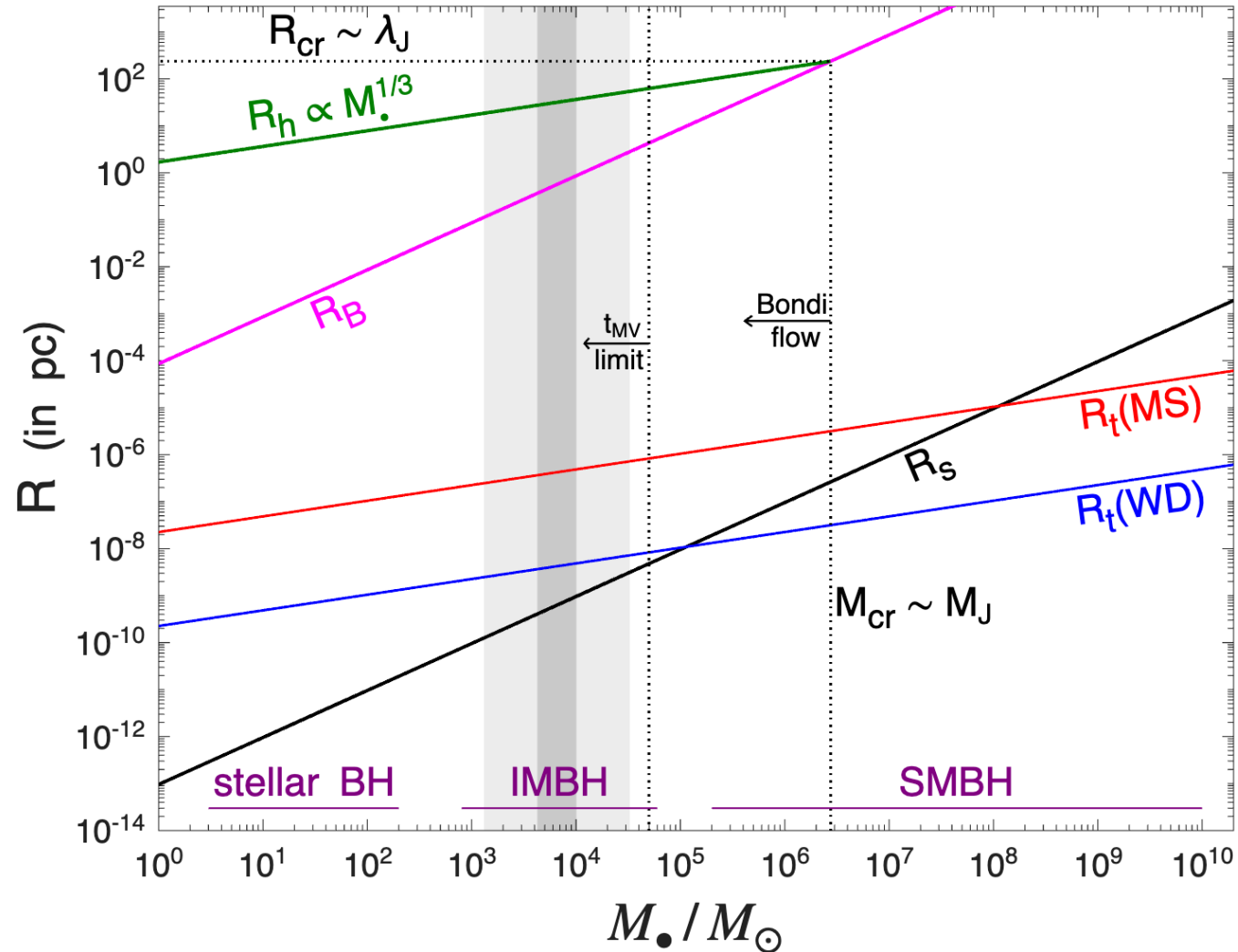
$$= 6.55^{+3.51}_{-2.29} \times 10^3 n_0^{-2/3} c_{S,6}^2 M_{\odot}$$

- Also consistent with the observed afterglow emission coming from  $r < R_B$

$$k = -1.60 \pm 0.17 \text{ (consistent with } -3/2)$$

$$n(r) = n_d (r/R_d)^{-k}, R_d = 10^{18} \text{ cm}$$

$$\log_{10} n_{d,0} = 0.36 \pm 0.28$$



# Bondi Hoyle Lyttleton Accretion:

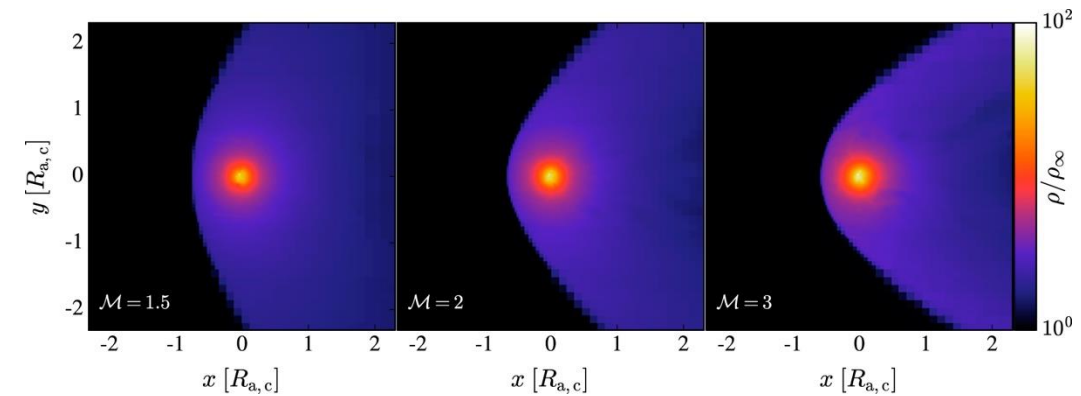
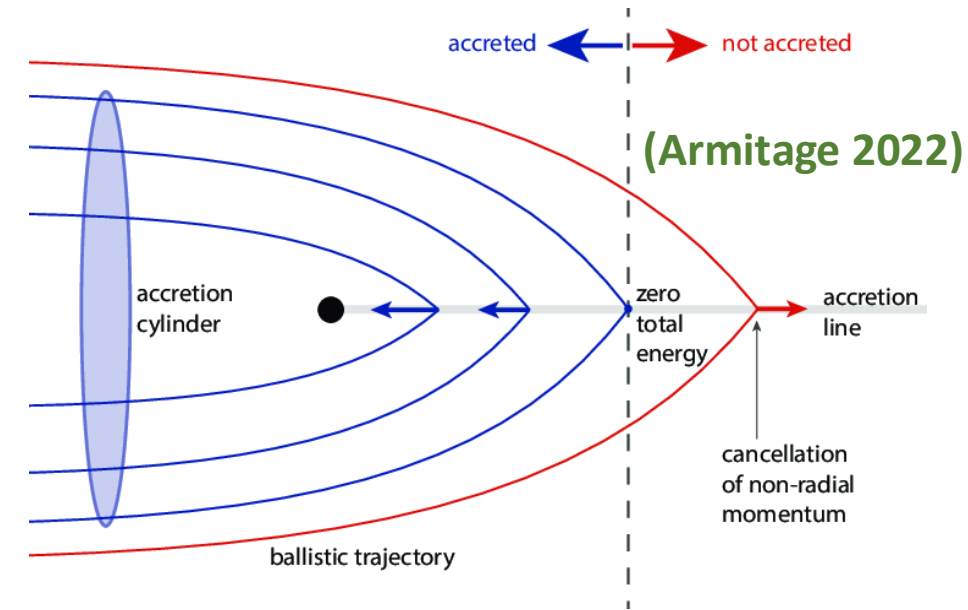
Modified Bondi Radius ( $v_{\text{BH}}$  added):

$$R_{\text{BHL}} \approx \frac{R_{\text{B}}}{1 + \mathcal{M}^2} = \frac{2GM_{\bullet}}{c_{\text{S}}^2(1 + \mathcal{M}^2)}; \quad \mathcal{M} \equiv \frac{v_{\text{BH}}}{c_{\text{S}}}$$

Modified inferred IMBH Mass:

$$M_{\bullet} = 6.55_{-2.29}^{+3.51} \times 10^3 n_0^{-2/3} c_{\text{S},6}^2 (1 + \mathcal{M}^2) M_{\odot}$$

$$t_{\text{MV,z}} > \frac{r_{\text{g}}}{c} \Rightarrow \frac{M_{\text{BH}}}{M_{\odot}} < 5 \times 10^4 \Rightarrow v_{\text{BH}} \lesssim 28 n_0^{1/3} \text{ km/s}$$



(Kaaz, Antoni & Ramirez-Ruiz 2019)

# Relevant Timescales: Main Sequence vs. White Dwarf

Disruption to 1<sup>st</sup> periastron passage ( $r_t \rightarrow r_p$ ):

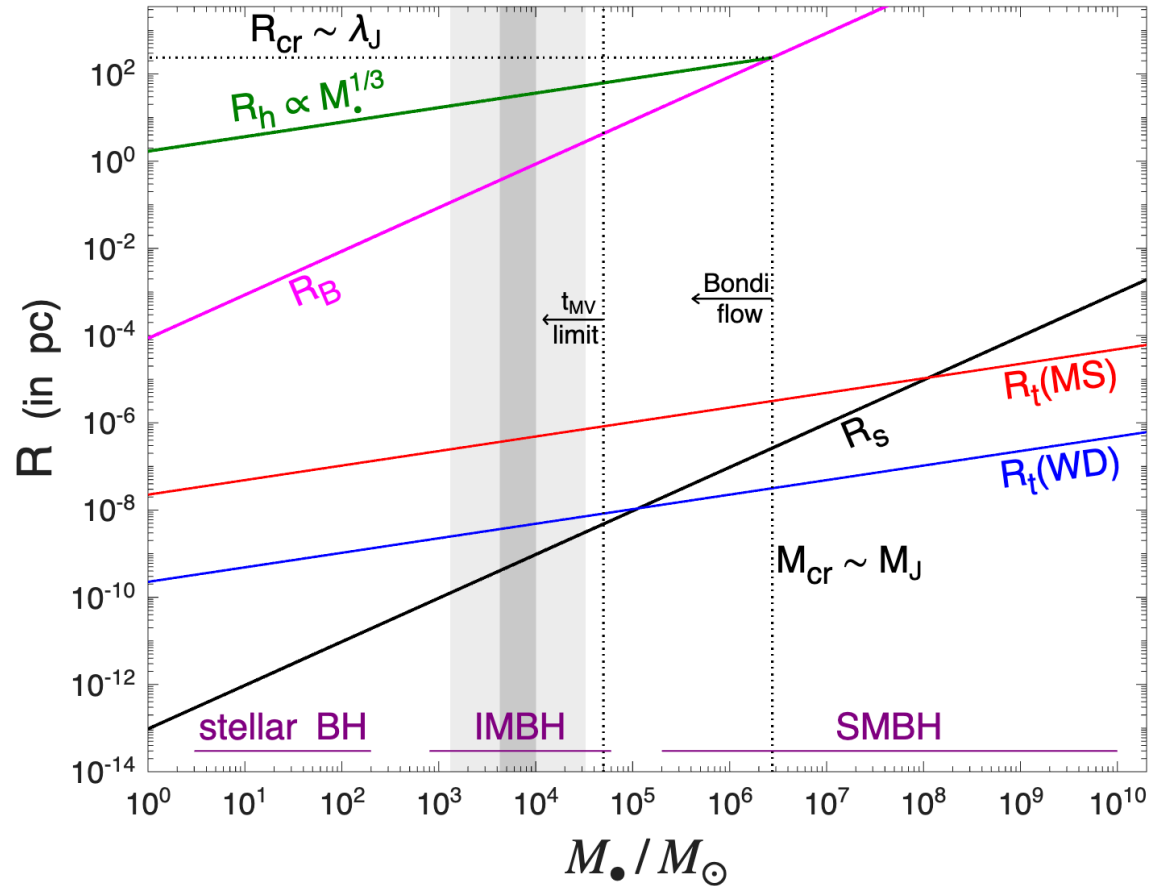
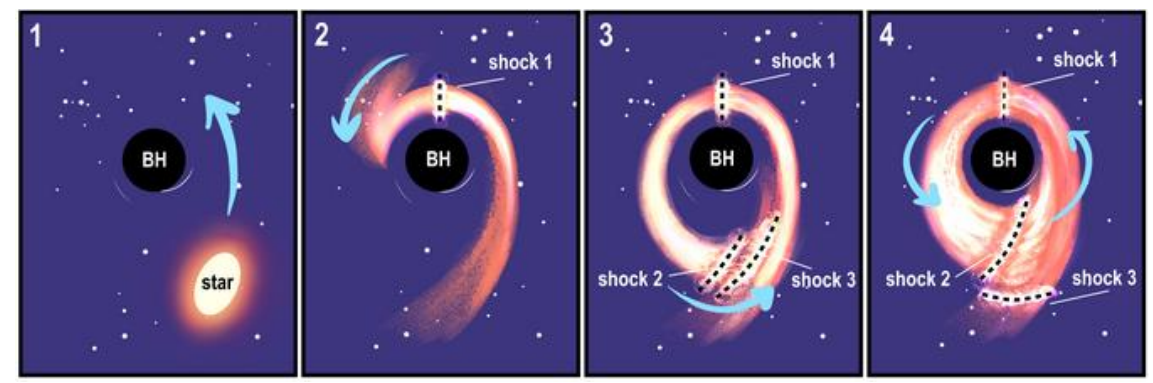
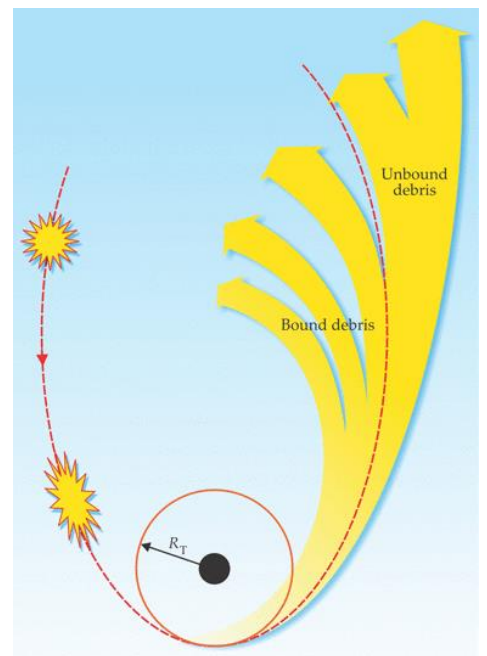
$$t_1 = \sqrt{\frac{\pi^2 R_*^3}{2GM_*}} = \begin{cases} 3.54 \times 10^3 R_{*,0}^{3/2} M_{*,0}^{-1/2} \text{ s (MS)}, \\ 3.54 R_{*,0}^{3/2} M_{*,0}^{-1/2} \text{ s (WD)}. \end{cases}$$

Orbital time of the most bound debris:

$$t_{\min} \approx \begin{cases} 3.5 \times 10^4 A_{\beta,-1} \eta^2 M_{\bullet,4}^{1/2} R_{*,0}^{3/2} M_{*,0}^{-1} \text{ s (MS)}, \\ 3.5 \times 10^1 A_{\beta,-1} \eta^2 M_{\bullet,4}^{1/2} R_{*,0}^{3/2} M_{*,0}^{-1} \text{ s (WD)}. \end{cases}$$

Where  $A_{\beta} \sim 1$  for frozen in approx, or  $\sim \beta^{-3}$  for efficient dissipation near  $r_p$   
 ( $\beta \equiv r_t/r_p =$  penetration factor)

- The observed timescales greatly prefer a MS star over a WD
- For a WD  $r_p \lesssim r_{\text{ISCO}}$  is possible, in which case no accretion disk or jet would form



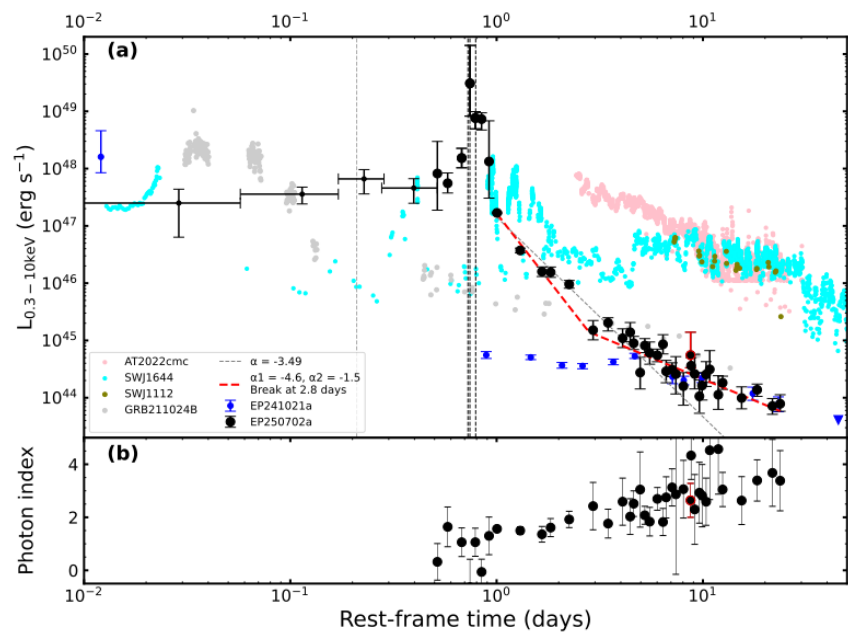
# Relevant Timescales: Main Sequence vs. White Dwarf

Disruption to 1<sup>st</sup> periastron passage ( $r_t \rightarrow r_p$ ):

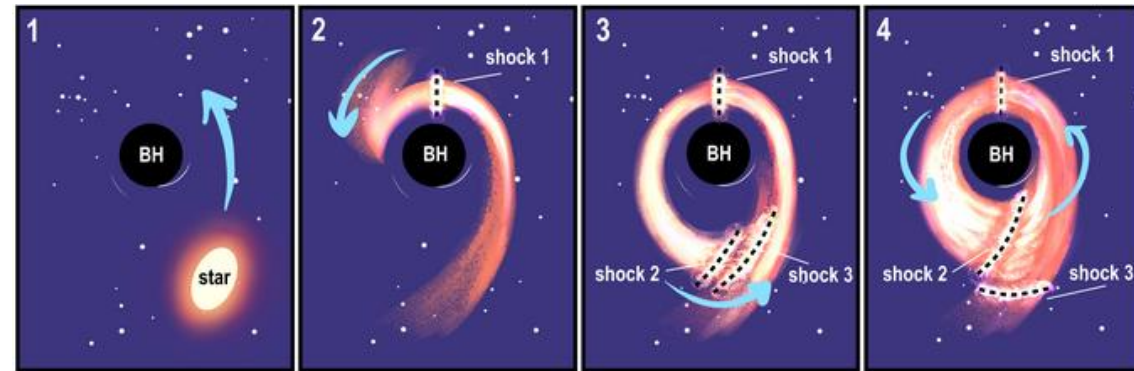
$$t_1 = \sqrt{\frac{\pi^2 R_*^3}{2GM_*}} = \begin{cases} 3.54 \times 10^3 R_{*,0}^{3/2} M_{*,0}^{-1/2} \text{ s (MS)}, \\ 3.54 R_{*,,-2}^{3/2} M_{*,0}^{-1/2} \text{ s (WD)}. \end{cases}$$

Orbital time of the most bound debris:

$$t_{\min} \approx \begin{cases} 3.5 \times 10^4 A_{\beta,-1} \eta^2 M_{\bullet,4}^{1/2} R_{*,0}^{3/2} M_{*,0}^{-1} \text{ s (MS)}, \\ 3.5 \times 10^1 A_{\beta,-1} \eta^2 M_{\bullet,4}^{1/2} R_{*,0}^{3/2} M_{*,0}^{-1} \text{ s (WD)}. \end{cases}$$



(Li et al. 2025 EP collaboration)



For  $R_{\text{circ}} \approx 2r_p = 2r_t/\beta$ ,  $t_{\text{acc}} \approx t_{\text{vis}}(R_{\text{circ}})$ :

$$t_{\text{acc}} \approx 4.5 \times 10^4 \beta^{-3/2} \alpha_{-1}^{-1} h^{-2} M_{*,0}^{-1/2} R_{*,0}^{3/2} \text{ s}$$

Approximate rise and peak timescales:

$$t_{X,\text{rise}} \sim t_{\text{circ}} + t_{\text{acc}}, \quad t_{\text{main}} \sim t_{\min} + t_{\text{acc}},$$

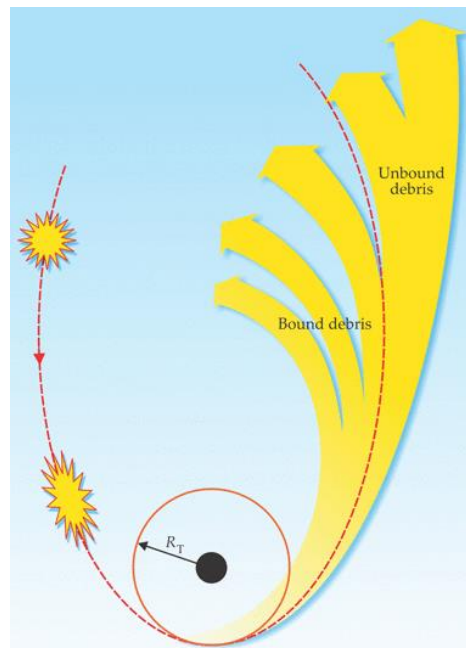
$$t_{\text{circ}} \approx 3.5 \times 10^4 f_{0.5} \beta_{0.5}^{-3} \eta^2 M_{\bullet,4}^{1/2} R_{*,0}^{3/2} M_{*,0}^{-1} \text{ s},$$

$$t_{\min} \approx 1.1 \times 10^4 \beta_{0.5}^{-3} \eta^2 M_{\bullet,4}^{1/2} R_{*,0}^{3/2} M_{*,0}^{-1} \text{ s},$$

$$t_{\text{acc}} \approx 3.2 \times 10^4 \beta_{0.5}^{-3/2} \alpha_{-1}^{-1} h_{-0.3}^{-2} M_{*,0}^{-1/2} R_{*,0}^{3/2} \text{ s},$$

Energetics limit on the jet beaming factor:

$$f_b \leq 6.4 \times 10^{-4} \eta_{j,-2} \eta_{\gamma,-1} M_{*,0} \left( \frac{f_{\text{fb}}}{0.5} \right) \left( \frac{1.4 \times 10^{54} \text{ erg}}{E_{\gamma,\text{iso}}} \right)$$

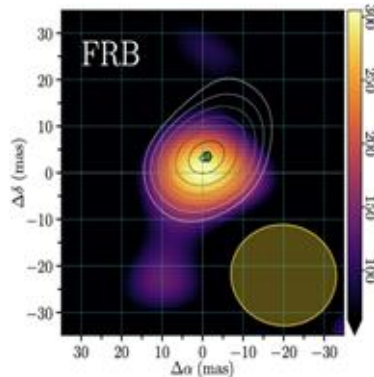
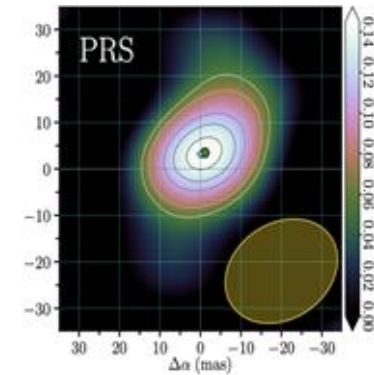


# Persistent Radio Sources (PRSs) of Repeating FRBs: Implications for Magnetar Progenitors (Rahaman, Acharia, Beniamini & JG 2025)

- A handful of confirmed/candidate PRSs associated with repeating FRBs
- Appear to have large  $DM_{\text{host}}$ , large + variable  $R$ , low- $Z$  high-SFR hosts
- Model: synchrotron emission from a compact Magnetar Wind Nebula (MWN)

Property	FRB 20121102A	FRB 20190417A	FRB 20190520B	FRB 20201124A	FRB 20240114A
$z$ (redshift)	0.193	0.128	0.241	0.098	0.130
Host galaxy	Dwarf	Dwarf	Dwarf	Spiral	Dwarf
$DM$ [ $\text{pc cm}^{-3}$ ]	558	1379	1204	413	528
$DM_{\text{host,rest}}$	$\lesssim 203$	$> 1228$	$137 - 707$	$150 - 220$	$142 \pm 107$
$RM_{\text{rest}}$ [ $\text{rad m}^{-2}$ ]	$(0.44 - 1.5) \cdot 10^5$	$(5.04 - 6.44) \cdot 10^3$	$(-3.6 - 2.0) \cdot 10^4$	$-661 \pm 42$	$449 \pm 13$
$\text{offset}_{\text{PRS-FRB}}$ [pc]	$< 40$	$< 26$	$< 80$	$< 188$	$\lesssim 28$
$R_{\text{proj}}$ [pc]	$< 0.7$ (at 5 GHz)	$< 23$	$< 9$	$< 700$	$< 0.4$
$\nu_{\text{obs}}$ [GHz]	1 - 26	1.4	1.5, 3, 5.5	6, 15, 22	0.65, 1.3, 5
$F_{\nu}$ [ $\mu\text{Jy}$ ]	180 (at 3 GHz)	190 (at 1.4 GHz)	202 (at 3 GHz)	8, 20, 30 (6, 15, 22)	66, 72, 46 (.65, 1.3, 5)
$\alpha$ (spectral index)	$-0.2 - -1$	$-1.2 \pm 0.4$	$-0.41 \pm 0.04$	$1.00 \pm 0.43$	$-0.34 \pm 0.21$
$L_{\nu}$ [ $\text{erg s}^{-1} \text{Hz}^{-1}$ ]	$2 \times 10^{29}$ (1.4 GHz)	$8 \times 10^{28}$ (1.4 GHz)	$3 \times 10^{29}$ (1.7 GHz)	$2 \times 10^{27}$ (6 GHz)	$2 \times 10^{28}$ (5 GHz)

PRS of FRB 20121102A

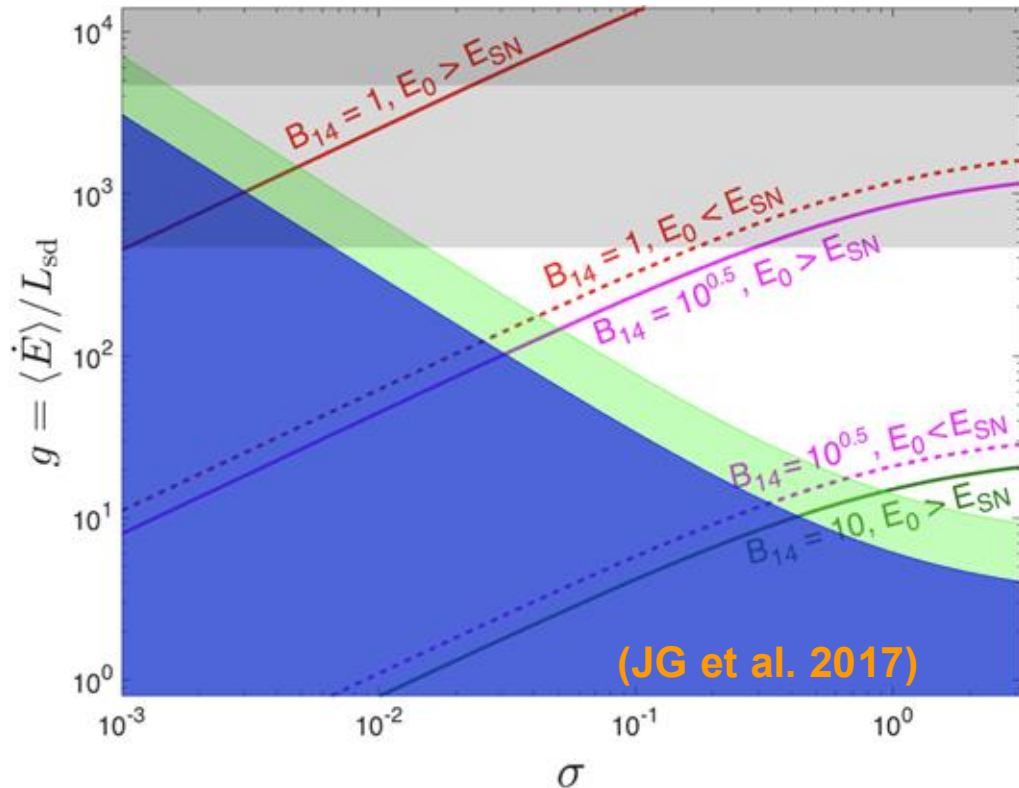


(Snelders et al. 2025)

Co-spatiality confirmed

# One Known Galactic Magnetar Wind Nebula: **Swift J1834-0846**

- Quite rare (1 out of over 30 Galactic magnetars)
- MWN size: diffusion-dominated cooling length of X-ray emitting  $e^\pm$
- Spindown power or  $B_{\text{dipole}}$  decay cannot power the MWN
- $B_{\text{int}}$  decay can power the MWN for a current  $B_{\text{int}} \gtrsim 10^{15.5}$  G through outflows associated with bursting activity (e.g. giant flares)



$$P = 2.48 \text{ s}$$

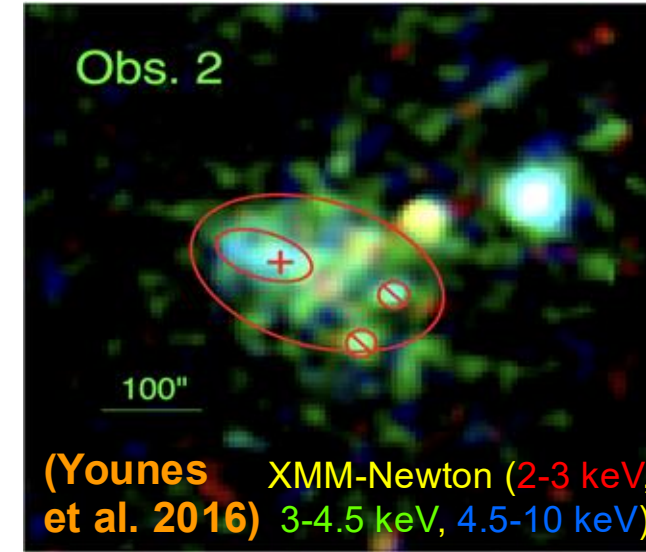
$$\dot{P} = 7.96 \times 10^{-12} \text{ s s}^{-1}$$

$$\tau_c = 4.9 \text{ kyr} \quad (n = 3)$$

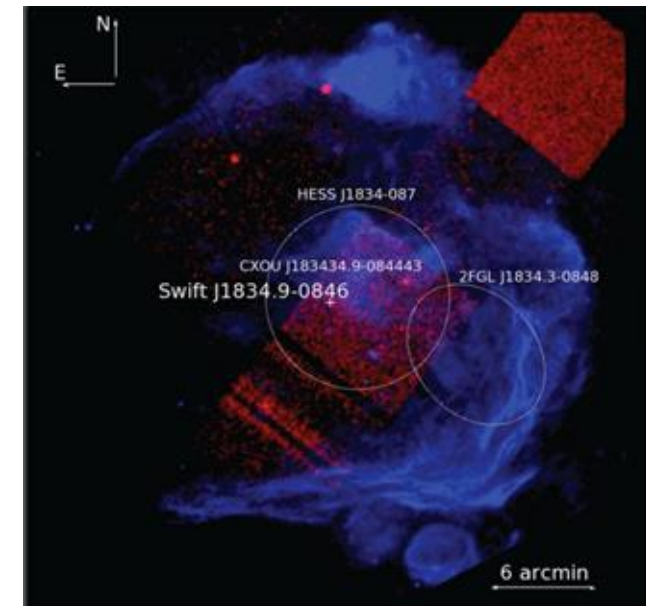
$$t = \tau_c - 10^5 \text{ yr}$$

$$B_d = 10^{14} \text{ G}$$

$$L_{\text{sd}} = 2 \times 10^{34} \text{ erg s}^{-1}$$

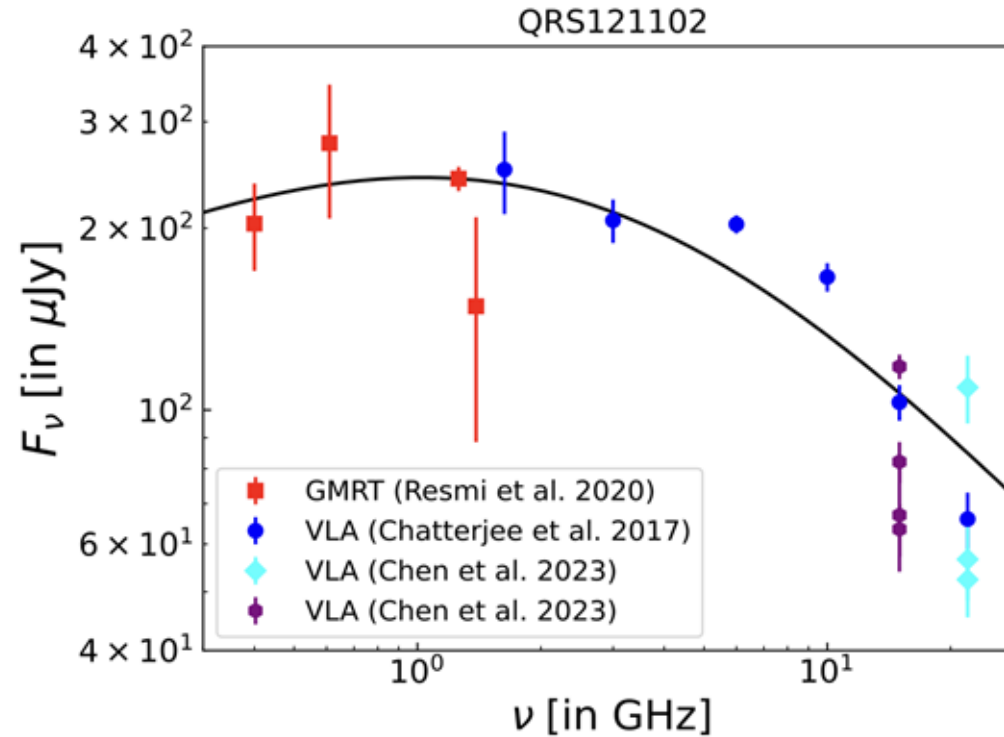
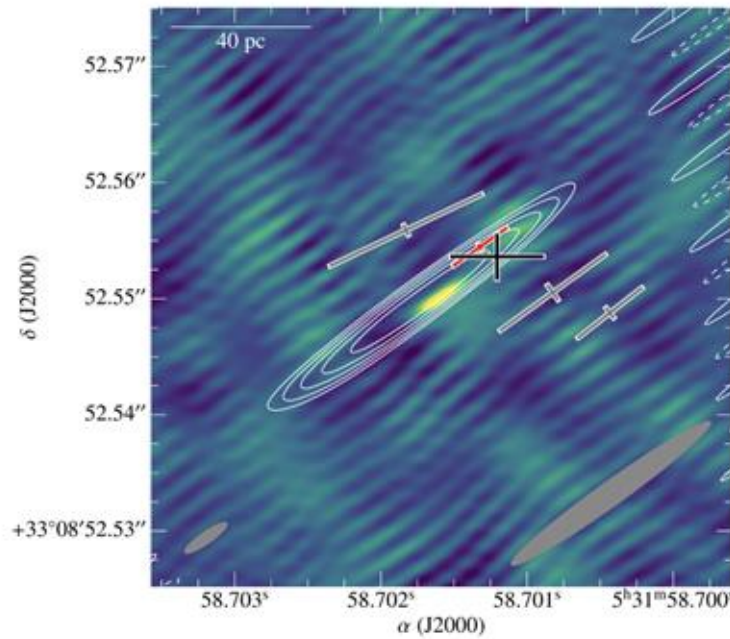


Associated with SNR W41



# Persistent Radio Sources (PRSs) of Repeating FRBs: Implications for Magnetar Progenitors (Rahaman, Acharia, Beniamini & JG 2025)

## PRS of FRB 121102A: the best constrained source



$$L_\nu \sim 2$$

$$\times 10^{29} \frac{\text{erg}}{\text{s Hz}}$$

$$\nu_{\text{sa}} < 0.5 \text{ GHz}$$

$$\nu_{\text{m}} < 3 \text{ GHz}$$

$$\nu_{\text{c}} > 22 \text{ GHz}$$

$$R_{\text{max}} = 0.7 \text{ pc (imaging)}$$

(Marcote et al. 2017)

$$R_{\text{eq}} \sim 0.1 \text{ pc (equipartition)}$$

$$R_{\text{min}} = 0.03 \text{ pc (scintillation)}$$

(Chen et al. 2023)

$$R_{\text{min}} < R_{\text{eq}} < R_{\text{max}}$$

**PRS is very compact**

# Persistent Radio Sources (PRSs) of Repeating FRBs: Implications for Magnetar Progenitors (Rahaman, Acharia, Beniamini & JG 2025)

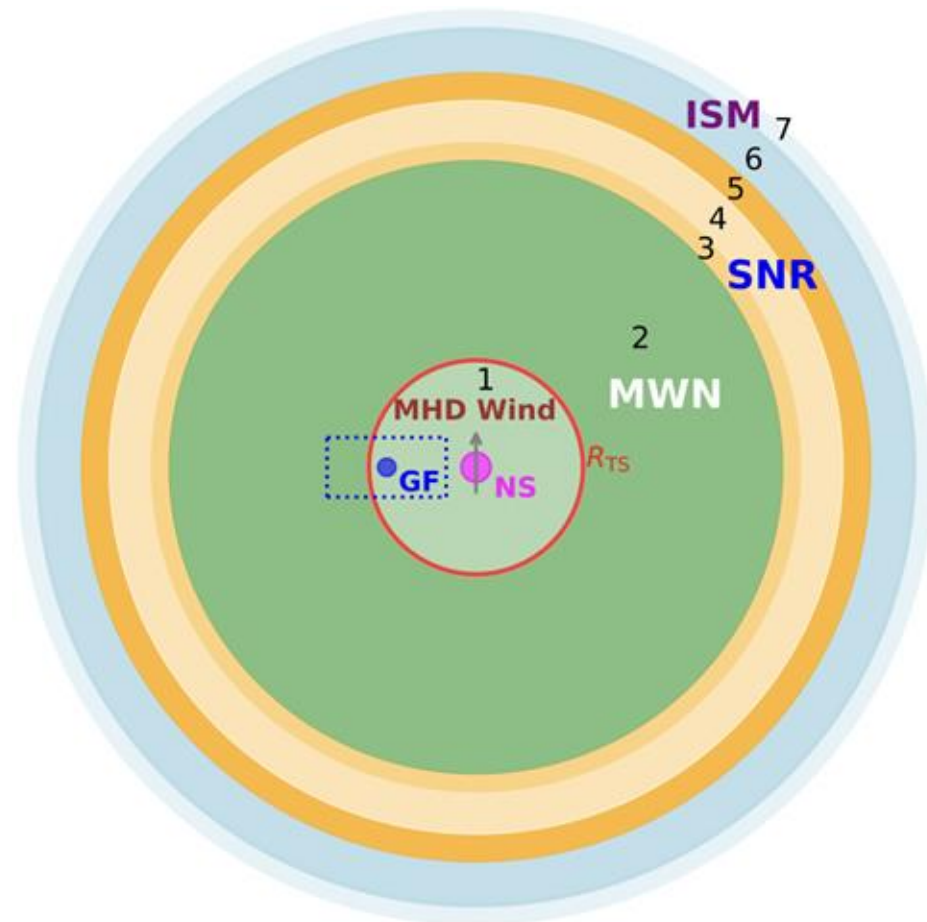
- Magnetar Wind Nebula (MWN = PRS candidate) is **confined** in a SuperNova Remnant (SNR)
- **Can a millisecond-magnetar work?** (Murase et al. 2016; Metzgar et al. 2017; Margalit & Metzgar 2018; Omand et al. 2018; Murase et al. 2021; Bhattacharya et al. 2024)
- **No** – the **compact size** and **minimal age** exclude this!!!

$$t = \frac{R_{\text{SNR}}}{v_{\text{SNR}}} = R_{\text{SNR}} \sqrt{\frac{M_{\text{SNR}}}{2(E_{\text{rot}} + E_{\text{SN}})}}$$

$$\approx \begin{cases} 2.5 R_{17.3} M_3^{\frac{1}{2}} P_{i,-3} \text{ yr} & \text{for } E_{\text{rot}} > E_{\text{SN}}, \\ 63.4 R_{17.3} M_{10}^{\frac{1}{2}} E_{50}^{-\frac{1}{2}} \text{ yr} & \text{for } E_{\text{rot}} < E_{\text{SN}}. \end{cases}$$

$$E = E_{\text{SN}} + E_{\text{rot}} \quad (\text{Total SNR Energy})$$

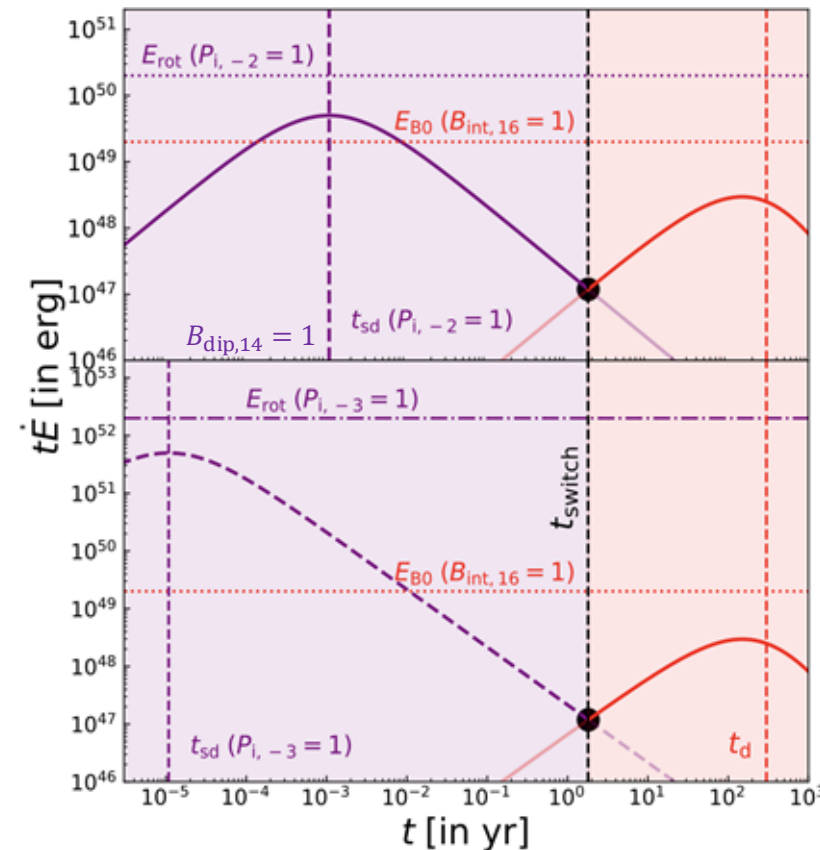
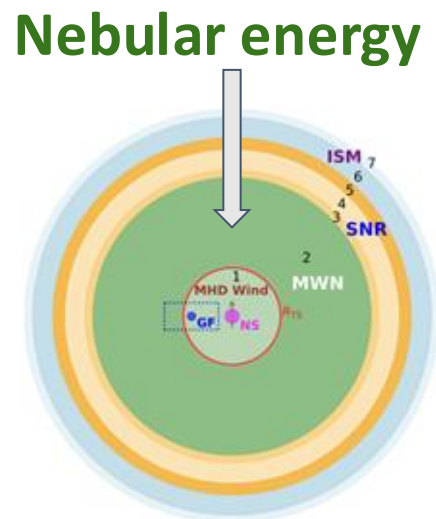
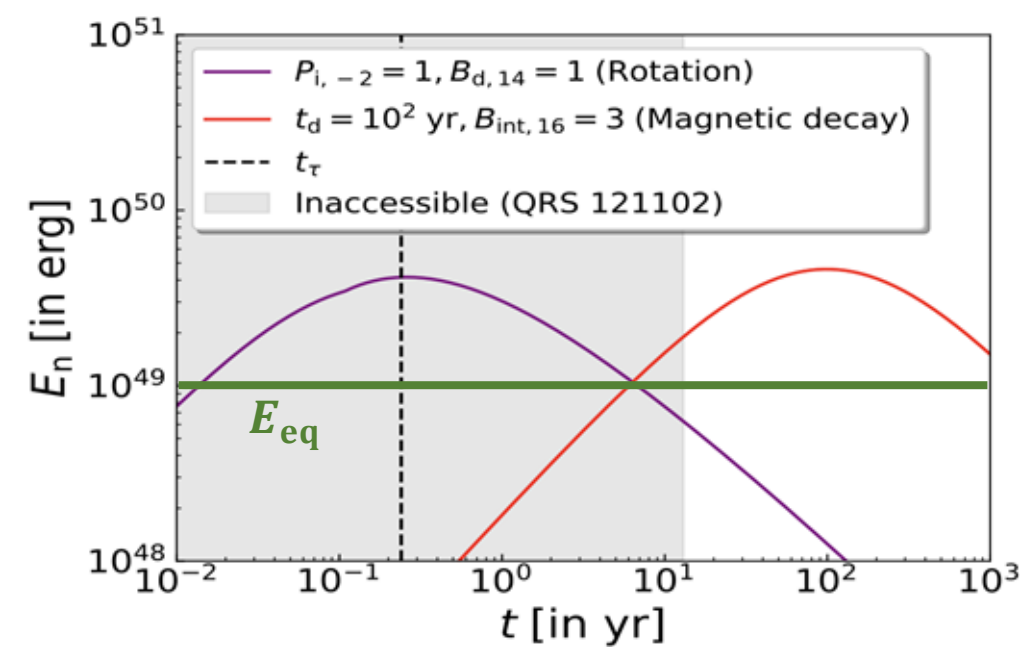
**This source is already observed for over 13 years**



# Persistent Radio Sources (PRSs) of Repeating FRBs: Implications for Magnetar Progenitors (Rahaman, Acharia, Beniamini & JG 2025)

- Equipartition/minimum nebular energy:  $E_{eq} \sim 10^{49}$  erg
- To power the FRB:  $B_{dip} \geq 10^{14}$  G (Lu & Kumar 2018, Beniamini & Kumar 2025)
- For an age of  $t > 13$  years spindown cannot power the MWN

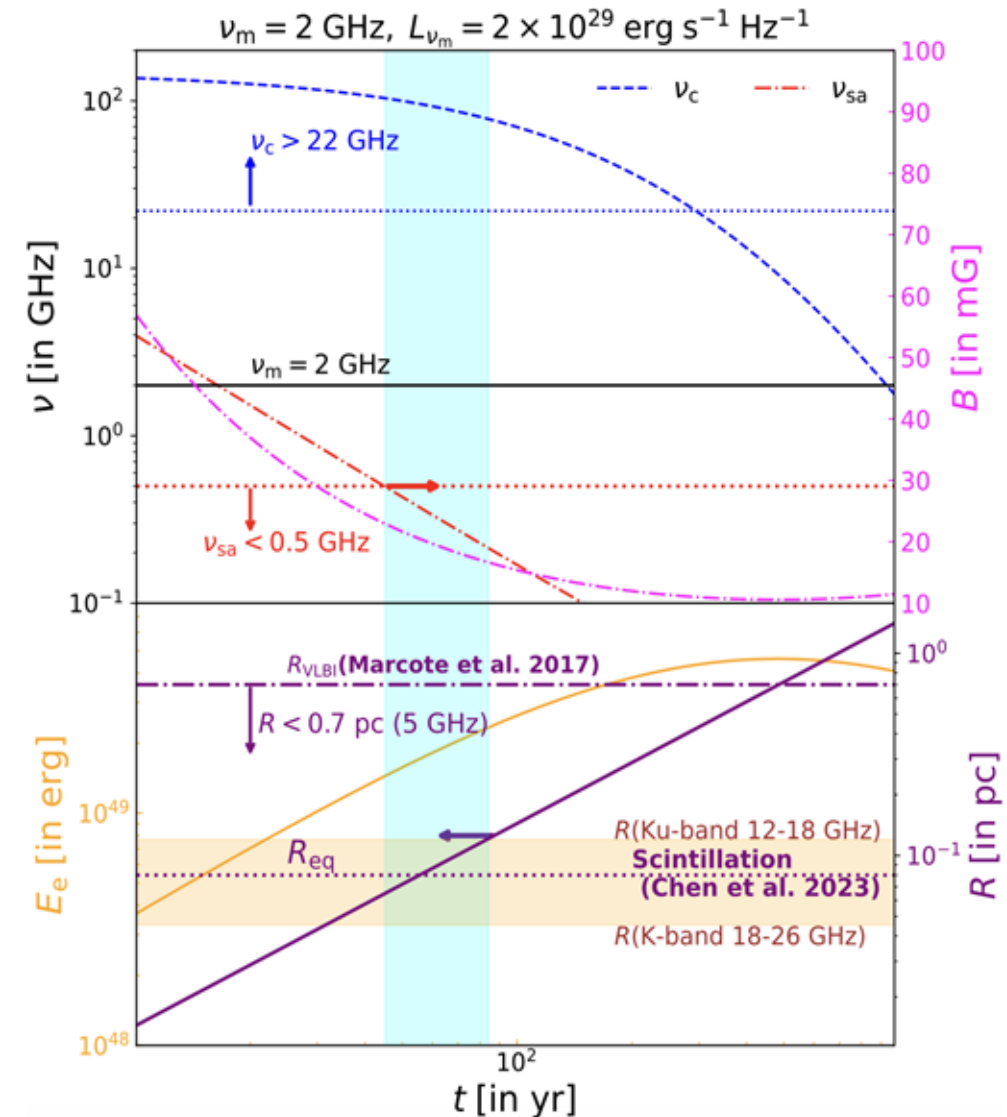
- After a characteristic time,  $t_{switch}$ , the nebular energy input is dominated by  $B_{int}$  decay
- We require  $B_{int}$  decay time:  $t_d \sim 10^{2.5}$  yr  $\gg t_{sd}$  (Other B-powered models need months: Murase+16, Metzger+17, Margalit & Metzgar 18, Omand+18, Murase+21, Bhattacharya+24)



# Persistent Radio Sources (PRSs) of Repeating FRBs: Implications for Magnetar Progenitors (Rahaman, Acharia, Beniamini & JG 2025)

Model favored by all of the observations:  
**Extreme magnetar & weak SN explosion**

- Extreme initial internal B-field:  
 $B_{\text{int}} \sim (1 - 3) \times 10^{16} \text{ G}$  with a rather small decay time  $t_d \sim 10^2 - 10^{2.5} \text{ yr}$
- Weak SN explosion:  $E_{\text{SN}} \sim 10^{50} - 10^{51} \text{ erg}$  given to an an ejected mass of  $M_{\text{ej}} \sim (3 - 10) M_{\odot}$
- Age of PRS/FRB source:  $13 \text{ yr} < t \lesssim 100 \text{ yr}$
- The slowest allowed  $B_{\text{int}}$  decay time  $t_{d,\text{max}} \sim 500 \text{ yr}$  favors a sub-energetic SN explosion  $E_{\text{SN}} \sim 10^{50} \text{ erg}$  with  $M_{\text{ej}} \gtrsim 10 M_{\odot}$  & a low-ionization fraction ( $\sim 3\%$ )
- Similar results hold for the PRS of FRB 20190520B
- PRS of FRB 20201124A is rather poorly constrained

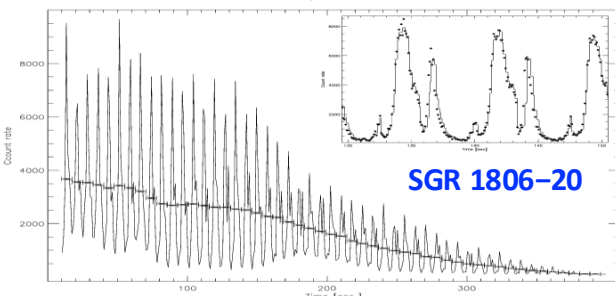
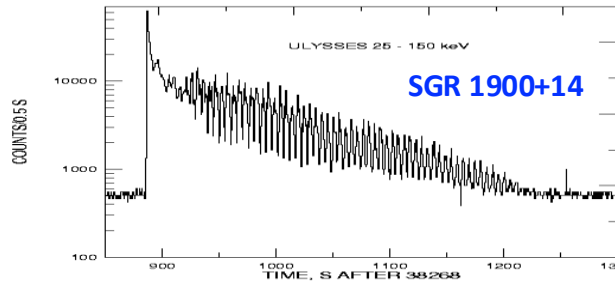
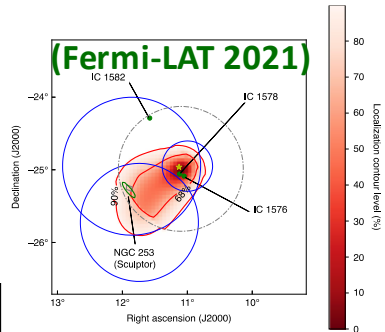
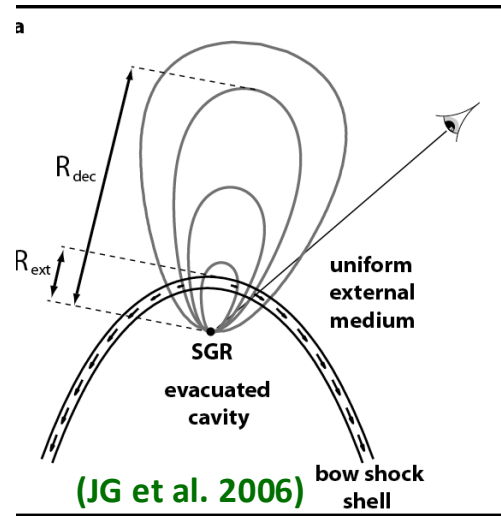
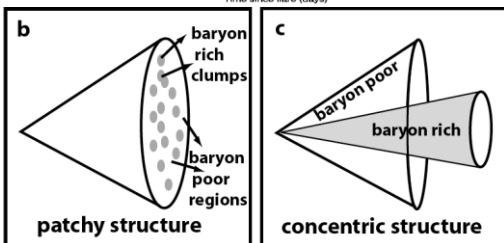
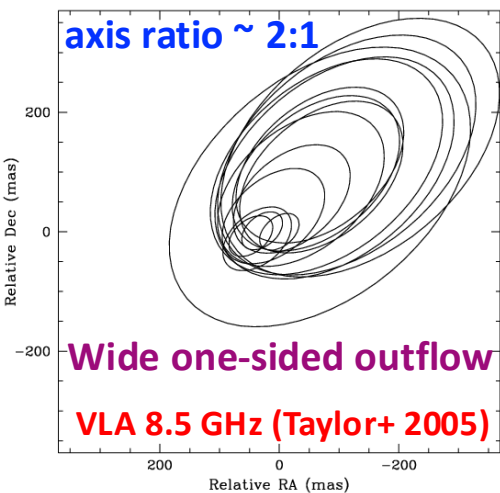
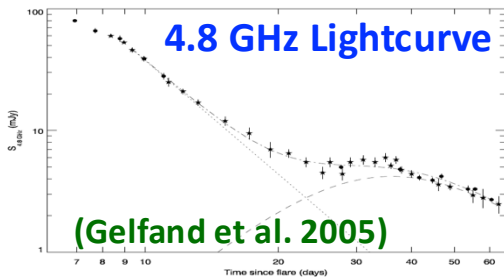
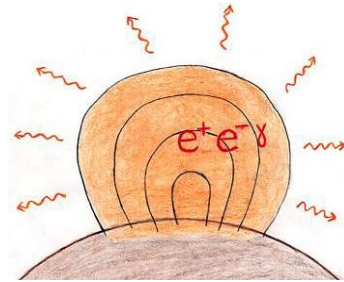


# Extragalactic Magnetar Giant Flares (GFs)

- There are **3 known Galactic GFs** (including the 5.3.1979 GF from SGR 0526-66 in the **LMC**)
- Similar energy in pulsating tail ( $\sim 10^{44}$  erg):  $e^+e^-\gamma$  that is trapped on closed field lines
- The **initial spike energy varies greatly** ( $E_{\text{spike}}/E_{\text{tail}} \sim 1 - 10^{2.5}$ ): what cannot be trapped
- 2 of the 3 Galactic GFs created a **radio nebula**, implying  $u = \Gamma\beta \sim 1$  outflow:  $E_k \sim E_{\text{spike}}$
- Recently: 10 good candidates for **extragalactic GFs** (only the initial spike is detectable)
- Sculptor galaxy** (3.5 Mpc):  $\Gamma \sim 100$ ,  $E_k \sim E_{\text{spike}} \sim 10^{46.5}$  erg (similar to SGR 1806-20)

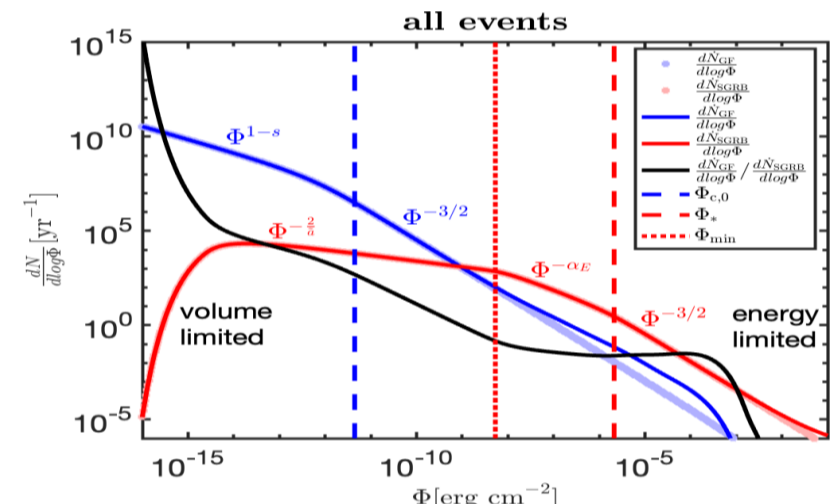
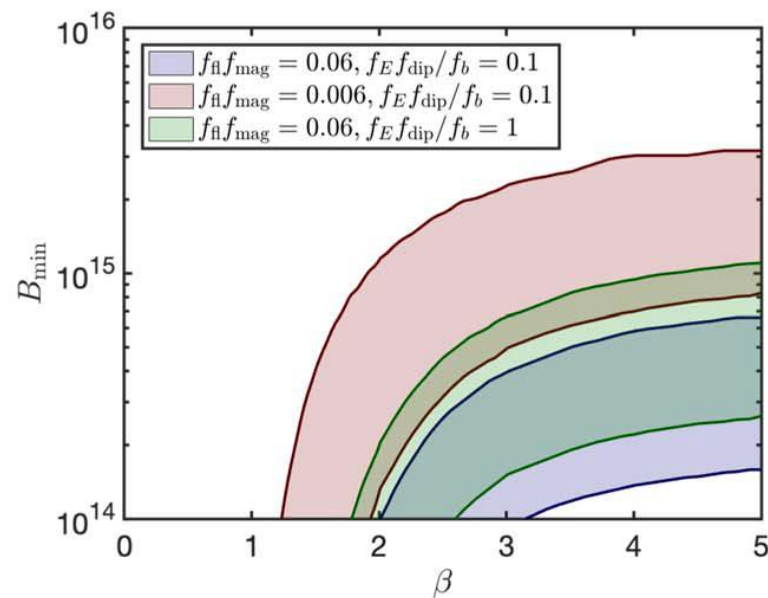
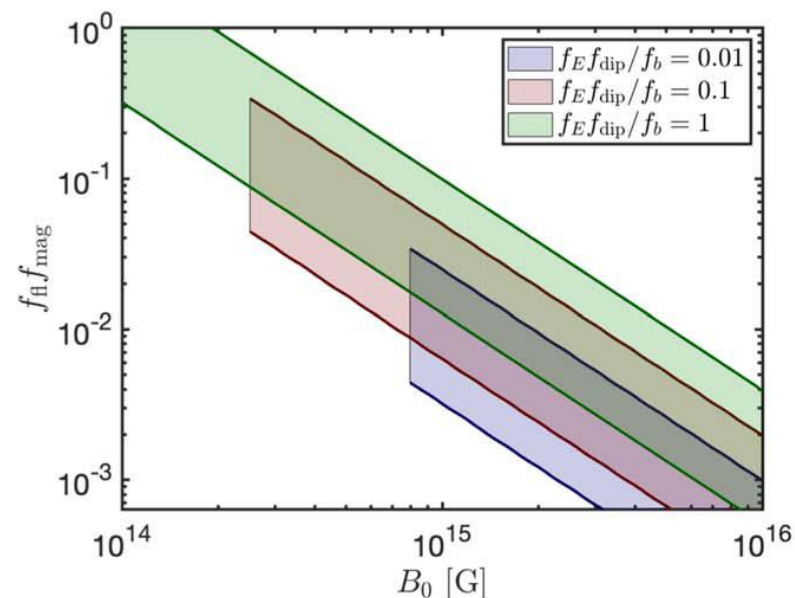
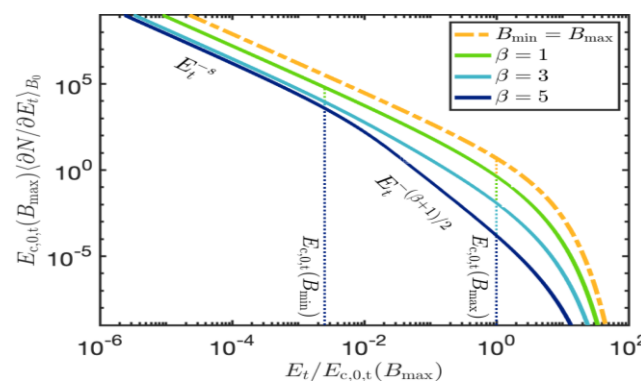
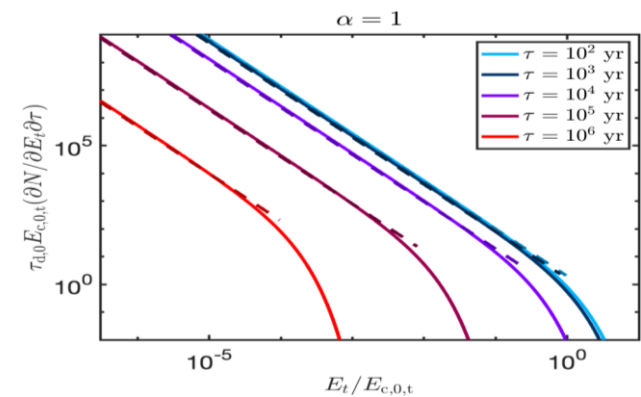
Observed delay of emission from outflow collision with an external bow-shock sell:  $\Delta t_{\text{obs,r}} = \frac{R_{\text{ext}}(1-\beta)}{\beta c} \sim \frac{R_{\text{ext}}}{2c\Gamma^2} \sim 17R_{16}\Gamma_2^{-2} \text{ s}$

(LAT  $\sim$  GeV photons at 19, 180, 284 s)



# Extragalactic Magnetar Giant Flares (GFs) (Beniamini et al. 2025)

- Each magnetar is born with **initial B-field**  $B_0$  of energy  $E_{B,0}$ , which **decays** on timescale  $\tau_{d,0}$  and powers the GFs:  $\int dE_t E_t \frac{\partial^2 N}{\partial E_t \partial \tau} = f_{fl} |\dot{E}_B|$
- Power law energy distribution**:  $\frac{\partial^2 N}{\partial E_t \partial \tau} \propto E_t^{-s} e^{-E_t/E_{c,t}}$  ( $s \approx 1.7$  from obs.)  
with **cutoff energy**:  $E_{c,t} = f_E f_{dip} E_B(\tau)$ ,  $f_{dip} = E_{dip}/E_B$ ,  $f_E = E_{c,t}/E_{dip}$
- Allow **beaming**: observed isotropic energy  $E = E_t/f_b$  ( $E_t =$  true energy)
- Allow for a **distribution in  $B_0$** :  $P(B_0) \propto B_0^{-\beta}$   $B_{min} < B_0 < B_{max}$
- Detailed predictions**: can constrain magnetar properties by fits to data



**The End**